

The Radio and Electronic Engineer

The Journal of the Institution of Electronic and Radio Engineers

Electronics and Energy

QUITE suddenly, the likelihood of existing sources of energy becoming exhausted has become front page news. The facts of growing demand and diminishing supplies, which have been well-known to geophysicists and engineers for a long time, are at last being widely appreciated as posing a real threat to the maintenance of living standards in the developed countries and thus, ultimately, to improving standards throughout the whole world. Clearly, if there is to be action in meeting this situation, engineers of all disciplines will need to cooperate and come up with some new approaches.

Last year, the Council for Environmental Science and Engineering (CESE) was set up jointly by CEI and CSTI under the chairmanship of Sir Kingsley Dunham, F.R.S., with representatives of all the senior engineering and scientific institutions (Professor H. M. Barlow, F.R.S., is the IERE's representative) and energy conservation is going to be as important a part of the Council's future deliberations as the perhaps more obvious problems of environmental pollution. The recent Graham Clark Lecture by Sir Kingsley, 'Natural resources, the engineer and the environment', which was reported in last month's Journal, reviewed the background factors for fossil fuels, coal, oil and natural gas, nuclear energy and solar energy, and this was followed up by a letter to *The Times* on 24th January from the Chairman of CESE and 16 of his colleagues calling for a new strategy:

'We would press for action similar to that taken before World War II when the need for rearmament was realized. That problem was solved only by setting up ministries in which leading industrialists, engineers, scientists and others were brought into positions of authority where they worked alongside civil servants on a full-time basis. The magnitude of the energy crisis demands a similar approach. It is not merely the short-term industrial and commercial problems that must be dealt with; research and development problems of almost frightening complexity urgently need attention'.

'The highest priority must be given to developing Britain's indigenous fuel resources, utilizing all fuels to their maximum efficiency and conserving their use with regard to their role, not only as providers of heat and power, but also as raw materials for many vital products'.

Both Sir Kingsley and Professor J. F. Coales (Vice-Chairman of CEI) subsequently expanded on the realities in broadcast interviews. Professor Coales referred to getting heat from the centre of the Earth and to the possibilities of using the Sun's radiation by photoelectric devices, but stressed that these were only at the 'ideas' stage at present. Later he said: 'The situation is such, we believe, that you have got to go for the things that you are most likely to bring to a successful conclusion and force these through'.

CEI's Board welcomed the initiative of CESE in setting the pace for positive action. The Chairman of CEI, Sir Leonard Atkinson, has subsequently been in correspondence with Lord Carrington, Secretary of State for Energy in the late Government, offering the co-operation of CEI in dealing with the energy problems of the country. The Council is now to seek from Constituent Members the names of appropriate persons whose expertise could be made available in this context to the new Secretary of State, Mr. Eric Varley.

What are to be the electronic engineers' contributions to these vital issues? Already the National Electronics Council has set up a working party to consider how the Industry and the research departments of Government and the Universities can help. Without wishing to anticipate the directions of investigation which will be recommended, electronic control and communications will be vitally important since greater automation in all energy industries must lead to more efficiency. For example, there is great scope in the coal mines for using the latest remote control techniques—'spin-offs' from the space programme—to enable otherwise difficult or even impossible seams to be worked. On the wider front it has for some time been apparent that in an era of rising costs, capital investment in the best possible equipment from the beginning of a project is much more effective than at a later stage, while amortization charges for hardware are generally far more favourable in such contexts than the continuing costs of manual control.

During the pre-World War II period referred to above, electronic engineers responded to the challenge of the time with the war-winning concept of radar. Perhaps there is no similar wide-ranging solution to be found for our present energy problems but, less spectacularly, the materials aspects of recent electronic developments may lead to greater efficiency in using electronics for solving some of the problems of world energy supplies. Where a 'breakthrough' is needed is in finding an answer to the growing need for new kinds of portable power.

In all these areas however political and economic problems will certainly rival those of technology . . .

Contributors to this issue*



Dr. M. J. Buckingham graduated in physics from the University of Reading in 1967. Since then he has been engaged in research into the properties and applications of semiconductor devices at the J.J. Thomson Physical Laboratory, University of Reading. About two years ago he took part in a study of the problems associated with the detection of gravitational radiation and his joint paper on this subject with Professor Faulkner was awarded the Clerk Maxwell Premium as the most outstanding paper of 1972.

Professor Faulkner was awarded the Clerk Maxwell Premium as the most outstanding paper of 1972.



Professor E. A. Faulkner (Fellow 1966, Member 1964) is a graduate of the University of Oxford. After appointments in industry and with the Australian C.S.I.R.O. he took up a teaching and research appointment at the J.J. Thomson Physical Laboratory, University of Reading, in 1960, and in 1970 he was appointed to the Department's Chair of Solid-State Electronics. A strong advocate of university-industry collaboration, Professor Faulkner is consultant in linear circuit design for a number of leading electronics firms and he is a director of Brookdeal Electronics Limited. He has published two books and nearly 70 papers in scientific and engineering journals, including several in the Institution's Journal for two of which he has been awarded Premiums. He has been a member of the IERE Papers Committee for several years and he has served on the Thames Valley Section Committee.

laboration, Professor Faulkner is consultant in linear circuit design for a number of leading electronics firms and he is a director of Brookdeal Electronics Limited. He has published two books and nearly 70 papers in scientific and engineering journals, including several in the Institution's Journal for two of which he has been awarded Premiums. He has been a member of the IERE Papers Committee for several years and he has served on the Thames Valley Section Committee.



Dr. C. F. Ho (Member 1965, Graduate 1969) is a senior lecturer in the Electrical Engineering Department of the University of Hong Kong, where he was appointed to a lectureship in 1967; he was awarded his doctorate in 1971. Dr. Ho is a graduate of the University of London, obtaining his B.Sc. at the then Battersea College of Technology in 1959, and he subsequently worked as a research engineer with the Automatic Telephone & Electric Co., Liverpool. Between 1962 and 1964 he was at the University of Manitoba where he obtained his Master's degree and for the next two years he was a senior applications engineer with Fairchild Semiconductor (H.K.) Ltd. Dr. Ho's current research interests are in solid-state device circuitry and control system stability and he has contributed several papers to the Institution's Journal on these subjects.

Automatic Telephone & Electric Co., Liverpool. Between 1962 and 1964 he was at the University of Manitoba where he obtained his Master's degree and for the next two years he was a senior applications engineer with Fairchild Semiconductor (H.K.) Ltd. Dr. Ho's current research interests are in solid-state device circuitry and control system stability and he has contributed several papers to the Institution's Journal on these subjects.

*See also page 166.



Dr. W. G. Fiennes went up to New College, Oxford, in 1964 to read physics; gaining a first in honour moderations, he then took the nuclear and theoretical physics options, and graduated with a second. In 1967 he joined the Lubrication Laboratory at Imperial College under Dr. A. Cameron (now 'Professor') to study the electrical characteristics of lubricating oil films.

The electrical aspects of this work were supervised by Professor Anderson, and they formed the subject of a thesis which was successfully submitted for a Ph.D. in 1971. Since that time Dr. Fiennes has worked as a research physicist in the Materials Research Laboratory of Smiths Industries, electrical ceramics being his prime concern.



Professor J. C. Anderson (Member 1949) graduated at the University of London in 1951, where he subsequently gained his Ph.D. in 1960 and his D.Sc.(Eng.) in 1967. After three years at Electric and Musical Industries, he became a lecturer in telecommunications at Northern Polytechnic. In 1957 he went to the University of Witwatersrand, Johannesburg, as a senior lecturer in Physics and later took

up a research fellowship at Royal Holloway College, University of London, followed by a period with Laboratories RCA in Zurich. In 1961 he joined Imperial College, London, as a lecturer in the Department of Electrical Engineering. He was appointed a Reader in the Department in 1962 and since 1965 he has occupied the Chair of Electrical Materials. He is the author of numerous papers in the scientific and technical literature and has been awarded Institution Premiums on two occasions. Professor Anderson served on the Papers Committee for several years and he was Chairman of Organizing Committees for IERE conferences on 'Thin Films' (1966), 'Thick Films' (1968) and 'Hybrid Micro-electronics' (1973).



Mr. C. J. Taylor (Graduate 1969) joined the Post Office in 1962 and after training worked on the automatic telex and telegraph transmission equipment in Fleet Building, London. Through part-time study from 1962-1969 at East Ham Technical College, he received an H.N.C. in electrical and electronic engineering with three endorsements and completed the CEI Part II Academic Test in 1972. Mr. Taylor left the Post

Office in 1968 to join the Marconi Company at Basildon, Essex, where he was concerned with aeronautical navigational and communication systems. From 1969 to 1972 he worked for Data Recording Instrument Company, Staines, on the design and quality aspects of using magnetic media on computer peripherals. He is now working for the Department of Posts and Telegraphs, Papua, New Guinea, on the development of the country's radio communications network.

Disk pack testing— A new approach

C. J. TAYLOR (Graduate)*

Based on a paper presented at the IERE Conference on Video and Data Recording held in Birmingham on 10th to 12th July 1973.

SUMMARY

Methods of testing disk packs on an amplitude detection principle are widely used at present for initial testing, but the detection methods used in computer systems are based on a time detection principle which is less sensitive to changes of amplitude.

This paper outlines the usefulness of amplitude detection as a method for testing disk packs and compares it against a technique based on time detection.

1 Introduction

A magnetic disk pack is the storage medium used on an exchangeable disk store (e.d.s.). In order to achieve the market requirements of greater storage capacity, faster access time, higher data rate and better reliability, the e.d.s. is designed with higher data and track packing densities, faster rotational speed and a shorter actuator access time. To achieve these requirements the design of the disk pack involves a thinner oxide coating, better surface finish and improved oxide coating methods.

As the data and track packing density is increased on an e.d.s., the effects of pulse crowding become evident. Timing distortions and signal to noise ratio are the limiting factors, and the most critical aspect in disk pack testing is to detect defect areas which would cause system errors.

Most types of disk pack test equipment used do not at present test the timing distortion produced from a disk pack but measure only the amplitude variations. In order to understand the contribution of the disk pack to the system performance, the critical areas in data detection are considered.

2 Limitations to Packing Density

The ideal step function response from a digital magnetic recording system would be the unit impulse (derivative). This is degraded by the losses in the system to a bell-shaped characteristic pulse.

A periodic signal corresponding to an all 'ones' pattern is represented by a square wave in record current waveform, and the replayed waveform at low packing density would be a sequence of characteristic pulses of alternate polarity. As packing density increases, pulse crowding sets in and adjacent pulses overlap giving a reduced amplitude. When a coded pattern is replayed at high density, timing distortion or peak shift occurs due to the overlap of adjacent pulses. The drop in amplitude and magnitude of peak shift can be approximately derived by the superposition of characteristic pulses, and the ideal characteristic pulse would be narrow and of large amplitude.¹ It has been shown^{2,3} that the amplitude of this pulse, e , can be found in terms of the magnetic recording head and disk pack surface characteristics:

$$e = \frac{8\mu_m n}{(\mu_m + 1)g} Kvw \frac{B_r c}{\mu_0} \tan^{-1} \left(\frac{g}{a+d} \right) \quad (1)$$

where K = head efficiency

n = number of turns on head

μ_m = head permeability

w = track width

v = head/surface velocity

c = oxide coating thickness

d = head to disk surface separation

g = half length of head gap

$$a = \frac{B_r c}{2\pi\mu_0 H_c} \quad (2)$$

* Formerly with the Data Recording Instrument Co. Ltd., Staines, Middlesex; now with the Department of Posts and Telegraphs, Papua, New Guinea.

where B_r = oxide coating retentivity

H_c = oxide coating coercivity

Also the width of the pulse at the 50% point can be found from:^{2,3}

$$P_{50} = 2\sqrt{(a+d)(a+d+c)+g^2} \quad (3)$$

The resolution of the system is limited by the width of the characteristic pulse P_{50} , which, from equation (3), will have a low value with a thin coating of high coercivity, low retentivity-thickness product, small head-to-medium separation and narrow head gap. The amplitude, however, from equation (1) reduces with reduced retentivity-thickness product, so a compromise is required for best overall system performance.⁴ The head 'flies' over the surface of the disk on a self-generated air bearing at a height of typically 2 μm . Any increase to the flying height will cause amplitude drop and timing distortion and disturbances to the air film may be caused by surface imperfections, foreign matter or non-flatness of the disk.⁴

3 Detection and Decoding

Two detection methods are commonly used in digital recording, peak detection and crossover detection. Unlike a tape system, which may use either method, a disk file operates over a range of surface velocities, packing densities and head flying heights. The same detection circuitry is generally switched between a number of heads which may show some variation in sensitivity. The 'read' electronics is therefore required to operate with signal levels having a wide range of amplitudes, and peak detection with a fixed threshold level is unsuitable. Crossover detection, which is less sensitive to amplitude variation, is generally used. The signal is first differentiated, and the detected cross-overs correspond to the peaks of the original signal.

The type of code most commonly used in disk files is double frequency modulation, which requires two flux changes per bit of information, although later methods, such as modified frequency modulation, permit more economic use of the medium.⁵

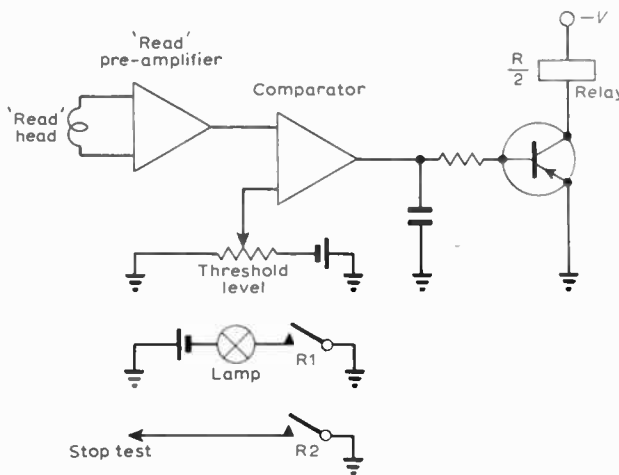


Fig. 1. Basic amplitude detection circuit.

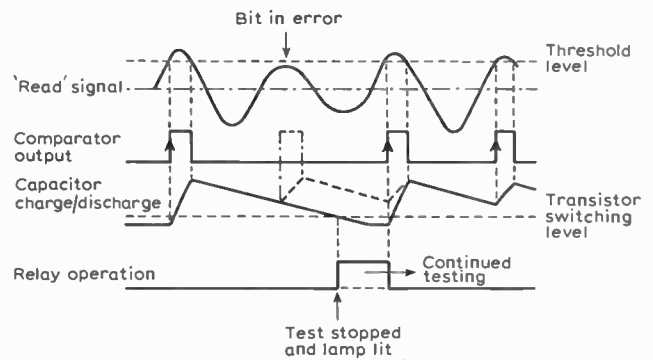


Fig. 2. Timing diagram of low amplitude detector—showing one bit in error.

4 Disk Pack Testing

Since it is known that the effects of variations in oxide thickness, head-to-disk separation and magnetic characteristics, which cause timing distortions, also cause amplitude variations, testing of disk packs using an amplitude based method is generally used. This Section describes the amplitude method currently used and compares it with a method based on time detection in order to test their significance in system terms.

4.1 Amplitude Testing

The amplitude method of detecting disk pack defects is based on the detection of amplitude variations from a pre-determined reference level. If the amplitude exceeds a certain limit or falls below a certain limit, then the point at which this occurs is called an error.

Figure 1 shows a basic low amplitude detection circuit. A disk pack written with a symmetrical waveform is read by the recording head and the signal amplified by the pre-amplifier. The 'read' signal is presented to the comparator. When the 'read' signal equals the threshold level, the comparator switches and gives an output, the capacitor C is charged by this output, and, as long as it is charged, the transistor remains switched off. While the 'read' signal is below the threshold level, no output is present at the comparator. If the output is missing for a period such that the capacitor can discharge, then the transistor switches and the relay is operated. The relay contacts operate a lamp and stop the testing so that the error can be seen. The time-constant of the charging capacitor network is set such that the circuit can detect if one bit is in error. A timing diagram showing a bit in error is given in Fig. 2.

The method used to detect changes in amplitude is based upon storing the average amplitude obtained from the magnetic disk surface on a particular track, and then comparing this with each pulse of signal. If the individual pulses are above or below a certain limit, with respect to the average amplitude, then this is called an error. Considering the diagram of the basic amplitude detection circuit, the threshold level adjustment would now be replaced by a memory device, rather like an integrator, which would store the average amplitude level. The limits could be set from this by having a further potentiometer arrangement. The circuit would then function in the same way, but an extra operation would be neces-

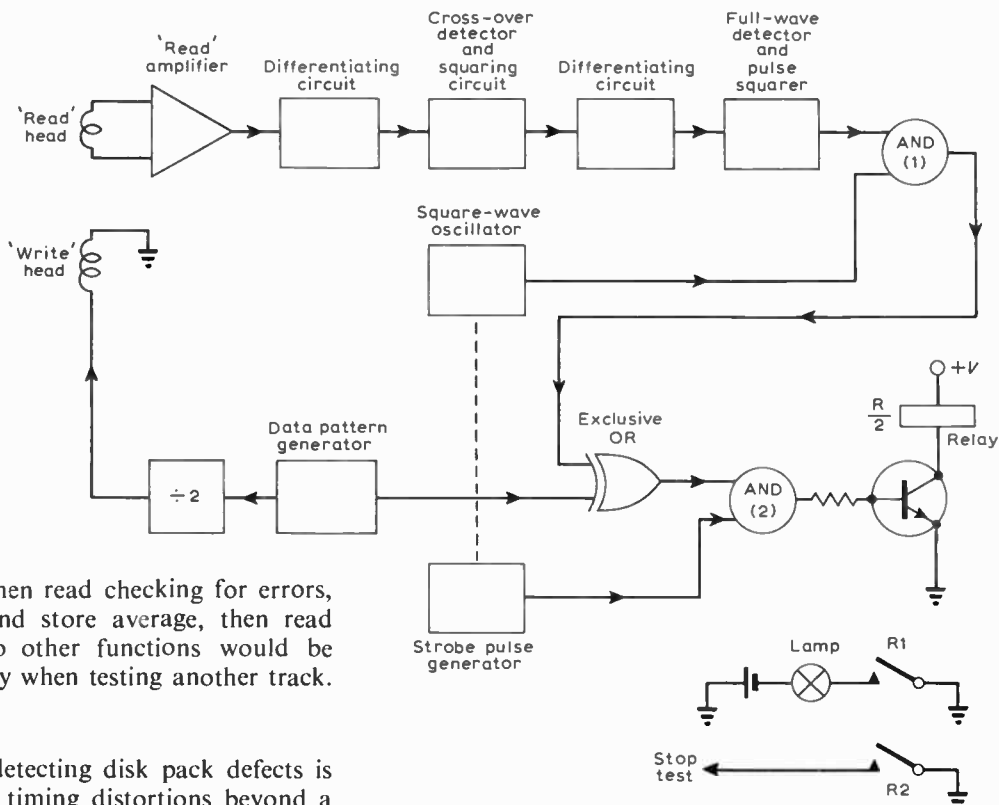


Fig. 3. Basic time detection circuit.

sary, i.e. instead of write then read checking for errors, it would be write, read and store average, then read checking for errors. Also other functions would be needed to clear the memory when testing another track.

4.2 Timing Testing

The timing method of detecting disk pack defects is based on the detection of timing distortions beyond a pre-determined distortion limit. If the pulses read from a disk pack are distorted such that they occur late or early in time and exceed the distortion limits, then the

place at which these occur is called an error. Figure 3 shows the basic error detection circuitry. Under normal operation the disk pack is written with an asymmetrical waveform from the data pattern generator and the read signals are then compared with the written data pattern.

The 'read' waveform is normally decoded by first differentiating then by squaring the signal. This process gives cross-over detection with the pulses occurring at the peaks of the original 'read' waveform. In order to reproduce the original double frequency data pattern, this signal is further differentiated, full-wave detected and squared giving a decoded 'read' signal.

In testing the surface of a disk pack, the decoded 'read' signal is compared logically with the original written data pattern such that differences between the two patterns give a pulse output. These outputs will be caused either by extra pulses or missing pulses in the 'read' waveform. Due to timing difficulties in the logic it is customary to strobe such outputs using a very narrow strobe pulse which occurs nominally in the centre of each expected decoded 'read' pulse.

It is clear that a timing distortion with a magnitude of up to half of the decoded 'read' signal pulse width will be successfully strobed. In order to test disk packs for timing distortion, the positive period of the square wave oscillator is reduced to a narrower 'window'. In order that the decoded 'read' pulse occurs during the window, the overall timing distortion must be less than half the difference between the respective pulse widths. A timing diagram showing one bit in error is shown in Fig. 4.

To enable easier design of the logic circuits, two separate 'windows' are generated from the squarewave oscillator output, such that each alternate decoded

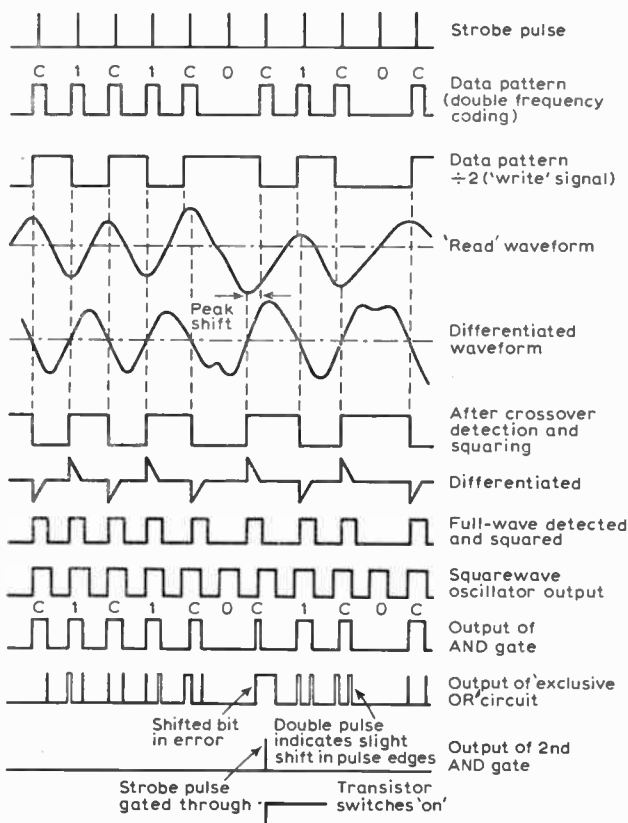


Fig. 4. Timing diagram of timing distortion detector—showing one bit in error.

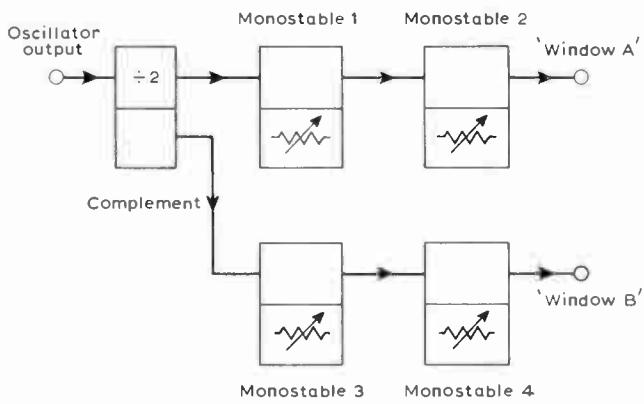


Fig. 5. Timing window generation.

'read' pulse can be tested independently. Figure 5 shows how the two windows are formed and how they can be adjusted for various window widths. Figure 6 shows the timing diagram of the window generator.

5 Correlation of Both Methods to System Performance

In order to relate the relevance of both methods to system performance a number of disk packs were tested by both amplitude and timing detection methods and also on a computer system.

Twenty disk packs were measured whose surfaces had the following basic parameters:

- Coating material gamma ferric oxide having the following properties:
- Coercive force 22000 to 26000 A/m (275–325 Oe)
- Retentivity 0.175 to 0.210 Wb/m² (1750–2100 G)
- Coating thickness between 2 μm to 3 μm (80 to 120 μin) at the 11.5 cm (4.5 in) radius track location, increasing proportionately to between 3 μm to 4 μm (120 to 160 μin) at the 16.5 cm (6.5 in) radius track location.

Number of surfaces 20 per disk pack.

The magnetic recording heads used in all the measurements were capable of reaching a bit packing density of 86.6 bit/mm (2200 bit/in) and a track packing density of 3.95 tracks/mm (100 tracks/in).

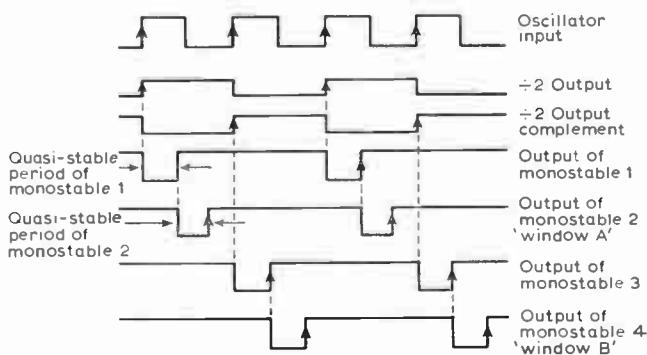


Fig. 6 Timing diagram of timing window generation.

The mechanical requirements of the disk packs and disk surfaces were such that 20 heads could be 'flown' on each disk pack. Each head, when in operation on its disk surface, was at a nominal flying height of approximately 2 μm (80 μin). All measurements were made under controlled environmental conditions.

The following basic test conditions were common to all methods of testing:

Number of tracks tested per surface	0 to 202 (203)
Number of surfaces tested per disk pack	0 to 19 (20)
Speed of machine	2400 rev/min
Packing density range	58–86.6 bit/mm (1500–2200 bit/in)
Head track width	0.178 mm (0.007 in)
Track spacing	0.254 mm (0.010 in)
Method of recording	double frequency

5.1 Amplitude Testing

Considering the basic system examined in Section 4, the disk packs were tested for two main types of error. The recording frequency used was kept constant at 2.5 × 10⁶ flux reversals per second. The types of errors tested were as follows:

Missing pulse error—any single bit or train of bits up to 500 μs in length, whose amplitude is less than 60% of the average base-to-peak amplitude, measured at the highest amplitude 50 μs sector of that track location.

Peak modulation error—any average base-to-peak amplitude measured at the highest amplitude 50 μs sector

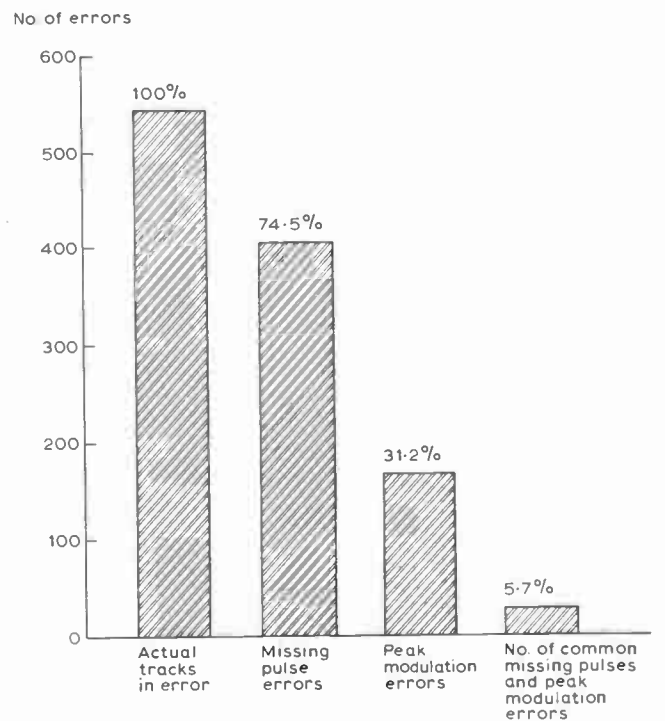


Fig. 7. Amplitude testing error analysis.

of that track location, that is greater than 146% of the average base-to-peak amplitude of the track.

An analysis of the results is illustrated in Fig. 7.

5.2 Timing Testing

Considering the system described in Section 4.2, the disk packs were tested for two main types of error. Using double frequency coding, the two frequencies were 2.5×10^6 flux reversals per second and 5.0×10^6 flux reversals per second. The data pattern used was repeated 1250 times on each track location. The 48 bits were arranged for a 'worst case' data pattern as follows:

0101 0010 0110 1100 0100 0111 0111 0011 1011 1101
0000 1001

The 'timing window' lengths were set to 45% of the cell time and then repeated with the 'timing window' lengths set to 25% of the cell time, the cell time being defined as that period of the waveform when an all '0's pattern is generated.

Two types of error can occur—a 'missing' data bit or an 'extra' or spurious bit—these were classified as follows:

Permanent or 'hard' error—an error which is detected during both the 'large' and 'small' timing window lengths.

Timing or 'soft' error—an error being detected in the 'small' window while the data are correct in the 'large' window.

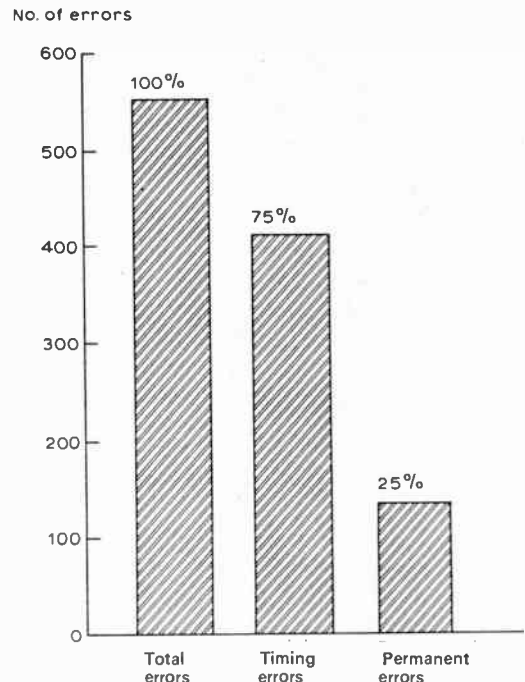


Fig. 8. Timing testing error analysis.

An analysis of the total number of errors found on the packs is shown in Fig. 8. The permanent errors are shown as a percentage of permanent errors plus timing errors. A comparison of amplitude tested errors and timing errors is illustrated in Fig. 9. From the results, approximately 16% of the amplitude errors were con-

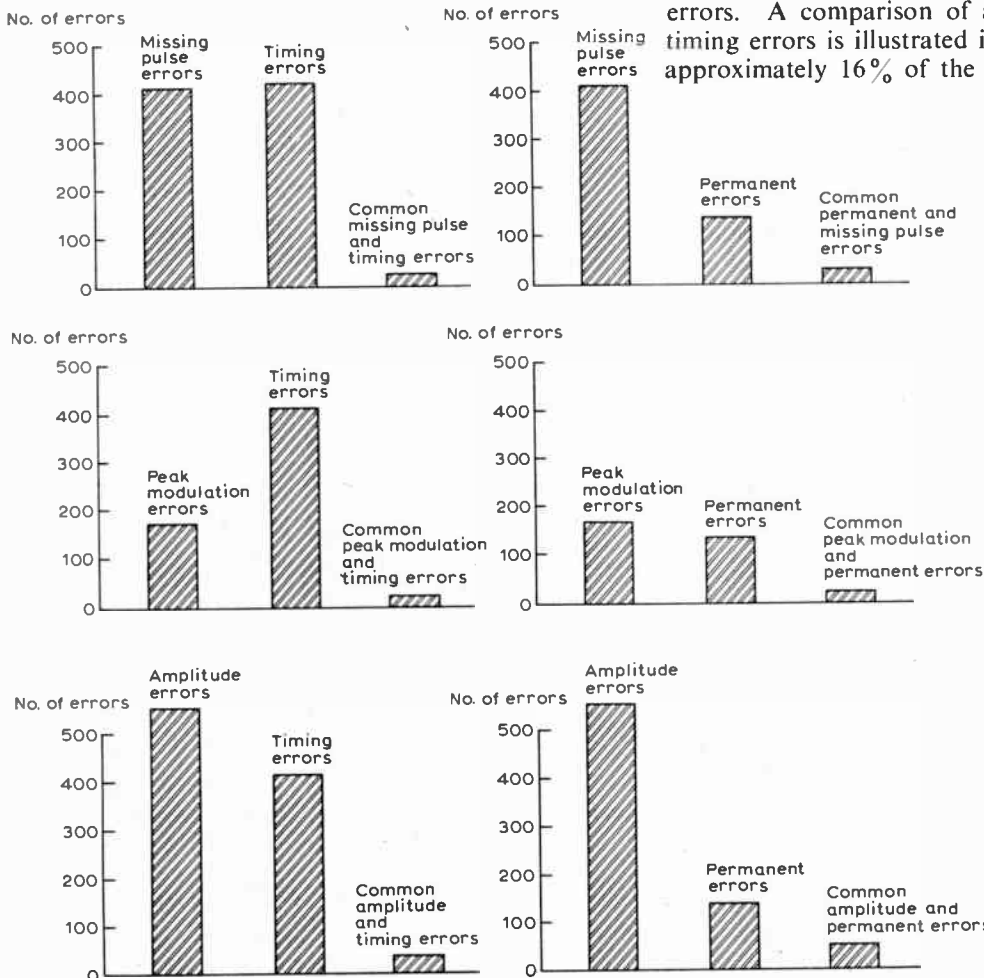


Fig. 9. Comparison of amplitude and timing tested errors.

firmed as timing tested errors; 9% of amplitude errors were found as 'permanent' errors (this represents 32.2% of all 'permanent' errors found). This shows a low correlation between the amplitude-tested errors and the timing-tested errors.

5.3 System Testing

The digital computer system used had a phase locked method of decoding. The coding used was double frequency modulation and the two frequencies were 2.5×10^6 flux reversals per second and 5.0×10^6 flux reversals per second. Crossover detection was used in the magnetic disk drive. A program was used by the system that was able to check for data errors on the type of pack tested.

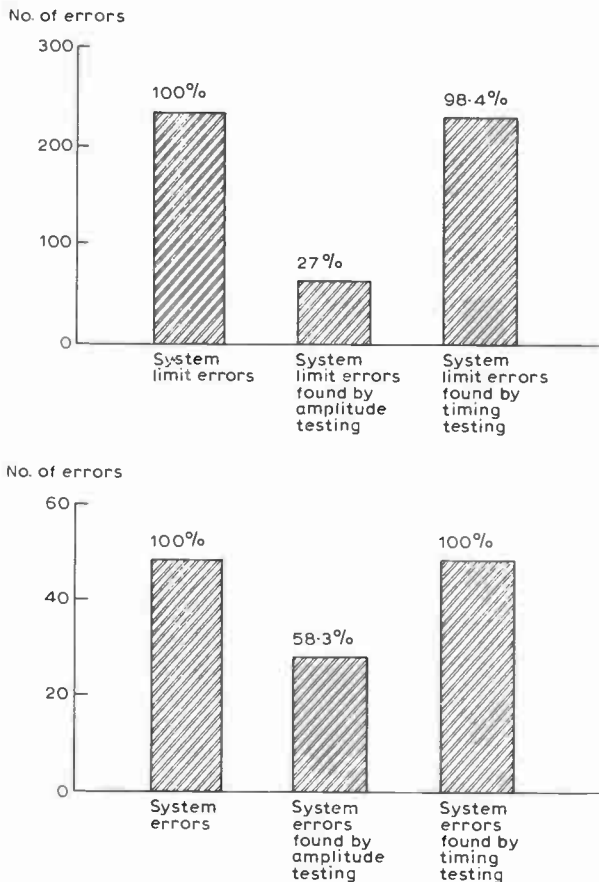


Fig. 10. Comparison of system, amplitude and timing errors.

The disk packs were first tested on the system with all the equipment calibrated correctly. They were then retested with the decoding circuitry recalibrated so that a 'worst case' system could be simulated. The results thus showed system errors and system 'limit' errors. The number of system 'limit' errors found by the amplitude and timing testing methods were compared. This is illustrated in Fig. 10.

Analysis of the results shows that 100% of the system errors were found by timing testing, compared with 58.3% found by amplitude testing; 98.4% of the system 'limit' errors were found by timing testing compared with 27% found by amplitude testing; 88.2% of the errors found by amplitude testing were not found as system errors or system 'limit' errors.

6 Conclusions

The results given in the paper indicate good correlation between the timing method of detection and system performance, while correlation with the amplitude method was relatively poor.

The amplitude method of testing could be supplemented by testing the disk packs on a computer system, but this has the disadvantage of adding an extra stage to the testing process.

The advantages of using the timing testing method can, therefore, be summarized as follows:

- (i) Final testing can be confined to a one-stage process, since there is a high success in finding system errors.
- (ii) Greater reliability in test results is obtained.
- (iii) When testing for system errors, no correlation of test limits is required, since true functional characteristic measurement of the disk packs is achieved.
- (iv) An increased yield of good surfaces will be produced, since a reduced number of disk pack errors will be classed incorrectly.

The conclusion of this paper is that a new method of disk pack testing based on time detection would provide significant benefit in both cost savings and reliability in test results.

7 References

1. Hoagland, A. S., 'Digital Magnetic Recording' (Wiley, New York, 1963).
2. Bonyhard, P. I., Davies, A. V. and Middleton, B. K., 'A theory of digital magnetic recording on metallic films', *IEEE Trans. on Magnetics*, MAG-2, pp. 1-5, 1966.
3. Middleton, B. K., 'The dependence of recording characteristics of thin metal tapes on their magnetic properties and on the replay head', *IEEE Trans.*, MAG-2, pp. 225-9, 1966.
4. Dudson, M. F., and Davies, A. V., 'Magnetic recording for computers', *Proc. IEE Reviews*, 119, pp. 956-84, 1972.
5. Cullum, C. D., 'Encoding and signal processing advances in magnetic recording', *Annals New York Acad. Sci.*, 189, pp. 52-62, 1972.

Manuscript first received by the Institution on 16th February 1973 and in final form on 18th December 1973 (Paper No. 1570/CC 188)

The theory of inherent noise in p-n junction diodes and bipolar transistors

M. J. BUCKINGHAM, Ph.D.,*

and

Professor E. A. FAULKNER,

Ph.D., C.Eng., F.I.E.E., F.I.E.R.E.*

SUMMARY

A new calculation is made of the noise (excluding excess noise) in p-n junction diodes and bipolar transistors. The theory is based on an analysis of the current waveforms caused by thermal motion of individual carriers and by individual recombination events in a one-dimensional model; unlike that of van der Ziel (1955) it does not rely on arbitrary assumptions about thermal fluctuations in carrier concentration and does not involve a transmission-line analogy. When depletion-layer recombination effects are neglected, the results are found to be identical to those obtained by van der Ziel, although one of his postulates was invalid. The theory of van der Ziel and Becking (1958) which also leads to the same results does not appear to be consistent with the new treatment.

* J. J. Thomson Physical Laboratory, University of Reading, Whiteknights, Reading RG6 2AL.

List of Principal Symbols

q	magnitude of electronic charge
k	Boltzmann's constant
ϵ_0	permittivity of free space
ϵ_r	dielectric constant
θ	absolute temperature
I_S	reverse saturation current in ideal diode
I_D	terminal current in ideal diode
G_J	conductance of ideal diode
G_E	conductance of ideal emitter-base junction
G_0	low-frequency value of G_J
G_{E0}	low-frequency value of G_E
B_J	susceptance of ideal diode
B_E	susceptance of ideal emitter-base junction
$Y_J \equiv G_J + jB_J$	admittance of ideal diode
$Y_E \equiv G_E + jB_E$	admittance of ideal emitter-base junction
τ_R	minority carrier lifetime in bulk region
D	diffusion constant
p	hole concentration in N-region
p_n	equilibrium hole concentration in N-region
$p' = p - p_n$	excess hole concentration in N-region
μ	mobility
$L_0 = (D\tau_R)^{\frac{1}{2}}$	low-frequency diffusion length
W	width of N-region
x'	location of an event in N-region
T	time interval over which averaging is performed
A	cross-sectional area of junction
l_x	length of carrier path in x direction
τ_f	mean-free time in bulk material
ν	mean number of events per second
N	number of carriers per unit volume
$\tau_J = W^2/2D$	
σ	bulk material conductivity
I_E	static current flowing in emitter lead of transistor
I_C	static current flowing in collector lead of transistor
I_B	static current flowing in base lead of transistor
I_{BR}	depletion-layer recombination component of static base current
α	ratio of alternating collector to emitter currents in actual transistor
α_0	low-frequency value of α
α_s	ratio of alternating collector to emitter currents in ideal transistor
α_{0s}	low-frequency value of α_s
$h_{fe} = dI_C/dI_B$	current gain of actual transistor
h_{fe0}	low-frequency value of h_{fe}
$\beta_0 = I_C/I_B$	ratio of static collector current to static base current

1 Introduction

The current-voltage characteristic exhibited by an 'ideal' p-n junction diode—by which we mean a junction in which depletion-layer recombination and surface effects are negligible—may be understood on the basis of the Shockley theory¹ of minority carrier injection into the bulk regions. The static characteristic relating the terminal current I_D to the applied voltage V for such a junction at absolute temperature θ , is

$$I_D = I_S [\exp (qV/k\theta) - 1] \tag{1}$$

where I_S is the reverse saturation current.

Equation (1) does not correctly describe the current-voltage characteristics of the silicon diodes which are commonly used nowadays, because in such devices the static terminal current arises almost entirely from depletion-layer recombination.² However, the study of noise processes in the ideal diode is of fundamental importance to an understanding of the noise properties of bipolar transistors.

It is generally accepted that the noise in an ideal diode can be represented by a current generator $i_{ND}(t)$ with a spectral density given by the relation

$$\frac{\delta \overline{i_{ND}^2(t)}}{\delta f} = 2q(I_D + 2I_S) + 4k\theta(G_J - G_0) \tag{2}$$

where G_J is the conductance of the junction and G_0 is the low-frequency value of G_J . This formula has certain essential properties: it gives the usual shot noise expressions $2qI_D$ and $2qI_S$ for low frequencies under strong forward and reverse bias conditions respectively, whilst reducing at zero applied voltage ($I_D = 0$) to the value $4k\theta G_J$ predicted by Nyquist's theorem for any passive component.

There are several explanations given in the literature to account for equation (2), at least in the low-frequency region where the second term on the right-hand side is zero. It is often stated, incorrectly, that the current crossing the depletion layer consists of a current $I_S \exp (qV/k\theta)$ resulting from injection and a voltage independent current I_S flowing in the opposite direction resulting from minority carrier generation; this argument, used in conjunction with the assumption that each of these currents is associated with a shot noise generator with spectral density $2qI$, gives the first term on the right-hand side of (2). A study of the Shockley theory¹, however, shows that the currents I_F and I_R which flow in each direction across the depletion layer of a forward-biased ideal p-n junction diode, and which are responsible for maintaining the enhanced minority-carrier concentration at the edge of the depletion layer, are enormously greater than the diffusion current I_D . Correspondingly, the values of I_F and I_R for zero bias are very much greater than the reverse saturation current; I_S is in fact a function of the width of the bulk region and also of the carrier lifetime τ_R in that region, and these parameters do not have an effect on the equilibrium current flow across the junction.

By far the most important paper on transistor noise was published by van der Ziel³ in 1955. Using the standard Shockley theory¹ of the junction he takes a one-dimensional model in which the current consists entirely

of holes, and makes a calculation of the total noise current by integrating the contributions to each volume element of the semiconductor material in the vicinity of the junction. The calculation is stated to be based on the following two assumptions: (a) the recombination current ΔI in each element of length Δx shows 'shot noise' $i_x(t)$ with a mean-square value given in the frequency range δf by the Schottky formula

$$\delta \Delta \overline{i_x^2(t)} = 2q \Delta I \delta f. \tag{3}$$

(b) The carrier concentration p in each element of length Δx and unit area shows thermal fluctuations $p(t)$ with mean-square value in the frequency range δf given by the relation

$$\delta \Delta \overline{p^2(t)} = \frac{4p \Delta x}{D_p} \delta f \tag{4}$$

where D_p is the diffusion constant for holes in the bulk N-region.

An objection that could be made to equation (4) is that it does not appear to be physically realistic because it does not contain any boundary conditions. In reference 3 it was presented as a hypothesis which was said to be indirectly confirmed by the fact that the calculated spectral density of the terminal noise current showed the correct form. Subsequently⁴ a proof was offered based on a somewhat ill-defined transmission line analogy, and it was also stated⁵ to have been proved by Petritz.⁶

The method by which van der Ziel³ calculates the junction noise current from (3) and (4) is somewhat confusing because it involves an analogy between the minority carrier distribution in the bulk semiconductor and the voltage distribution in a distributed R-C transmission line. A close examination of his calculation reveals that equation (4) has been inserted into the electrical analogue as a voltage generator and not as a voltage; we conclude that equation (4) is incorrect and must be replaced by a formulation which will be discussed later.

In this paper we shall present a theory of junction noise which is based on accepted physical principles and which confirms the results of van der Ziel.³ The theory offers no support for the so-called 'corpuscular approach' of van der Ziel and Becking.⁷

2 Current-Voltage Relationships

In considering the ideal diode there is no loss of generality involved if we assume that the current flow is due entirely to the injection of holes into the N-region of length W . We find by solving the diffusion equation for a one-dimensional situation that the static terminal current is

$$I_D = \frac{qAD_p p'_0}{L_0} \frac{\cosh (W/L_0)}{\sinh (W/L_0)} \tag{5}$$

where D_p is the diffusion constant for a hole in the N-region, L_0 is the diffusion length and p'_0 is the excess minority carrier concentration at the boundary plane, $x = 0$, between the depletion layer and the N-type bulk region. The reverse saturation current is

$$I_S = \frac{qAD_p p_n}{L_0} \frac{\cosh (W/L_0)}{\sinh (W/L_0)} \tag{6}$$

where p_n is the equilibrium hole concentration in the N-region.

From the solution of the time-dependent diffusion equation we find that the complex quantity Y_J representing the admittance of an ideal one-dimensional diode, is

$$Y_J \equiv G_J + jB_J = G_0 \tanh\left(\frac{W}{L_0}\right) \cdot \frac{(1 + j\omega\tau_R)^{\frac{1}{2}}}{\tanh\left[\left(1 + j\omega\tau_R\right)^{\frac{1}{2}} \frac{W}{L_0}\right]} \quad (7)$$

where τ_R is the minority carrier lifetime, and the low-frequency conductance, G_0 , is the derivative of the static characteristic in equation (1), given by

$$G_0 = \frac{q}{k\theta} (I_D + I_S) = \frac{q^2 D_p}{k\theta L_0} \cdot (p'_0 + p_n) \cdot \frac{\cosh(W/L_0)}{\sinh(W/L_0)} \quad (8)$$

It is not difficult to show that

$$G_J = G_0 \tanh\left(\frac{W}{L_0}\right) \times \frac{\left[a \sinh\left(\frac{2aW}{L_0}\right) + b \sin\left(\frac{2bW}{L_0}\right) \right]}{\left[\cosh\left(\frac{2aW}{L_0}\right) - \cos\left(\frac{2bW}{L_0}\right) \right]} \quad (9a)$$

and

$$B_J = G_0 \tanh\left(\frac{W}{L_0}\right) \times \frac{\left[b \sinh\left(\frac{2aW}{L_0}\right) - a \sin\left(\frac{2bW}{L_0}\right) \right]}{\left[\cosh\left(\frac{2aW}{L_0}\right) - \cos\left(\frac{2bW}{L_0}\right) \right]} \quad (9b)$$

where a and b are parameters defined by the relation

$$(a + jb) = (1 + j\omega\tau_R)^{\frac{1}{2}} \quad (10)$$

In the ideal one-dimensional bipolar transistor the solution of the static diffusion equation leads to expressions of similar form to (5) for the terminal currents. Assuming a base width W , and that the collector-base junction is short-circuited, we find that for a p-n-p device

$$I_E = \frac{qAD_p p'_0}{L_0} \cdot \frac{\cosh(W/L_0)}{\sinh(W/L_0)} \quad (11)$$

and

$$I_C = \frac{qAD_p p'_0}{L_0} \cdot \frac{1}{\sinh(W/L_0)} \quad (12)$$

where I_E and I_C are the emitter and collector currents and the other symbols have the same meanings as in equation (5). For an actual transistor the expression describing the emitter current contains a term in addition to that given in (11), arising from recombination in the emitter-base depletion layer.

We introduce the complex admittance $Y_E \equiv G_E + jB_E$ now to relate the current flowing in the emitter lead to the signal voltage applied across the emitter-base junction. We find by solving the time-dependent diffusion equation that in the absence of depletion-layer recombination the low-frequency conductance G_{E0} is identical to G_0 given in equation (8) and the conductance G_E and

susceptance B_E are given by equations (9a) and (9b) respectively. The complex parameter α_s , also obtained from the solution of the time-dependent diffusion equation, relates the alternating current flowing in the collector and emitter leads:

$$\alpha_s = 1/\cosh[(a + jb)W/L_0] \quad (13a)$$

which for low frequencies reduces to

$$\alpha_{0s} = 1/\cosh(W/L_0) \quad (13b)$$

The subscript s appearing in equations (13a) and (13b) indicates that the parameters relate to the 'ideal' situation as described by Shockley.¹

We shall find it convenient when discussing noise in transistors to express the admittance, Y_E , and the product $\alpha_s Y_E$ as power series in frequency. We find that, to second order in frequency

$$Y_E = G_{E0} \tanh\left(\frac{W}{L_0}\right) \cdot \frac{(1 + j\omega\tau_R)^{\frac{1}{2}}}{\tanh\left[\left(1 + j\omega\tau_R\right)^{\frac{1}{2}} \frac{W}{L_0}\right]} \quad (14a)$$

$$\simeq G_{E0} \left[1 + \frac{2j\omega\tau_J}{3} + \frac{4}{45} \omega^2 \tau_J^2 \right] \quad (14b)$$

and

$$\alpha_s Y_E = G_{E0} \tanh\left(\frac{W}{L_0}\right) \cdot \frac{(1 + j\omega\tau_R)^{\frac{1}{2}}}{\sinh\left[\left(1 + j\omega\tau_R\right)^{\frac{1}{2}} \frac{W}{L_0}\right]} \quad (15a)$$

$$\simeq \alpha_{0s} G_{E0} \left[1 - \frac{j\omega\tau_J}{3} - \frac{7}{90} \omega^2 \tau_J^2 \right] \quad (15b)$$

where $\tau_J = W^2/2D_p$, and we have used the fact that in an actual transistor, $W/L_0 \ll 1$. The series in (14b) and (15b) are convergent for $\omega < 2\pi^2/\tau_J$.

3 Mean-Square Values and Complex Correlation Coefficient

The purpose of this analysis is to develop equivalent circuits which will enable the signal/noise ratio to be calculated in practical engineering applications. The equivalent circuits will contain voltage and current noise generators, $v_N(t)$ and $i_N(t)$ respectively, which are specified by their spectral densities, and complex coefficients are introduced to represent the causal connexion between one generator and another.

The spectral density of a generator $x(t)$ is defined over the time interval T as the quantity

$$\frac{\overline{\delta x^2(t)}}{\delta f} = \frac{2}{T} \cdot \overline{X(j\omega)X^*(j\omega)} \quad (16)$$

where $\overline{\delta x^2(t)}$ is the mean-square value of the Fourier components of $x(t)$ belonging to the frequency range δf centred at the frequency f , $X(j\omega)$ is the Fourier transform of the function $x(t)$ over the time interval T , and the averaging of $X(j\omega)X^*(j\omega)$ is carried out over a frequency interval much greater than $1/T$. The asterisk denotes complex conjugate. We may also define the 'cross spectrum' between two generators $x_1(t)$ and $x_2(t)$ by the relation

$$\frac{\overline{\delta x_1(t)x_2(t)}}{\delta f} = \frac{2}{T} \cdot \text{Re} \overline{X_1(j\omega)X_2^*(j\omega)} \quad (17)$$

where $X_1(j\omega)$ and $X_2(j\omega)$ are the Fourier transforms of $x_1(t)$ and $x_2(t)$ over the time interval T , and the averaging, again, is carried out over a frequency interval much greater than $1/T$.

Averages like that in (17) frequently appear in the discussion of noise in bipolar transistors, and van der Ziel in a paper published in 1958⁵ treats them in terms of a correlation impedance. Here we choose to describe such averages by means of a complex coefficient, Γ_{12} , which differs in general from the real correlation coefficient, γ_{12} , used to describe the correlation between two fluctuating quantities. γ_{12} is in fact the real part of Γ_{12} .

The complex correlation coefficient Γ_{12} between $x_1(t)$ and $x_2(t)$ is defined over the time interval T by the relation

$$\Gamma_{12} = \frac{\overline{X_1(j\omega) X_2^*(j\omega)}}{[\overline{X_1(j\omega) X_1^*(j\omega)} \overline{X_2(j\omega) X_2^*(j\omega)}]^{1/2}} \quad (18)$$

and Γ_{12} is related to the familiar real correlation coefficient γ_{12} by the equation

$$\text{Re } \Gamma_{12} = \gamma_{12} = \frac{\overline{\delta x_1(t) x_2(t)}}{[\overline{\delta x_1^2(t)} \overline{\delta x_2^2(t)}]^{1/2}} \quad (19)$$

Correspondingly, the formula for the mean-square value of the sum of $x_1(t)$ and $x_2(t)$ in the frequency range δf is

$$\delta \overline{[x_1(t) + x_2(t)]^2} = \delta \overline{x_1^2(t)} + \delta \overline{x_2^2(t)} + 2 \text{Re } \Gamma_{12} \cdot [\overline{\delta x_1^2(t)} \overline{\delta x_2^2(t)}]^{1/2} \quad (20)$$

The importance of the complex correlation coefficient to the engineer is that it expresses the existence of any causal connexion between two generators which may enable the resultant noise to be optimized by suitable circuit design. If there is a complete causal connexion between $x_1(t)$ and $x_2(t)$ we are able to relate the Fourier transforms of $x_1(t)$ and $x_2(t)$ by means of some constant system function $A(j\omega)$:

$$X_1(j\omega) = A(j\omega) X_2(j\omega) \quad (21)$$

in which case it is evident that

$$\Gamma_{12} = A(j\omega)/|A| \text{ and } |\Gamma_{12}| = 1. \quad (22)$$

In general, the magnitude of the complex correlation coefficient is a measure of the degree of causal connexion between two generators, irrespective of the value of the real coefficient γ_{12} . (In equation (21), if we put $A(j\omega) = 1/j\omega$, we obtain $\gamma_{12} = 0$.)

As a practical design example of the use of the complex correlation coefficient Γ_{12} , we may consider the amplifier circuit of Fig. 1(a) where the noise generators are represented in the usual way as input voltage and current generators.

In Fig. 1(b) the Norton equivalent circuit of 1(a) has been drawn for the purpose of calculating the signal/noise ratio. The total mean-square noise current in a frequency band δf centred on a frequency f is now calculated from the expression

$$\begin{aligned} \delta \overline{[i_{N1}(t) + i_{N2}(t)]^2} &= \delta \overline{i_{N1}^2(t)} + \delta \overline{i_{N2}^2(t)} + 2 \delta \overline{i_{N1}(t) i_{N2}(t)} \\ &= \delta \overline{i_{N1}^2(t)} + |Y_s|^2 \delta \overline{V_N^2(t)} + \\ &\quad + 2[\delta \overline{V_N^2(t)} \cdot \delta \overline{i_{N1}^2(t)}]^{1/2} \text{Re}(Y_s \Gamma_{vi}) \quad (23) \end{aligned}$$

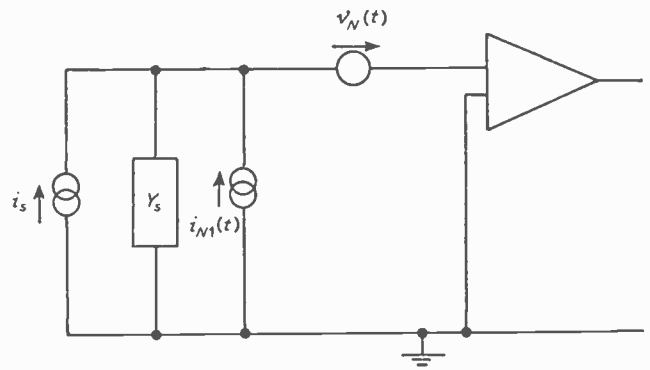
where because of the correlation term the optimum value of Y_s is seen to be, in general, quite different from that which would have been predicted on the assumption that the correlation between the equivalent noise voltage and current generators could be fully expressed by a real coefficient γ_{vi} . This formulation shows, for example, how the noise figure of a transistor can be improved by the use of an inductive source to 'tune out' the input capacitance.

4 The Method of Analysis, Application to Resistor Noise

The devices discussed in the following analysis are assumed to have perfect metal contacts connected together by wire of negligible impedance, which we call the *external circuit*. The noise is assumed to be due to a random succession of *events* each of which generates a time-varying current

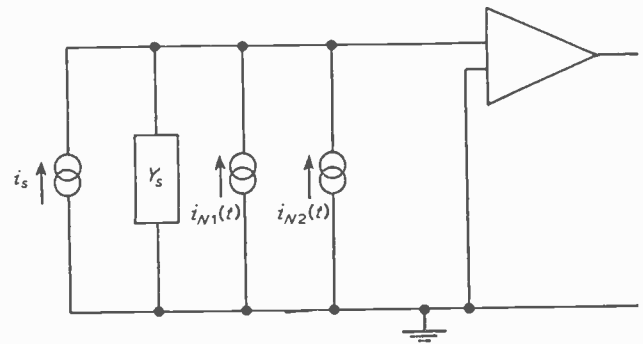
$$i_j = a_j f(t) \quad (24)$$

into the external circuit. (The analysis could, of course, be carried out in terms of open-circuit voltages rather than short-circuit currents; the latter approach is somewhat simpler.)



(a)

(a) Representation of the noise generators in an amplifier circuit. The signal source, i_s , has admittance Y_s and the complex correlation coefficient for the current and voltage generators is Γ_{vi} .



(b)

(b) Norton equivalent circuit of (a) in which the complex correlation coefficient for the noise current generators is $\Gamma_{12} = Y_s^* \Gamma_{vi} / |Y_s|^2$.

Fig. 1.

The spectral density of the noise is given by the relation⁸

$$\frac{\overline{\delta i_N^2(t)}}{\delta f} = 2\nu \overline{a_j^2} |F(j\omega)|^2 \quad (25)$$

where $F(j\omega)$ is the Fourier transform of $f(t)$, and ν is the mean number of events per second. It is implicit in equation (25) that the power in any given frequency range is averaged over a large number of events.

In calculating i_j for an event in bulk material or in a p-n junction, it is not possible to ignore carrier interactions. We take account of these interactions by considering each individual carrier as existing in a continuous medium which is characterized by such bulk parameters as electrical conductivity σ , diffusion constant D , and recombination time τ_R , each of these parameters being defined by the appropriate macroscopic flow equation. Each event is described in terms of an initial carrier action (i.e. creation, destruction, or motion) which is assumed to cause a departure from equilibrium. The initial action is followed by a relaxation process determined by the bulk parameters of the material, and this restores the equilibrium situation. The initial action, and/or the subsequent relaxation, may be accompanied by the generation of currents in the external circuit, and these currents are assumed to make up i_j of equation (24). Obviously this procedure does not give a correct picture of an individual event; but it gives the correct result for the spectral density when averaged over a large number of events.

In a two-carrier system the relaxation consists of two parts: the very rapid majority-carrier relaxation which restores charge equilibrium (i.e. removes potential differences) and the slower minority-carrier relaxation which restores the equilibrium distribution of the minority-carrier population. In the vicinity of a p-n junction the minority-carrier relaxation results in a current flow around the circuit, but in locations far from a junction the effect of the minority carrier is negligible.

In our treatment we use a one-dimensional model of the system in which events can be regarded as giving rise to 'sheets' of disturbed carrier concentration; this approach simplifies the calculations without sacrificing generality in any significant way.

As an example of the method, we now calculate the formula for thermal noise in bulk material. The material is assumed to have conductivity σ , diffusion constant D , mobility μ , mean-free time τ_f , and to contain N carriers of charge q per unit volume. These parameters refer to all carriers without distinction between minority and majority carriers, because in the bulk material far from a junction we are dealing essentially with a one-carrier system. The specimen is of length d and cross-sectional area A .

An event is initiated by a carrier path of length l_x in the x direction. In our one-dimensional model this generates two charge sheets, initially of surface charge density $\pm q/A$. A potential difference occurs between one side of the double charge sheet and the other, with instantaneous value v_{N0} given by

$$v_{N0} = q l_x / \epsilon_0 \epsilon_r A. \quad (26)$$

The charge now decays through the conductance g formed by the bulk material separating the two sheets and also through the conductance G of the whole specimen which is assumed short-circuited. The flow during the decay is represented by the equation

$$v_N(g+G) + \frac{\epsilon_0 \epsilon_r A}{l_x} \frac{dv_N}{dt} = 0 \quad (27)$$

for which the solution is

$$v_N(t) = v_{N0} \exp[-t(g+G)l_x/\epsilon_0 \epsilon_r A]. \quad (28)$$

Thus the total variation of voltage with time is given by

$$v_N(t) = \frac{q l_x}{\epsilon_0 \epsilon_r A} u(t) \exp[-t(g+G)l_x/\epsilon_0 \epsilon_r A] \quad (29)$$

where $u(t)$ is the unit step function.

Now the relaxation time $\tau_1 = \epsilon_0 \epsilon_r A / l_x(g+G)$ is extremely short by electronic standards, so we may approximate the voltage to a δ -function; observing that in equation (29)

$$\int v_N dt = q/(g+G)$$

we write

$$v_N(t) = q\delta(t)/(g+G). \quad (30)$$

Thus the current i_j flowing in the external circuit can be written as

$$\begin{aligned} i_j &= q\delta(t)G/(g+G) \\ &\approx q\delta(t)l_x/d \end{aligned} \quad (31)$$

the approximation of g for $(g+G)$ being very accurate because the specimen length d is assumed enormously greater than the free path length l_x . We now have from (25)

$$\frac{\overline{\delta i_N^2(t)}}{\delta f} = 2\nu q^2 \overline{l_x^2}/d^2 \quad (32)$$

where $\nu = NAd/\tau_F$ and the diffusion mobility μ is given by the relation†

$$\mu = q \overline{l_x^2} / 2\tau_F k\theta \quad (33)$$

whence

$$\frac{\overline{\delta i_N^2(t)}}{\delta f} = 4NA\mu q k\theta/d = 4Gk\theta. \quad (34)$$

This is the well-known formula for the thermal noise in a resistor, which we have derived without the use of transform methods (apart from using the fact that the transform of a δ -function is unity) in order to clarify the physical situation in this simple case.

In the transform approach, we begin by noticing that the 'initial condition' of equation (26) can be exactly represented by inserting a δ -function term in the flow equation (27), giving

$$(g+G)v_N(t) + \frac{\epsilon_0 \epsilon_r A}{l_x} \frac{dv_N(t)}{dt} = q\delta(t). \quad (35)$$

Replacing the functions of time by their transforms, we

† See, for example, Shockley, W., 'Electrons and Holes in Semiconductors', Chap. 8 (D. Van Nostrand, New York, 1963).

now obtain

$$(g + G)v_N(j\omega) + \frac{\epsilon_0 \epsilon_r A}{l_x} j\omega v_N(j\omega) = q$$

$$i_j(j\omega) = Gv_N(j\omega) = \frac{G}{(g + G)} \cdot \frac{q}{(1 + j\omega\tau_1)}$$

$$\approx \frac{l_x q}{d(1 + j\omega\tau_1)} \quad (36)$$

By using (25) and (33) we arrive at the following expression for the spectral density of the noise current:

$$\frac{\delta i_N^2(f)}{\delta f} = \frac{4Gk\theta}{1 + \omega^2\tau_1^2} \quad (37)$$

This expression reduces to the formula in (34) for values of angular frequency ω which are well below $1/\tau_1$.

5 Thermal Fluctuations in Minority Carrier Flow

If the carrier under discussion in the calculation of Section 4 had been a minority carrier, the majority-carrier relaxation that gives rise to equation (32) would have left a perturbation in the minority carrier concentration, and this would be restored by a second relaxation process. In bulk material far from a junction, the minority-carrier relaxation is not accompanied by any flow of charge around the circuit, since it is continuously compensated by majority carrier flow; however, for an event in the vicinity of a junction the minority flow comes partly from across the junction and in this case there is a resultant flow around the external circuit.

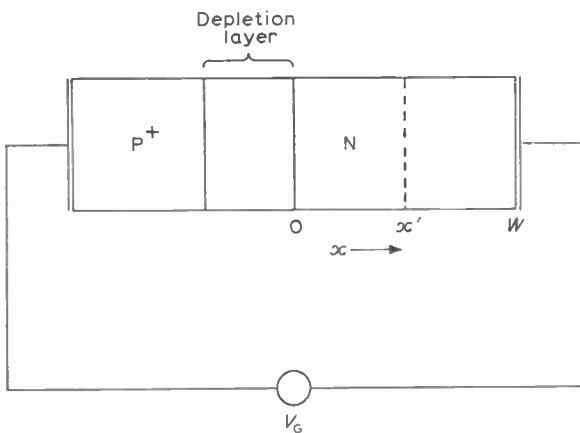


Fig. 2. One-dimensional model of a p⁺-n junction showing the bulk regions and the depletion layer (not to scale). The plane $x = x'$ is the location at which an event occurs.

In Fig. 2 we show a one-dimensional model of a p⁺-n junction. A forward bias is maintained by the voltage generator V_G in the external circuit, and we derive the current through the external circuit by calculating the minority carrier distribution p in the N-region and hence the concentration gradient $(dp/dx)_0$ at the $x = 0$ plane which is situated at the edge of the depletion layer.¹ Strictly speaking, the same procedure should be applied to the free electron distribution in the P-region to give an additional contribution to the total current, but this

would introduce unnecessary duplication in the calculation and for the purposes of this discussion we may ignore the second contribution—or, equivalently, assume that we are dealing with a p⁺-n junction in which it is negligibly small.

The applied voltage V_G maintains a minority carrier concentration

$$p_0 = p_n \exp(qV/k\theta) \quad (38)$$

at the $x = 0$ plane, and a metal contact, or a second p-n junction maintains a concentration p_w at the $x = W$ plane.

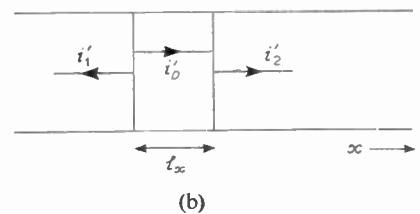
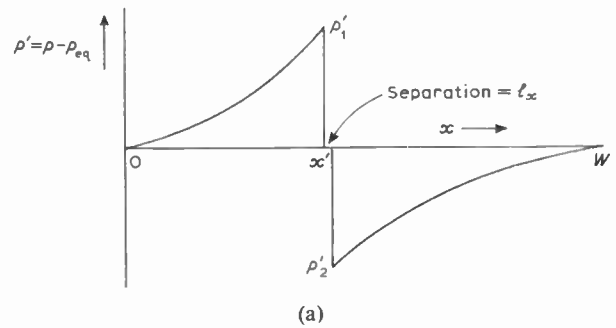


Fig. 3. (a) Departure from the equilibrium minority carrier concentration due to an event consisting of a minority carrier path of length l_x at the x' plane and (b) the corresponding carrier flows.

We now consider the effect of an event consisting of a minority carrier path of length l_x at the x' plane. The considerations of majority-carrier relaxation given in Section 4 show that this makes a contribution given by equation (27) to the noise voltage in the circuit; this is part of the thermal noise in the bulk resistance, which we shall assume to be negligible in comparison with the junction incremental impedance. The effect of the event on the minority carrier concentration is illustrated in Fig. 3, where p' represents the departure from the equilibrium carrier concentration.

The carrier path is equivalent to a current flow which can be represented by the function $q\delta(t)$, between two planes separated by a distance l_x . The resulting values of p' at these two planes are p'_1 and p'_2 respectively.

As in the case of the majority-carrier relaxation, the minority-carrier relaxation occurs mainly by direct return flows i'_{D1} and i'_{D2} from each plane towards the other. These flows are found by solving the time-dependent diffusion equation¹ for the region between the two planes

and are given in transform terminology by the relations

$$i'_{D1}(j\omega) = \frac{qDA}{L} \frac{[p'_1(j\omega) \cosh(l_x/L) - p'_2(j\omega)]}{\sinh(l_x/L)} \quad (39a)$$

$$i'_{D2}(j\omega) = \frac{qDA}{L} \frac{[p'_1(j\omega) - p'_2(j\omega) \cosh(l_x/L)]}{\sinh(l_x/L)} \quad (39b)$$

where

$$L = \sqrt{D\tau_R/(1+j\omega\tau_R)}. \quad (40)$$

It is clear from these equations that i'_{D1} and i'_{D2} are not necessarily equal, the difference being represented by recombination and by changes in the carrier store. However, in this context the difference is negligible because l_x is very much smaller than $\sqrt{(D\tau_R)}$ or any of the other linear dimensions involved in the problem; hence throughout the frequency range of interest we may write $l_x/L \ll 1$ and we find

$$i'_{D1}(j\omega) = i'_{D2}(j\omega) = i'_D(j\omega) = \frac{qDA}{l_x} [p'_1(j\omega) - p'_2(j\omega)]. \quad (41)$$

There are further carrier flows i'_1 and i'_2 outwards towards the $x = 0$ and $x = W$ planes respectively, and these are given in transform terminology by

$$i'_1(j\omega) = Ak_1(j\omega)p'_1(j\omega) \quad (42a)$$

$$i'_2(j\omega) = Ak_2(j\omega)p'_2(j\omega) \quad (42b)$$

where

$$k_1 = \frac{qD}{L} \coth(x'/L) \quad (43a)$$

$$k_2 = \frac{qD}{L} \coth[(W-x')/L]. \quad (43b)$$

From considerations of current continuity we now write

$$i'_1(t) - i'_D(t) + q\delta(t) = i'_2(t) + i'_D(t) - q\delta(t) = 0$$

$$i'_1(j\omega) - i'_D(j\omega) + q = i'_2(j\omega) + i'_D(j\omega) - q = 0 \quad (44)$$

giving, in conjunction with equations (41) and (42), and the condition $k_1, k_2 \ll qD/l_x$, the result

$$i'_1(j\omega) = -i'_2(j\omega) = \frac{l_x k_1 k_2}{D[k_1 + k_2]}. \quad (45)$$

Equation (45) shows that the thermal motion causes primarily a current flow *through* the material, rather than a fluctuation in carrier concentration as was supposed by van der Ziel.³ The contribution to this power spectrum by an element of length Δx at the plane $x = x'$ is, from equation (25),

$$\Delta \left(\frac{\delta i'^2_{N1}(t)}{\delta f} \right) = \Delta \left(\frac{\delta i'^2_{N2}(t)}{\delta f} \right) = \frac{2pAl_x^2}{\tau_F D^2} \left| \frac{k_1 k_2}{k_1 + k_2} \right|^2 \Delta x. \quad (46)$$

By the use of Einstein's relation in conjunction with (33) we find

$$D = \bar{l}_x^2 / 2\tau_F$$

whence

$$\Delta \left(\frac{\delta i'^2_{N1}(t)}{\delta f} \right) = \Delta \left(\frac{\delta i'^2_{N2}(t)}{\delta f} \right) = \frac{4pA}{D} \left| \frac{k_1 k_2}{k_1 + k_2} \right|^2 \Delta x. \quad (47)$$

This is the formulation we shall use to replace equation (4) postulated by van der Ziel.³

It follows from equations (42) and (45) that if the time-varying parts of the carrier concentrations at planes x and $x + \Delta x$ are $p(t)$ and $p(t) + \Delta p(t)$ respectively, then the limit of the mean-square value of $\Delta p(t)$ as Δx approaches zero is given by the relation

$$\overline{\delta \Delta p^2(t)} = \frac{4p\Delta x}{AD} \delta.$$

This formula has the same form as van der Ziel's postulate (4); but it is important to notice that it refers to fluctuations in the *difference* in carrier concentration across the element and that the mean-square value of the fluctuation in carrier concentration itself at any plane can only be determined by integration across the whole region with the insertion of the appropriate boundary conditions. In the present example the boundary conditions are that $\overline{p^2(t)} = 0$ at $x = 0$ and at $x = W$.

Now we are primarily interested in the minority carrier flows i_o and i_w across the $x = 0$ and $x = W$ planes respectively. From the time-dependent diffusion equation we find

$$i_o(j\omega) = Ak_o(j\omega)p_1(j\omega) = \frac{l_x}{D} \frac{k_o k_2}{(k_1 + k_2)} \quad (48a)$$

$$i_w(j\omega) = Ak_w(j\omega)p_2(j\omega) = -\frac{l_x}{D} \frac{k_1 k_w}{(k_1 + k_2)} \quad (48b)$$

where

$$k_o = \frac{qD}{L} \operatorname{cosech}(x'/L) \quad (49a)$$

$$k_w = \frac{qD}{L} \operatorname{cosech}[(W-x')/L] \quad (49b)$$

and hence from (25)

$$\Delta \left(\frac{\delta i'^2_{No}(t)}{\delta f} \right) = \frac{4pA}{D} \left| \frac{k_o k_2}{k_1 + k_2} \right|^2 \Delta x \quad (50a)$$

$$\Delta \left(\frac{\delta i'^2_{Nw}(t)}{\delta f} \right) = \frac{4pA}{D} \left| \frac{k_1 k_w}{k_1 + k_2} \right|^2 \Delta x. \quad (50b)$$

These expressions refer to the thermal contribution to the minority carrier noise currents across the $x = 0$ and $x = W$ planes. Although the description of the individual event (in terms of a particle immersed in a continuous medium) is unrealistic, the averaged expressions (50a) and (50b) may be taken to be accurate when applied to regions containing a large number of carriers, and over times which include a large number of collisions. We may check their validity by considering the simple (but practically important) case where bulk recombination is negligible and the frequency range is low enough to ensure that carrier-storage effects are also negligible. In this case we have the condition $W \ll L$, and we find that (50a) and (50b) reduce to

$$\Delta \left(\frac{\delta i'^2_{No}(t)}{\delta f} \right) = \Delta \left(\frac{\delta i'^2_{Nw}(t)}{\delta f} \right) = \frac{4pAq^2 D}{W^2} \Delta x. \quad (51)$$

For this case the carrier concentration varies linearly across the P-region, and equation (51) can be integrated easily to give the spectrum of the total noise current. The

result is

$$\frac{\delta i_{N0}^2(t)}{\delta f} = \frac{\delta i_{NW}^2(t)}{\delta f} = \frac{2q^2 AD}{W} (p_0 + p_w) \quad (52)$$

which may be expressed in terms of the diffusion current I_D , as follows:

$$\frac{\delta i_{N0}^2(t)}{\delta f} = \frac{\delta i_{NW}^2(t)}{\delta f} = 2qI_D \frac{(p_0 + p_w)}{(p_0 - p_w)} \quad (53)$$

If we now insert $p_w = 0$ in equation (53) (corresponding to the situation in a bipolar transistor with reverse-biased collector junction), we see that the noise spectrum deduced from the integration of (51) is simply equal to the shot noise that would be predicted in I_D on the assumption of independent carrier motion across the $x = W$ plane, which is clearly correct in this particular case.

It seems surprising at first sight to find the shot noise in the current crossing the $x = W$ plane, which can be deduced from the carrier motion in the vicinity of the plane, associated with generators supposed to be distributed throughout the N-region. However, it must be borne in mind that in the bulk model we are using, the boundary concentrations p_0 and p_w are supposed constant so that a time-varying current crossing the $x = W$ plane can only arise from time-variations in the carrier concentration in the region between the boundary planes. Furthermore, these disturbances cause equal currents to flow across both planes, so that the generation mechanism does not need to be associated with one boundary more than the other. These considerations bring out the essential part played by the interactions throughout the minority-carrier store in maintaining correlation between the flows across the two boundary planes. The question of whether the flow causes the carrier-concentration disturbances or vice versa does not really arise.

Another interesting aspect of (53) is that it correctly describes the high noise level in a saturated transistor where $p_w \approx p_0$. Although this is often discussed in terms of two independent currents flowing in opposite directions across the base region, such an interpretation does not seem to accord with a diffusion model of junction action.

6 Bulk Region Recombination Noise

In the theory of the ideal junction¹ it is assumed that recombination in the depletion layer is negligible. Where this is not so, the current-voltage characteristic takes a different form² from equation (1); Lauritzen⁹ gives an account of the noise generation in this case, and we briefly discuss it, for a forward-biased junction, in Section 9. In this Section we shall consider only the noise generation by recombination events which occur in the bulk material.

A recombination event does not result in any change in the charge distribution, so there is no majority-carrier relaxation. The initial action is equivalent to a minority-carrier flow $q\delta(t)$ 'from nowhere' into the x' plane, resulting in a departure from the equilibrium carrier concentration, as shown in Fig. 4.

The minority carrier relaxation occurs by flows i_1'' and i_2'' towards the $x = 0$ and $x = W$ planes respectively; as in

equations (42) and (44) we have

$$i_1''(j\omega) = -Ak_1(j\omega)p_1'(j\omega) \quad (54a)$$

$$i_2''(j\omega) = Ak_2(j\omega)p_2'(j\omega) \quad (54b)$$

$$i_1''(j\omega) - i_2''(j\omega) - q = 0. \quad (55)$$

We now obtain the following expressions for the minority current flows i_0'' and i_w'' across the $x = 0$ and $x = W$ planes respectively:

$$i_0''(j\omega) = \frac{qk_0}{(k_1 + k_2)} \quad (56a)$$

$$i_w'' = \frac{-qk_w}{(k_1 + k_2)}. \quad (56b)$$

For the situation where the width of the N-region is much less than the diffusion length ($W \ll L$) these relations reduce at low frequencies to

$$i_0''(j\omega) = q \left(1 - \frac{x'}{W}\right) \quad (57a)$$

$$i_w''(j\omega) = -q \frac{x'}{W} \quad (57b)$$

showing that the total minority-carrier outflow for each event is equal to the charge q on one carrier, as would be expected. The charge equilibrium is maintained by a majority-carrier flow q through the metal contact in the case of a diode, or through the base lead in the transistor. It follows that in the low-frequency part of the spectrum the component of base current arising from bulk region recombination shows full shot noise.

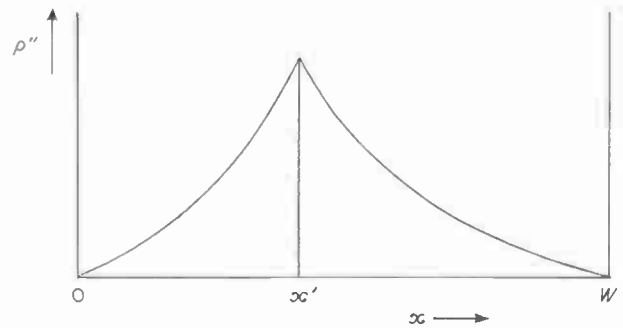


Fig. 4. Departure from the equilibrium minority carrier concentration due to a recombination event at the $x = x'$ plane.

Now the number of recombination events occurring per second in an element Δx is $pA\Delta x/\tau_R$, where τ_R is the carrier lifetime. The generation rate—which is of course equal to the recombination rate when p has its equilibrium value of p_n —is $p_n A\Delta x/\tau_R$. Hence the contributions of this element to the power spectra of the noise currents across the $x = 0$ and $x = W$ planes respectively, are

$$\Delta \left(\frac{\delta i_{N0}^2(t)}{\delta f} \right) = \frac{2(p + p_n)Aq^2}{\tau_R} \left| \frac{k_0}{k_1 + k_2} \right|^2 \Delta x \quad (58a)$$

$$\Delta \left(\frac{\delta i_{NW}^2(t)}{\delta f} \right) = \frac{2(p + p_n)Aq^2}{\tau_R} \left| \frac{k_w}{k_1 + k_2} \right|^2 \Delta x. \quad (58b)$$

These expressions will be used in Section 10.

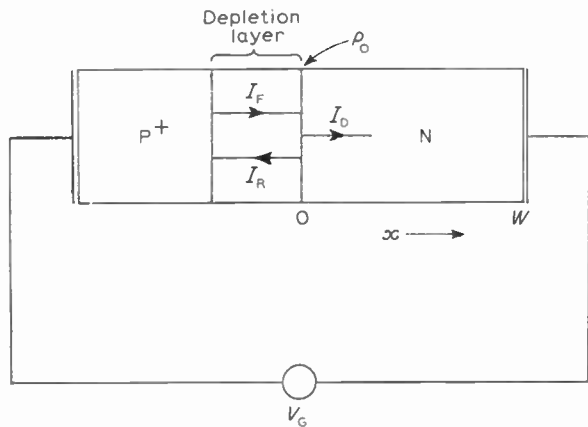


Fig. 5. Current flows I_F and I_R across a p-n junction which, for forward bias, are very much larger than the nett current, I_D .

7 Noise due to Carriers Crossing the Depletion Layer

Before calculating the noise due to the passage of carriers across the depletion layer we must examine in more detail the principles of p-n junction action.

In the standard treatments of the junction, which are based on the work of Shockley¹, it is assumed that the minority-carrier concentration p_0 at the plane $x = 0$ at the edge of the depletion layer follows the applied voltage V exactly, according to the relation

$$p_0 = p_n \exp(qV/k\theta). \quad (59)$$

This is due to the fact that the minority-carrier population in this region is in thermal equilibrium with the majority-carrier bath on the far side of the junction. The equilibrium is maintained by current flows I_F and I_R from one side of the junction to the other, which for forward bias are very large by comparison with the nett current I_D flowing across the $x = 0$ plane (Fig. 5); in fact, in calculations of the carrier distribution the current I_D is approximated to zero, which is equivalent to the assumption of constant quasi-Fermi levels across the depletion layer.

A simple statistical argument leads to the expressions

$$I_F = (qp_n DA/\bar{l}_x) \cdot \exp(qV/k\theta)$$

$$I_R = (qp_0 DA/\bar{l}_x)$$

where \bar{l}_x is the mean free path in the x direction. Because I_F and I_R are not exactly equal, equation (59) cannot be exactly true: any flow I_D must correspond to a difference between I_F and I_R , and for a given nett current flow I_D there must be an excess applied voltage ΔV given by the relation

$$\Delta V = I_D \cdot \frac{dV}{dI_F} = I_D \frac{k\theta}{qI_F}. \quad (60)$$

Thus the effect we are discussing is equivalent to a resistance of value $k\theta/qI_F$ in series with the junction. This is much less than the low-frequency incremental resistance of the junction, which is $k\theta/q(I_D + I_S)$, and in impedance calculations will normally be negligible. However, it is extremely relevant to the present discussion because it represents the relaxation mechanism by which the carrier

equilibrium is restored after a carrier crosses the depletion layer of a forward-biased junction. For our present purposes we need only to consider the conductance

$$G_S = qI_F/k\theta \quad (61)$$

and the junction admittance Y_J given by equation (7); we neglect other contributions to the total impedance, such as bulk resistance and contact resistance, although in practice they may have more effect on the total impedance than G_S .

When a carrier crosses the depletion layer of a forward-biased junction with short-circuited terminals, the resulting change in minority-carrier concentration p_0 at the $x = 0$ plane relaxes by means of current flows through two parallel paths. These consist of a flow directly back across the depletion layer, represented by a change in I_R , and a flow through the N-region represented by a change in I_D . The initial action is equivalent to a current generator $q\delta(t)$ across G_S in the a.c. equivalent circuit, shown in Fig. 6. Because Y_J approaches infinity at infinite frequency, the current $q\delta(t)$ instantaneously flows around the external circuit and the charge is stored in Y_J ; a relaxation $qg(t)$ follows, and the total current flow in the external circuit is given by the relations

$$i_D(t) = q[\delta(t) - g(t)]$$

$$i_D(j\omega) = q \int_0^\infty [\delta(t) - g(t)] \exp(-j\omega t) dt. \quad (62)$$

The function $i_D(j\omega)$ which is actually what we require, is immediately available by analysis of Fig. 6. A Thévenin transformation applied to G_S and its parallel current generator gives a voltage generator $q\delta(t)/G_S$ in series with G_S , and we obtain

$$i_D(j\omega) = q \frac{Y_J}{G_S + Y_J} = q \left(1 - \frac{G_S}{G_S + Y_J} \right). \quad (63)$$

The repetition rate of these events is simply $(I_F + I_R)/q \approx 2I_F/q$ so the resulting contribution to the spectrum of the noise current $i_{ND}''(t)$ around the circuit is

$$\frac{\delta i_{ND}''^2(t)}{\delta f} = 4qI_F \left| \frac{Y_J}{G_S + Y_J} \right|^2 = 4k\theta G_S \left| \frac{Y_J}{G_S + Y_J} \right|^2. \quad (64)$$

Equation (64) has the following simple interpretation: the noise due to carriers crossing the depletion layer is equivalent to thermal noise in the effective series resistance $1/G_S$. In the frequency range in which devices are useful, this effect is negligible—as indicated by the fact that G_S is so large that it is not normally taken into account when the current-voltage relation is considered.

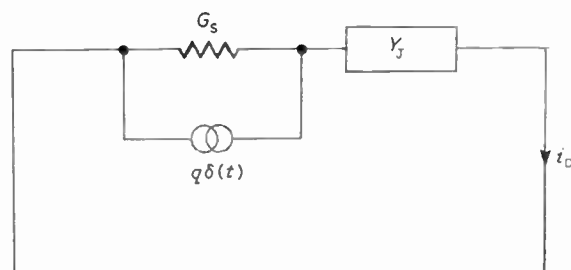


Fig. 6. A.c. equivalent circuit representing the crossing of the depletion layer by an individual carrier.

It is interesting to compare this result with that of van der Ziel and Becking in the Appendix to reference 7. We observe from (62) and (63) that the Fourier transform of the current $i_D(t)$ is the total admittance Y_T multiplied by q/G_S . Thus we have

$$Y_T = \frac{G_S Y_J}{G_S + Y_J} = G_S \int_0^\infty [\delta(t) - g(t)] \exp(-j\omega t) dt. \quad (65)$$

If we ignore the d.c. component of Y_J we have the condition

$$\int_0^\infty g(t) dt = 1 \quad (66)$$

and we may now rewrite (65) in the form

$$Y_T = G_S \int_0^\infty [1 - \exp(-j\omega\tau)] g(\tau) d\tau. \quad (67)$$

This is the form that was used by van der Ziel and Becking in their derivation. They interpreted it as a description of two delta-functions separated by a time τ , corresponding to the forward and return journeys of an individual carrier; the function $g(\tau)$ is supposed to be a distribution function for the time intervals. Accordingly they used the expression

$$\begin{aligned} \frac{\overline{\delta i_{ND}^2(t)}}{\delta f} &= 2qI_F \int_0^\infty g(\tau) |1 - \exp(-j\omega\tau)|^2 d\tau \\ &= 4qI_F \int_0^\infty g(\tau) (1 - \cos \omega\tau) d\tau \\ &= 4q \operatorname{Re} Y_T I_F / G_S = 4k\theta \operatorname{Re} Y_T. \end{aligned} \quad (68)$$

In this derivation, the repetition rate of the double-pulse event is taken as I_F/q .

Now although (68) is the correct expression for the total noise associated with the real component of the a.c.

$$\frac{\overline{\delta i_{ND}^2(t)}}{\delta f} = \frac{q^2 A L_0}{\tau_R} \frac{\left[p'_0 (R_1 + R_2) \operatorname{cosech} (W/L_0) + 4p_n \left(a \sinh \left(\frac{2aW}{L_0} \right) + b \sin \left(\frac{2bW}{L_0} \right) \right) \right]}{\left[\cosh \left(\frac{2aW}{L_0} \right) - \cos \left(\frac{2bW}{L_0} \right) \right]} \quad (71)$$

junction admittance, it has been derived on a totally incorrect basis. First of all, it involves a model of junction action in which the crossing of the depletion layer by a carrier is usually followed within an extremely short time (note by comparing equations (62) and (63) that the frequency components of $g(t)$ lie far outside the operating range) by a return crossing by the same individual carrier, the time delay τ being in some unspecified way determined by the function $g(\tau)$, itself a function of the diffusion constant D and the recombination time τ_R . In this model any recombination events occur within the time τ , so that the pulse caused by the forward flow is not followed by a second pulse. This model of junction action results in the substitution of the function

$$\int g(\tau) |1 - \exp(-j\omega\tau)|^2 d\tau$$

for the function

$$\left| 1 - \int g(\tau) \exp(-j\omega\tau) d\tau \right|^2 = \frac{|Y_T|^2}{G_S^2}$$

which was used in (64) in the calculation of the spectral density of the noise due to carriers crossing the junction.

Similar objections apply to the treatment of transistor noise given by van der Ziel and Becking.

8 Total Noise in the Ideal Diode

The total noise current at the terminals of an ideal diode is given by the minority-carrier noise current crossing the $x = 0$ plane. The corresponding value for the $x = W$ plane is not in general the same, the difference being made up by majority carrier flow at the metal contact. Accordingly we obtain the spectral density of the noise current by integrating the expressions (50a) and (58a) across the N-region, using the excess minority carrier distribution given by the solution of the one-dimensional static diffusion equation:

$$p' = p'_0 \cdot \frac{\sinh [(W-x')/L_0]}{\sinh (W/L_0)}. \quad (69)$$

The required integral, which is essentially the same as that used by van der Ziel,³ is

$$\begin{aligned} \frac{\overline{\delta i_{ND}^2(t)}}{\delta f} &= \frac{4A}{D} \int_0^W (p' + p_n) \left| \frac{k_2 k_0}{k_1 + k_2} \right|^2 dx' + \\ &+ \frac{2q^2 A}{\tau_R} \int_0^W (p' + 2p_n) \left| \frac{k_0}{k_1 + k_2} \right|^2 dx'. \end{aligned} \quad (70)$$

If we were not making the assumption that all the diffusion current is carried by holes, a similar integration would be required for the P-region, giving a result of the same form.

It is laborious but not difficult to evaluate the integrals in 70). The result is

where

$$R_1 \equiv (2a - 1) \cosh [(2a + 1)W/L_0] - (2a + 1) \cosh [(2a - 1)W/L_0]$$

and

$$R_2 \equiv 2 \cosh (W/L_0) \cos (2bW/L_0) + 4b \sinh (W/L_0) \sin (2bW/L_0).$$

By comparing (71) with the expression for the junction conductance given in equation (9) and remembering the relationships in (5) and (6) for I_D and I_S we find that the spectral density of the noise current may be written in the following simple way:

$$\begin{aligned} \frac{\overline{\delta i_{ND}^2(t)}}{\delta f} &= 4q(I_D + I_S) \frac{G_J}{G_0} - 2qI_D \\ &= 2q(I_D + 2I_S) + 4k\theta(G_J - G_0). \end{aligned} \quad (72)$$

This is the standard result given in equation (2).

9 Noise due to Recombination in the Depletion Layer

Most of the carriers which diffuse from the P-type bulk region into the depletion layer do not have sufficient energy to cross it, and return without a collision. On the basis of a one-dimensional model we can represent this action in terms of a sheet of charge between the plates of a short-circuited parallel plate capacitor (Fig. 7).

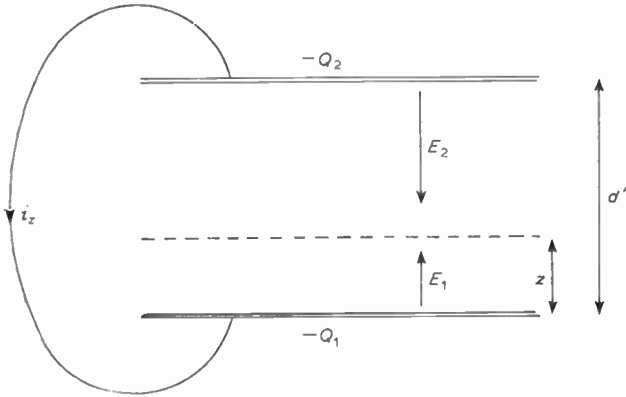


Fig. 7. Short-circuited, parallel plate capacitor with a sheet of charge located at a distance z from the lower plate. This model is used as a basis for discussing recombination in the depletion layer.

With plates of separation d' , and a sheet of charge Q located at a distance z from the lower plate, the charges on the two plates are such as to maintain the conditions

$$E_1 z = E_2 (d' - z)$$

$$Q_1 + Q_2 = Q$$

$$\frac{Q_1}{E_1} = \frac{Q_2}{E_2}$$

where E_1 and E_2 are the electric fields in the regions between the sheet of charge Q and the lower and upper plates respectively. The charges Q_1 and Q_2 on the plates are, therefore,

$$Q_1 = Qz/d'$$

$$Q_2 = Q(d' - z)/d'$$

Thus a positive carrier moving rapidly to the plane at z from the lower plate delivers a current

$$i_+ = q(z/d') \cdot \delta(t) \tag{73}$$

through the wire on the outward journey, and an equal but opposite current on the return journey, the nett result being zero on a time-scale appropriate to semiconductor devices. On the other hand, if a carrier is trapped at the z plane, whether on its outward or return journey, there is a resultant flow given by equation (73). This is equally true of carriers which have diffused out of the N-region, because as we have seen in Section 7 the nett effect of the carrier motion and the resultant relaxation is zero in the absence of recombination, so that an interruption of the carrier motion causes a resultant current to appear.

The capture of a hole is followed by the capture of an electron within a time which is dependent on the trap

dynamics. This gives rise to a current

$$i_- = q(1 - z/d') \cdot \delta(t) \tag{74}$$

and if the time delay is short in relation to the frequency range of interest, the pulses i_+ and i_- will be apparently simultaneous and the nett result will be a pulse with area equal to one carrier charge. Experimentally this is found to be the case in practical devices⁹ and the result is that the depletion-layer recombination current gives rise to full shot noise. Since the flow is due to charge interaction it appears only as a majority-carrier flow through the bulk regions, not as a minority-carrier flow across the $x = 0$ plane; in fact, these recombination events have no effect on the minority-carrier concentration in the bulk N-region. Hence in a transistor with short-circuited collector-base terminals the depletion-layer recombination gives rise to noise currents in the base and emitter leads, but not the collector lead. It can be represented by a parallel noise current generator with mean-square value $2qI_{BR} \delta f$ where I_{BR} is the relevant component of the base current.

10 Noise in Bipolar Transistors

It must be borne in mind, when discussing noise processes in the bipolar transistor, that the role of the metal contact in the diode is shared in the transistor between the collector, which deals with the minority diffusion current, and the base contact which is essentially continuous with the majority carrier bath. Thus, the noise current in the base lead contains a full shot noise component due to depletion-layer recombination, as discussed in the previous Section, which is uncorrelated with the contributions to the noise made by thermal and recombination processes occurring in the bulk base region; it may, therefore, be included as an additive term in the expressions for the total spectral densities of the noise currents in both the base and the emitter leads. However, for a zero-biased collector-base junction, and with the emitter-base junction short-circuited for a.c., the noise in the collector lead contains no component arising from depletion-layer recombination.

The introduction of depletion-layer recombination into the ideal model of Shockley¹ does not affect its validity because, for all practical situations, the quasi-Fermi levels can still be treated as constant within the depletion layer.

From equations (50a), (50b), (58a) and (58b) the spectral densities of the noise currents in the emitter and collector leads are

$$\frac{\delta i_{NE}^2(t)}{\delta f} = \frac{4A}{D} S_1 + \frac{2q^2 A}{\tau_R} S_2 + 2qI_{BR} \tag{75}$$

$$\frac{\delta i_{NC}^2(t)}{\delta f} = \frac{4A}{D} S_3 + \frac{2q^2 A}{\tau_R} S_4 \tag{76}$$

where the S parameters are integrals over the base width W , defined as

$$S_1 \equiv \int_0^W (p' + p_n) \left| \frac{k_0 k_2}{k_1 + k_2} \right|^2 dx'$$

$$S_2 \equiv \int_0^W (p' + 2p_n) \left| \frac{k_0}{k_1 + k_2} \right|^2 dx'$$

$$S_3 \equiv \int_0^W (p' + p_n) \left| \frac{k_1 k_W}{k_1 + k_2} \right|^2 dx'$$

$$S_4 \equiv \int_0^W (p' + 2p_n) \left| \frac{k_W}{k_1 + k_2} \right|^2 dx'$$

and the k parameters are defined in equations (43a), (43b), (49a) and (49b). The corresponding complex correlation coefficient is

$$\Gamma_{CE} \equiv \frac{-\frac{4A}{D} S_5 + \frac{2q^2 A}{\tau_R} S_6}{\left[\frac{\delta i_{NE}^2(t)}{\delta f} \frac{\delta i_{NC}^2(t)}{\delta f} \right]^{\frac{1}{2}}} \quad (77)$$

where

$$S_5 \equiv \int_0^W (p' + p_n) \left\{ \frac{k_2 k_0}{k_1 + k_2} \right\}^* \left\{ \frac{k_1 k_W}{k_1 + k_2} \right\} dx'$$

$$S_6 \equiv \int_0^W (p' + 2p_n) \left\{ \frac{k_0}{k_1 + k_2} \right\}^* \left\{ \frac{k_W}{k_1 + k_2} \right\} dx'.$$

Using equation (69) for the excess minority carrier concentration p' and the condition $p' \gg p_n$, these expressions may be evaluated without too much difficulty. In order to present the results in a tractable form we follow a similar procedure to that used in solving the same problem for the p-n junction diode: we compare our calculated results with the expressions for the transistor currents and parameters discussed in Section 2. By making the appropriate substitutions we arrive at the results

$$\frac{\delta i_{NE}^2(t)}{\delta f} = 4qI_E \left(\frac{G_E}{G_{E0}} - \frac{1}{2} \right) - 4qI_{BR} \left(\frac{G_E}{G_{E0}} - 1 \right) \quad (78)$$

and

$$\frac{\delta i_{NC}^2(t)}{\delta f} = 2qI_C \quad (79)$$

whilst the complex correlation coefficient in equation (77) is given by

$$\Gamma_{CE} = - \frac{2qI_C \frac{\alpha_s}{\alpha_{0s}} \frac{Y_E}{G_{E0}}}{\left[\frac{\delta i_{NE}^2(t)}{\delta f} \frac{\delta i_{NC}^2(t)}{\delta f} \right]^{\frac{1}{2}}} \quad (80)$$

In the low-frequency approximation this expression reduces to

$$\Gamma_{CE} = -\alpha_0^{\frac{1}{2}} \quad (81)$$

The spectral density of the short-circuit noise current in the base lead is derived readily from equations (78), (79) and (80):

$$\frac{\delta i_{NB}^2(t)}{\delta f} = 2qI_E \left[\frac{2G_E}{G_{E0}} - 1 + \alpha_{0s} - \frac{(\alpha_s Y_E + \alpha_s^* Y_E^*)}{G_{E0}} \right] - 2qI_{BR} \left[\frac{2G_E}{G_{E0}} - 2 + \alpha_{0s} - \frac{(\alpha_s Y_E + \alpha_s^* Y_E^*)}{G_{E0}} \right]$$

$$= 2qI_C \left[\frac{1}{\beta_0} + \frac{2G_E - (\alpha_s Y_E + \alpha_s^* Y_E^*)}{\alpha_{0s} G_{E0}} - \frac{2(1 - \alpha_{0s})}{\alpha_{0s}} \right] \quad (82)$$

As we should expect, for low frequencies this result reduces to $2qI_B$ where I_B is the total current flowing in the base lead. By making use of the Maclaurin expansions in equations (14b) and (15b) we find that, to second

order in frequency,

$$\frac{\delta i_{NB}^2(t)}{\delta f} \approx 2qI_C \left[\frac{1}{\beta_0} + \frac{(8 + 7\alpha_{0s})}{45\alpha_{0s}} \omega^2 \tau_J^2 \right] \quad (83)$$

where $\tau_J = W^2/2D$.

The result in (80), in conjunction with equations (78), (79) and (82), may be used to evaluate a complex correlation coefficient describing the causal connexion between the noise currents in the collector and base leads:

$$\Gamma_{CB} = \frac{-\Gamma_{CE} \left[\frac{\delta i_{NE}^2(t)}{\delta f} \frac{\delta i_{NC}^2(t)}{\delta f} \right]^{\frac{1}{2}} - \frac{\delta i_{NC}^2(t)}{\delta f}}{\left[\frac{\delta i_{NC}^2(t)}{\delta f} \frac{\delta i_{NB}^2(t)}{\delta f} \right]^{\frac{1}{2}}}$$

$$= -2qI_C \left[1 - \frac{\alpha_s Y_E}{\alpha_{0s} G_{E0}} \right] / \left[\frac{\delta i_{NC}^2(t)}{\delta f} \frac{\delta i_{NB}^2(t)}{\delta f} \right]^{\frac{1}{2}} \quad (84)$$

Expanding Γ_{CB} in a power series in ω using equation (15b), we find that to first order

$$\Gamma_{CB} \approx -2qI_C \frac{j\omega\tau_J}{3} / \left[\frac{\delta i_{NC}^2(t)}{\delta f} \frac{\delta i_{NB}^2(t)}{\delta f} \right]^{\frac{1}{2}} \quad (85)$$

It is evident from equations (79), (83) and (85) that for low frequencies Γ_{CB} varies linearly with ω , whilst the real correlation coefficient is zero.

11 Equivalent Circuits

For circuit design work the results we have obtained for the transistor must be expressed in the form of an equivalent circuit. For small signal conditions it is nowadays standard practice to use the so-called 'hybrid- π ' model of the transistor shown in Fig. 8. The circuit

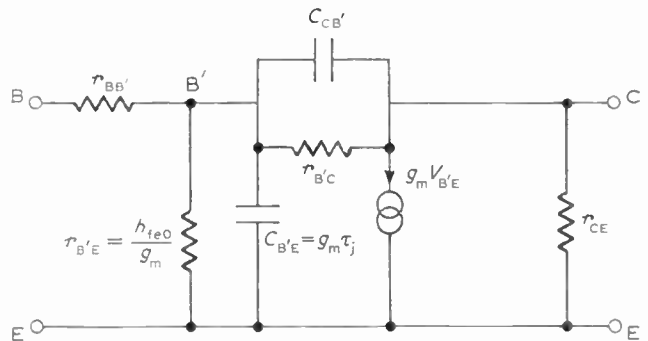


Fig. 8. 'Hybrid π ' model of transistor.

includes only resistors, capacitors, and a single current generator controlled by the voltage between the emitter terminal and the fictitious 'internal base terminal' B'.

The transfer parameter, which is often referred to as the 'mutual conductance' g_m , is usually assumed to be independent of frequency and equal to $\alpha_{0s} G_{E0} = qI_C/k\theta$, while the low-frequency current gain h_{fe0} is treated as an empirically determined quantity which is a function of the d.c. operating current I_C . In fact it is seen from equation (15a), which was derived on the assumption that base-resistance effects are negligible, that the transfer parameter $\alpha_s Y_E$ does vary with frequency, the second-order approximation being given in equation (15b). Although in practice this variation has a negligible effect on the frequency response of the transistor compared with the frequency variation of the common-emitter current gain, we shall need to incorporate it into the calculation of the equivalent noise generators.

For most design purposes it is convenient to separate the hybrid- π circuit of Fig. 8 into the 'intrinsic transistor' with terminals B', E, C, and the base resistance $r_{BB'}$ which is regarded as an external component in series with the external impedance connected to the B, E terminals. This is clearly the appropriate model in relation to the noise calculations of preceding Sections, which have been derived without the inclusion of any base-resistance effects. The admittance matrix Y of this transistor has the simple form

$$Y = \begin{pmatrix} \frac{1}{r_{B'E}} + \frac{1}{r_{B'C}} + s(C_{B'E} + C_{CB'}) & -\frac{1}{r_{B'C}} - sC_{CB'} \\ g_m - \frac{1}{r_{B'C}} - sC_{CB'} & \frac{1}{r_{B'C}} + \frac{1}{r_{CE}} + sC_{CB'} \end{pmatrix} \quad (86)$$

and in most design situations this can be approximated by

$$Y \simeq \begin{pmatrix} g_m \left(\frac{1}{h_{fe0}} + s\tau_J \right) - sC_{CB'} \\ g_m & 0 \end{pmatrix} \quad (87)$$

Making use of this intrinsic equivalent circuit in the form of a 'black box' specified by Y , we now draw the circuit of Fig. 9 in which the noise sources specified as short-circuit noise currents in equations (79) and (83) are represented as current generators $i_{p2}(t)$ and $i_{p1}(t)$ across the collector-base terminals and the 'intrinsic' base-emitter terminals. To second order in frequency we have

$$\frac{\delta i_{p1}^2(t)}{\delta f} = 2qI_C \left[\frac{1}{\beta_0} + \left(\frac{8+7\alpha_{0s}}{45\alpha_{0s}} \right) \omega^2 \tau_J^2 \right] \quad (88)$$

$$\frac{\delta i_{p2}^2(t)}{\delta f} = 2qI_C \quad (89)$$

and from (85) we have to first order in frequency

$$\Gamma_{21} = - \frac{2qI_C j\omega\tau_J/3}{\left[\frac{\delta i_{p1}^2(t)}{\delta f} \frac{\delta i_{p2}^2(t)}{\delta f} \right]^{1/2}} \quad (90)$$

Now the generators in Fig. 9 are not in a suitable form for circuit design work, partly because they are very strongly correlated and partly because they are not referred to the ports. It is standard practice nowadays to refer the noise generators in a 2-port to the input port (port 1) where they appear as a series voltage generator and a parallel current generator. The first step in

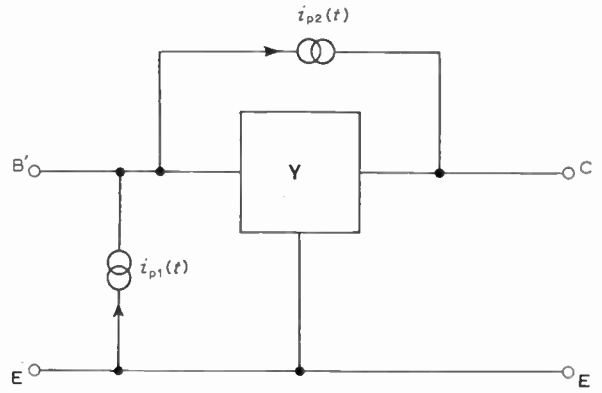
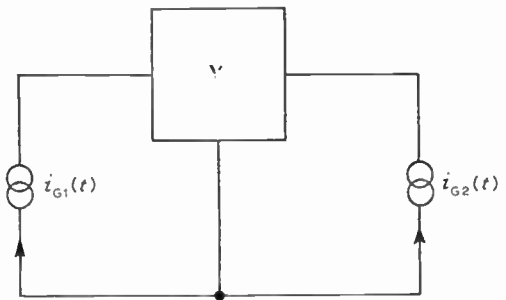
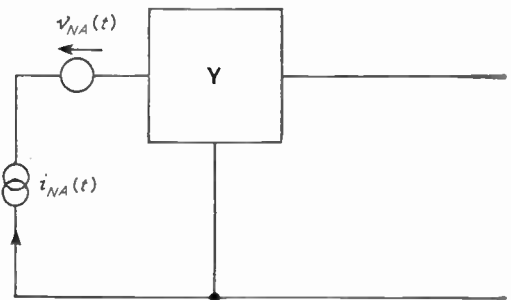


Fig. 9. The intrinsic transistor represented by a 'black box' specified by the admittance matrix Y .



(a) Equivalent version of the circuit shown in Fig. 9. The current generators are $i_{G1}(t) = i_{p1}(t) - i_{p2}(t)$ and $i_{G2}(t) = i_{p2}(t)$.



(b) For the purpose of calculating the output the generators in (a) are referred to the input. The values are $i_{NA}(t) = i_{G1}(t) + i_{G2}(t)y_{11}/y_{21}$ and $v_{NA}(t) = i_{G2}(t)/y_{21}$.

Fig. 10.

deriving such a circuit is to split up the collector-base generator $i_{p2}(t)$ into a collector-emitter generator $i_{p2}(t)$ and a base-emitter generator $-i_{p2}(t)$ in which case the current generators across the ports, as shown in Fig. 10(a), are $i_{G1}(t) = i_{p1}(t) - i_{p2}(t)$ and $i_{G2}(t) = i_{p2}(t)$. The collector-emitter generator $i_{G2}(t)$ is now referred to the input terminals by means of the well-known theorem that states that a current generator at port 2 of a linear 2-port can be represented for the purposes of calculating the current and voltage at port 2 as a voltage generator $i_{G2}(t)/y_{21}$ and a current generator $i_{G2}(t)y_{11}/y_{21}$ at port 1. The result is the equivalent circuit of Fig. 10(b) where we

obtain from equations (79), (83) and (87) the relations

$$\frac{\delta i_{NA}^2(t)}{\delta f} = 2qI_C \left[\frac{1}{h_{fe0}^2} + \frac{1}{\beta_0} + \omega^2 \tau_J^2 \left\{ \frac{8+7\alpha_{0s}}{45\alpha_{0s}} - \frac{2}{3\alpha_{0s}} + \frac{7}{45h_{fe0}} - \frac{1}{3h_{fe0}\alpha_{0s}} + \frac{1}{\alpha_{0s}^2} \right\} \right] \tag{91}$$

$$\frac{\delta v_{NA}^2(t)}{\delta f} = 2qI_C \left(1 + \frac{2\omega^2 \tau_J^2}{45} \right) / \alpha_{0s}^2 G_{E0}^2 \tag{92}$$

$$\Gamma_{vi} = + \frac{2qI_C}{\alpha_{0s} G_{E0}} \left[\frac{1}{h_{fe0}} - j\omega \tau_J \left(\frac{1}{\alpha_{0s}} - \frac{1}{3} - \frac{1}{3h_{fe0}} \right) \right] / \left[\frac{\delta i_{NA}^2(t)}{\delta f} \frac{\delta v_{NA}^2(t)}{\delta f} \right]^{\frac{1}{2}} \tag{93}$$

With the exception of the effects of depletion-layer recombination, this circuit is equivalent to those given by van der Ziel.³

Making the practical approximations

$$\left. \begin{aligned} \alpha_{0s} &\approx 1 \\ h_{fe0} &\gg \beta_0 \gg 1 \\ \omega^2 \tau_J^2 &\ll 1 \end{aligned} \right\} \tag{94}$$

we arrive at the results

$$\frac{\delta i_{NA}^2(t)}{\delta f} \approx 2qI_B + \frac{4}{3}qI_C \omega^2 \tau_J^2 \tag{95}$$

$$\frac{\delta v_{NA}^2(t)}{\delta f} \approx 2qI_C / G_{E0}^2 \tag{96}$$

$$\Gamma_{vi} \approx - \frac{4qI_C j\omega \tau_J / 3G_{E0}}{\left[\frac{\delta i_{NA}^2(t)}{\delta f} \frac{\delta v_{NA}^2(t)}{\delta f} \right]^{\frac{1}{2}}} \tag{97}$$

Although this equivalent circuit gives correct results if used to calculate the output at port 2, it must be emphasized that it cannot be used to calculate the noise currents flowing in the input circuit; this is evident from the fact that the current generator $i_{NA}(t)$ has a different value from the true base-emitter current generator.

In order to calculate the noise figure of the 'intrinsic transistor', in which base resistance effects are neglected, we use the circuit configuration shown in Fig. 11 where, by the use of Norton's theorem, the noise voltage generator $v_{NA}(t)$ is represented as an equivalent current generator with spectral density $|Y_1|^2 \delta v_{NA}^2(t) / \delta f$, and $Y_1 = G_1 + jB_1$ is the source admittance. The noise figure from this circuit and using equations (95) to (97) is

$$F = 1 + \frac{2qI_C}{4k\theta G_1} \times \left[\left(\frac{B_1^2}{G_{E0}^2} + \frac{4B_1 \omega \tau_J}{3G_{E0}} + \frac{2}{3}\omega^2 \tau_J^2 \right) + \frac{1}{\beta_0} + \frac{G_1^2}{G_{E0}^2} \right] \tag{98}$$

where the first-order term in frequency arises from the correlation. By completing the square (98) may be written in the form

$$F = 1 + \frac{2qI_C}{4k\theta G_1} \times \left[\left(\frac{B_1}{G_{E0}} + \frac{2}{3}\omega \tau_J \right)^2 + \frac{2}{9}\omega^2 \tau_J^2 + \frac{1}{\beta_0} + \frac{G_1^2}{G_{E0}^2} \right] \tag{99}$$

It is clear from this expression that by selecting the appropriate value of B_1 at a given frequency, it is possible to 'tune out' part of the frequency dependent contribution of (99), thereby improving the high-frequency noise

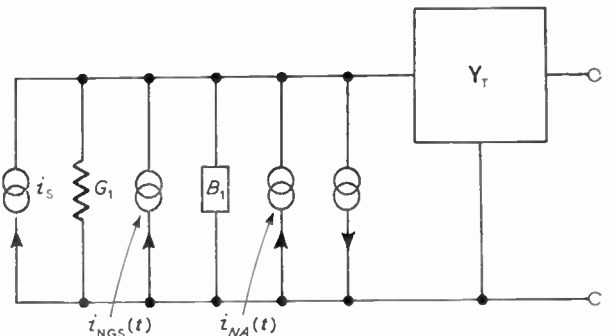


Fig. 11. Parallel representation of the source generator and the noise generators for calculating the noise figure of the transistor. The source admittance is $Y_1 = G_1 + jB_1$ and the corresponding noise current generator, $i_{NGS}(t)$, has a spectral density given by $\delta i_{NGS}^2(t) / \delta f = 4k\theta G_1$. The unmarked current generator has spectral density $|Y_1|^2 \delta v_{NA}^2(t) / \delta f$.

figure. The optimum value of B_1 to achieve this condition is $-\frac{2}{3}G_{E0} \omega \tau_J$ corresponding to a source inductance of $3/(2G_{E0} \omega^2 \tau_J)$.

After optimizing the susceptance B_1 in equation (99) we are left with the following expression for the noise figure:

$$F = 1 + \frac{2qI_C}{4k\theta} \left[\frac{G_1}{G_{E0}^2} + \frac{1}{G_1} \left(\frac{1}{\beta_0} + \frac{2}{9}\omega^2 \tau_J^2 \right) \right] \tag{100}$$

The minimum noise figure¹⁰ is now obtained from (100) by equating the terms in G_1 and $1/G_1$, the required condition for a minimum at a given frequency being

$$G_1 = G_{E0} \left(\frac{1}{\beta_0} + \frac{2}{9}\omega^2 \tau_J^2 \right)^{\frac{1}{2}} \tag{101}$$

Inserting this condition into equation (100), and remembering that $G_{E0} \approx qI_C / k\theta$, we obtain the following expression for the minimum noise figure:

$$F_{min} = 1 + \left(\frac{1}{\beta_0} + \frac{2}{9}\omega^2 \tau_J^2 \right)^{\frac{1}{2}} \tag{102}$$

which, in accordance with the behaviour of actual transistors, increases with increasing frequency. For low frequencies and a value of 100 for β_0 , the minimum noise figure from (102) is approximately 0.4 dB.

The importance of equation (102) lies in the fact that it represents a physical limitation on the noise performance that can be expected of any transistor. In practice the limiting value given by (102) will not be attainable because all actual transistors have a finite base resistance, as well as exhibiting an excess noise component which in our analysis we have neglected

entirely; thus the observed minimum noise figure will be degraded by comparison with that given in equation (102).

If in Fig. 11 the source admittance has to be real, then the susceptance B_1 is zero and it is not possible to 'tune out' inductively part of the frequency dependent contribution of the noise figure in equation (98). In this situation, at a given frequency, the optimum value of G_1 for a minimum in the noise figure is

$$G_1 = G_{E0} \left(\frac{1}{\beta_0} + \frac{2}{3} \omega^2 \tau_j^2 \right)^{\dagger} \quad (103)$$

and the minimum noise figure is

$$F_{\min} = 1 + \left(\frac{1}{\beta_0} + \frac{2}{3} \omega^2 \tau_j^2 \right)^{\dagger} \quad (104)$$

This result represents the best possible noise performance that can be achieved with a resistive source but, for the same reasons given above with regard to an inductive source, it is not attainable in practice.

A simplified noise model of the transistor which is useful to the circuit designer roughly approximates the circuit of Fig. 11 derived from our rigorous analysis. Referring to equation (95) we see that an important feature of this expression is that the frequency dependence of the current generator, which has a +3 dB point at $\omega = (1/\tau_j)\sqrt{(3/2\beta_0)}$, is due primarily to the frequency-dependence of the common-emitter current gain y_{21}/y_{11} rather than to the increase in the base noise current with frequency. For many design purposes it is possible to ignore the frequency-dependent term in equation (88) and correspondingly to approximate the complex correlation coefficient to zero, and the current generators in Fig. 10(a) may now be described by the following approximations:

$$\frac{\overline{\delta i_{G1}^2(t)}}{\delta f} \simeq 2qI_B \quad (105)$$

$$\frac{\overline{\delta i_{G2}^2(t)}}{\delta f} \simeq 2qI_C \quad (106)$$

$$\Gamma_{12} \simeq 0. \quad (107)$$

Obviously this is the model which would be predicted from the most naïve assumptions about the noise properties of the device—i.e. that the collector current and the base current each show 'full shot noise' and that the uncorrelated noise current generators appear at the input and the output ports in a common-emitter representation.

In Fig. 10(b), which is the equivalent of Fig. 10(a) with the generators referred to the input, the approximate expressions from the simplified model for the spectral densities and the correlation are (using (94)):

$$\frac{\overline{\delta i_{NA}^2(t)}}{\delta f} \simeq 2qI_C \left[\frac{1}{\beta_0} + \omega^2 \tau_j^2 \right] \quad (108)$$

$$\frac{\overline{\delta v_{NA}^2(t)}}{\delta f} \simeq 2qI_C / G_{E0}^2 \quad (109)$$

$$\Gamma_{vi} \simeq - \frac{2qI_C j\omega\tau_j / G_{E0}}{\left[\frac{\overline{\delta i_{NA}^2(t)}}{\delta f} \frac{\overline{\delta v_{NA}^2(t)}}{\delta f} \right]^{\dagger}} \quad (110)$$

Comparing these equations with (95), (96) and (97) we see that this simplified model underestimates the +3 dB frequency for the noise current generator by a factor of $\sqrt{3}$, and also gives a somewhat higher magnitude for the complex correlation coefficient Γ_{vi} . Since this coefficient is imaginary it has no effect on the noise figure when the source impedance is resistive but an overestimate of its magnitude leads to an overestimate of the improvement in noise figure that can be obtained by the use of an inductive source. Using the same optimizing procedure as before we find that the minimum noise figure for an inductive source is from equations (108) to (110)

$$F_{\min} = 1 + \frac{1}{\beta_0^{\dagger}} \quad (111)$$

where the optimum value of the tuning inductor is $1/G_{E0} \omega^2 \tau_j$, and the optimum value of G_1 is G_{E0}/β_0^{\dagger} . Although for low frequencies the expression in (111) does not differ from that in (102), we see that for higher frequencies the simplified model does not predict an increase in the minimum noise figure.

In the situation where the source is purely resistive the optimum value of G_1 for this simplified model is $G_{E0} (1/\beta_0 + \omega^2 \tau_j^2)^{\dagger}$ and the corresponding minimum noise figure is

$$F_{\min} = 1 + \left(\frac{1}{\beta_0} + \omega^2 \tau_j^2 \right)^{\dagger} \quad (112)$$

This expression differs from equation (104) obtained from the more rigorous analysis only by a factor $\frac{2}{3}$ in the frequency dependent term, and the high-frequency minimum noise figure obtained from the simplified model with an optimized inductive source is improved by comparison with that obtained using a purely resistive source. Because of the similarity between the results obtained from the rigorous analysis and the simplified model, the errors involved in using the latter in a practical design situation are usually negligible.

The approximations represented by equations (105) to (110) can be incorporated into the hybrid- π model of the transistor by means of the circuit shown in Fig. 12(a) where the equivalent emitter-base and collector-base capacitors have been moved to the outside of the diagram and the current generators of Fig. 10(a) have been referred to the terminals of the 'equivalent broadband device' which is represented in the Figure by a frequency-independent G matrix with parameters

$$\left. \begin{aligned} g_{11} &= qI_C / h_{fe0} k\theta & g_{12} &= 0 \\ g_{21} &= qI_C / k\theta & g_{22} &= 0 \end{aligned} \right\} \quad (113)$$

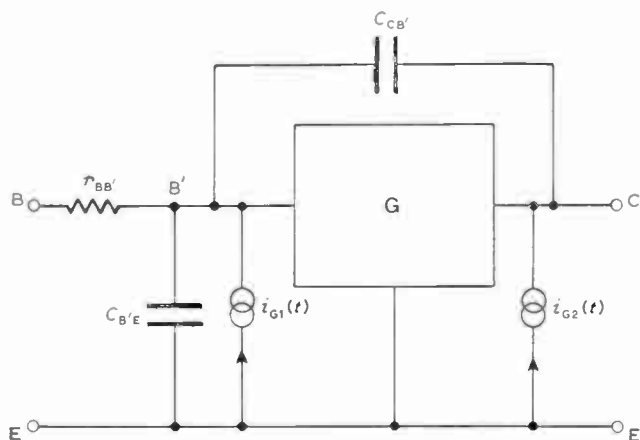
The spectral densities and the complex correlation coefficient for the noise generators in Fig. 12(b) are given by the relations

$$\frac{\overline{\delta i_{NT}^2(t)}}{\delta f} = 2qI_B \quad (114)$$

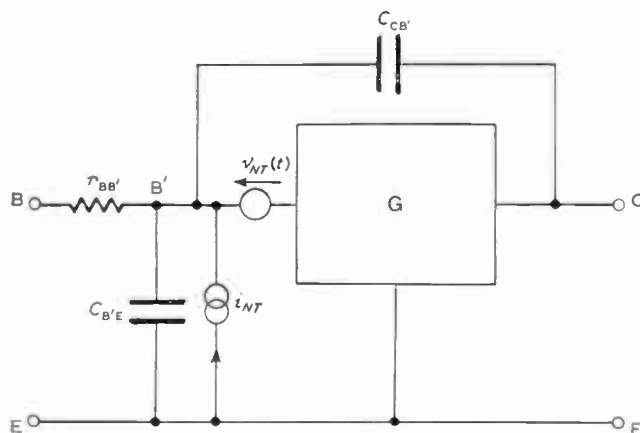
$$\frac{\overline{\delta v_{NT}^2(t)}}{\delta f} = 2qI_C / G_{E0}^2 \quad (115)$$

$$\Gamma_{vi} = 0 \quad (116)$$

and the obvious advantage of this formulation is that the



(a) 'Hybrid π ' model of the transistor showing a frequency-independent G matrix with the equivalent emitter-base and collector-base capacitors moved to the outside of the diagram. The spectral densities of the generators in this model are $\delta i_{G1}^2(t)/\delta f = 2qI_B$ and $\delta i_{G2}^2(t)/\delta f = 2qI_C$.



(b) Equivalent circuit of (a) for the purpose of calculating the output. The spectral densities of the generators are $\delta i_{NT}^2(t)/\delta f = 2qI_B$ and $\delta v_{NT}^2(t)/\delta f = 2qI_C/G^2$ and the complex correlation coefficient is zero.

Fig. 12.

generators are not only 'white' but uncorrelated. The increase of noise figure with frequency, according to this model, is due to the signal attenuation caused by the device capacitances and these can be considered along with the other reactances in the circuit.

Because the generators in Fig. 12(b) are uncorrelated they may be represented conveniently in terms of an equivalent series noise resistance¹⁰ R_{Nv} and parallel noise resistance R_{Ni} , where

$$R_{Nv} = \frac{1}{4k\theta} \frac{\delta v_{NT}^2(t)}{\delta f} \tag{117}$$

and

$$R_{Ni} = 4k\theta \frac{\delta i_{NT}^2(t)}{\delta f} \tag{118}$$

Substituting $qI_C/k\theta$ for G_{E0} in equations (114) to (116) we obtain the simple formulae

$$R_{Nv} = r_c/2 \tag{119}$$

$$R_{Ni} = 2r_c\beta_0 \tag{120}$$

where $r_e = 1/G_{E0}$. With typical values of the parameters¹¹ the effect of the finite base resistance on the minimum noise figure may be taken into account simply by adding $r_{BB'}$ to the series noise resistance given above.

12 Acknowledgments

The authors are grateful for many stimulating discussions with Professor C. W. McCombie, Dr. P. C. Banbury and Mr. R. S. Leigh of this Laboratory.

Thanks are also due to Professor H. Sutcliffe, University of Salford, and Messrs. B. V. Cake and I. Wilson, Atomic Energy Establishment, Winfrith, for valuable comments on the manuscript.

13 References

- Shockley, W., 'The theory of p-n junctions in semiconductors and p-n junction transistors', *Bell Syst. Tech. J.*, **28**, p. 435, July 1949.
- Sah, C. T., Noyce, R. N. and Shockley, W., 'Carrier generation and recombination in p-n junctions and p-n junction characteristics', *Proc. IRE*, **45**, p. 1228, September 1957.
- van der Ziel, A., 'Theory of shot noise in junction diodes and junction transistors', *Proc. IRE*, **43**, p. 1639, November 1955.
- van der Ziel, A., 'Fluctuation Phenomena in Semiconductors', p. 99 (Butterworths, London, 1959).
- van der Ziel, A., 'Noise in junction transistors', *Proc. IRE*, **46**, p. 1019, June 1958.
- Petritz, R. L., 'On noise in p-n junction rectifiers and transistors' *Phys. Rev.*, **91**, p. 231, 1953 (erratum p. 204).
- van der Ziel, A. and Becking, A. G. T., 'Theory of junction diode and junction transistor noise', *Proc. IRE*, **46**, p. 589, March 1958.
- Rice, S. O., 'Mathematical analysis of random noise', *Bell Syst. Tech. J.*, **23**, p. 282, 1944; **24**, p. 46, 1945.
- Lauritzen, P. O., 'Noise due to generation and recombination of carriers in p-n junction transition regions', *IEEE Trans. on Electron Devices*, **ED-15**, p. 770, October 1968.
- Faulkner, E. A., 'The design of low-noise audio frequency amplifiers', *The Radio and Electronic Engineer*, **36**, p. 17, July 1968.
- Faulkner, E. A., 'Optimum design of low-noise amplifiers', *Electronics Letters*, **2**, No. 11, p. 426, November 1966.

Manuscript first received by the Institution on 17th August 1973 and in final form on 6th November 1973. (Paper No. 1571/CC 189).

© The Institution of Electronic and Radio Engineers, 1974

Electrical conduction in thin lubricating oil films

W. G. FIENNES, B.Sc., Ph.D.*

and

Professor J. C. ANDERSON,

D.Sc.(Eng.), Ph.D., D.I.C., F.Inst.P., C.Eng., M.I.E.R.E.*

SUMMARY

Under conditions of hydrodynamic lubrication oil forms a thin film between the lubricated surfaces. An investigation of the electrical properties of such films is described, the measurements being made under dynamic conditions. It is shown that the electrical conduction is consistent with space-charge limited current in the presence of a uniform distribution of traps. The oil film is considered to form a pressure-frozen quasi-solid of glass-like material. A rise in current corresponding to the trap-filled limit is observed and imparts a conductivity switching type of behaviour to the film, reminiscent of amorphous glass switching of the Ovshinsky type.

* Department of Electrical Engineering, Imperial College, London SW7 2BT.

1 Introduction

Direct measurement of the thickness of oil films under conditions of dynamic lubrication is generally difficult. One method which has been used was suggested by Brix¹ and developed by Cameron and his co-workers.² This consists of passing a high current (up to 100 A) through the film from a low-voltage d.c. source and measuring the voltage drop across the film. It was found empirically that the voltage developed was proportional to the film thickness in many cases. The present work stems from an investigation of this effect and reports on the electrical conductivity of thin oil films under conditions of elasto-hydrodynamic lubrication. The analysis of the Brix-Cameron effect is being reported elsewhere.³

2 General Considerations

A lubricated contact presents a unique environment for a conductivity study. It is dynamic, and at every instant of time fresh material is being swept through the gap forming the contact. Some of the lubricant may have been passed through before and may consequently be conditioned in some way, while mixed with this will be 'new' oil which has only just been drawn out of the reservoir or sump. Thus the material under investigation is never reproducible. Although the same parts of the metallic surfaces pass repeatedly through the contact zone the electrodes which they form are presenting surfaces which are new on an electronic time scale, and the exact combination of anode and cathode surfaces is never repeated.

Another consequence of the dynamic nature of the contact is that the oil may be conditioned even as it passes between the electrodes. Thus if, for example, the cathode is injecting charge into the oil which builds up to an equilibrium concentration, there will be a concentration gradient down the length of the contact. The amount of charge in any one element depends upon the time which that element has spent in the contact zone.

Despite these considerations of the dynamic nature of the contact there is one redeeming feature. In the case of a rolling contact there is no relative motion between the opposing sides as they pass through the area of closest approach. Thus for the time that an element is actually passing through the contact, the element and the elements of metal surface which form its boundaries on two sides are in relative stasis, and there will be no shearing in the film. Nevertheless the history of such an element may be very varied. As it enters the contact zone it will be in a liquid phase at a relatively low pressure. During an appreciable fraction of the transit time through the contact it may be 'pressure-frozen', and at the exit it could cavitate and enter a vapour phase.

Thus although the mechanical properties of an oil film are reproducible even on a microscopic scale, the factors which may influence the electrical properties are continuously changing.

3 Experimental Method

The mechanical system used for this work was the same in principle to that used by Westlake.⁴ A 2.54 cm (1 in) diameter steel ball was loaded hydrostatically

against one side of a flat steel disk. The disk was perfectly free to rotate about its axis. Thus as the ball was driven by a small electric motor about an axis through and perpendicular to the axis of the disk, a pure rolling contact was established. The ball ran in a small bath of oil—sufficient to prevent starvation of the contact, and electrical contact was made to the ball and to the disk by means of mercury and copper slip-rings. The speed of rotation of the ball was continuously variable up to 2500 rev/min, and the contact loading covered the range 0–20 kg. Thus full control over the film profile was obtained.

Both the ball and disk were made from ball-bearing steel, type EN 31. The surface of the disk was polished with a polishing wheel as used for the preparation of metallurgical specimens. Despite the large area of the disk surface, satisfactory finishes could be obtained free of pits and scratches. For the finest surface 1 μm diamond paste was employed, and to produce the coarser finishes a carborundum grinding paste was used. The balls used were also polished with diamond paste, and always to the best surface finish obtainable.

Before using, all traces of grease and oil from previous runs were removed from the surface by means of solvents. The surfaces were finally washed in alcohol followed by acetone in conjunction with ultrasonic agitation. The ball-cup received similar treatment.

Several electrical configurations were used in conjunction with this mechanical arrangement. Average currents and voltages were measured by using an X–Y plotting table (Bryans type 26000 A3) having a frequency response of 5 Hz. The current was monitored from the p.d. across a 0.5 Ω resistor in series with the film and the voltage was measured directly between the electrodes. The input resistance of the recorder was sufficiently high not to shunt the oil film resistance significantly. A power supply (Roband) was used which was capable of delivering up to 10 A at 30 V and could be used in either a constant voltage or constant current mode.

The transient variations of the voltage were also examined using a c.r.o. For measurements in the high current regime the power supply was connected directly across the oil film and used in the current mode. At low currents the power supply was connected in series with a resistor—generally about 3 k Ω —and was used as a voltage source.

In order that the transient I/V characteristics at low current levels could be examined, the Roband power supply was replaced by one employing a solid circuit operational amplifier (Fenlow AD 5003). The circuit was designed to provide a varying current, and had a series output impedance greater than 10 M Ω . The input signal was obtained from a Marconi l.f. signal generator capable of delivering sine-, ramp- or square-wave signals of 15 V peak-to-peak and which could operate continuously or in a 'single-shot' mode. The c.r.o. was used as an X–Y plotter and the traces were photographed with a Polaroid camera.

A simple arrangement for studying static oil films between a polished steel ball and a polished steel flat was made. This was used only for comparative qualitative observations as it was not possible to make an accurate estimate of the film thickness. This was due to surface micro-asperities on the ball and plate which were inevitably present as well as to microscopic particles in the oil, which tend to bridge the gap.

4 Elastohydrodynamic Lubrication (e.h.l.)

Under e.h.l. conditions the opposing surfaces are separated by an unbroken film of lubricant which is drawn into the gap between the surfaces by their motion. Very high pressures are generated within the oil film which supports the load. Consequently appreciable elastic distortion occurs in the surfaces.

If two spheres of radii R_1 and R_2 are loaded together, the radius a of the area of contact can be calculated and is called the Hertz radius.

In a dynamic case the distortion of the surfaces is

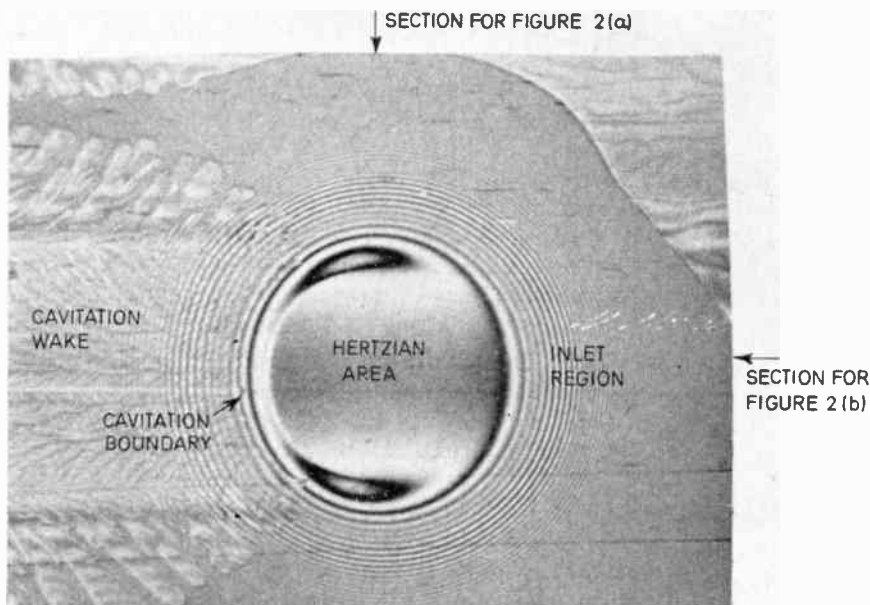


Fig. 1. Interferogram of an e.h.l. point contact.

basically Hertzian, but is modified by the load-supporting requirements and pressure generation in the lubricant film separating the two surfaces. Reynolds's equation shows that pressure generation in the lubricant occurs only when the two surfaces are converging, and thus pressures in the oil start to increase some way upstream of the edge of the equivalent Hertzian area. As the pressure in the lubricant increases the viscosity also approximately increases as:

$$\eta_p = \eta_0 \exp \alpha p \quad (1)$$

where η_p is the viscosity of oil at pressure p ,

η_0 is the viscosity of oil at zero pressure and

α is a constant, pressure coefficient of viscosity.

This expression is valid up to about 2000 lb/in², (14 MN/m²).

Interferometry was used to measure the profile of oil films formed when a ball is loaded against and rolls on a glass disk. Figure 1 is a typical photomicrograph from which measurements were taken. It is a picture of the interference fringes seen when the contact between ball and plate is viewed normally through the glass, using a microscope. The black contours are interference fringes linking points in the oil film of equal optical thickness. Thus after a correction has been made for the pressure dependence of the refractive index of the oil the film profile as shown in Figs. 2(a) and (b) may be obtained. These represent sections of the oil film, with the associated pressure distribution. Superimposed on each is the Hertzian pressure distribution for that particular load.

The section shown in Fig. 2(a) is taken through the centre of the contact in the direction of rolling of the ball. The vertical scale is exaggerated with respect to the horizontal. It can be seen that the oil film is of almost constant thickness throughout the contact, except at the exit, with the diameter of the flat portion being only very slightly less than the Hertzian. At the exit, the thickness increases very slightly, and then falls sharply before rising to follow the undistorted profile.

The pressure curve follows very closely the Hertzian pressure distribution in the central parallel part of the film but starts to rise some way ahead of the contact as

predicted by Reynolds's equation. Just before the exit constriction there is a very sharp peak in the pressure, predicted by theory. The magnitude of this peak has not been measured with any accuracy, but its existence has been verified and its value estimated to be at least as high as the Hertzian pressure p_{max} under most conditions. Beyond the peak the pressure falls rapidly and reaches zero a short way outside the Hertzian area.

Figure 2(b) shows a section at right-angles to that in Fig. 2(a), and taken through the points of minimum film thickness. Because of leakage of oil out of the side of the contact the central portion is not so parallel as in Fig. 2(a). In addition, just inside the Hertzian area on either side, the film thickness drops to a value of about 0.6-0.7 of that found in the centre of the contact, h_0 . This thickness is denoted by h_m . The pressure in the centre of the film again follows the Hertzian distribution, but drops off more rapidly at the edges due to leakage. The side-closures in the oil film and the constriction at the exit gives the interferogram of Fig. 1 its characteristic horse-shoe shape.

At the downstream edge, or exit, of the contact the predicted pressure becomes negative, and consequently the oil is placed in a state of tension. The film therefore ruptures, this happening at a film thickness of about 1.5 times the minimum thickness directly upstream. Bubbles of gas, previously in solution in the oil, as well as of oil vapour are formed. This cavitation will occur preferentially on scratches or marked surface irregularities, and frequently microscopic bubbles adhering to the surfaces assist in the process.

Wedeven⁵ has shown that in order for a full stable film to be maintained the contact must operate in a fully flooded condition. Thus there must be sufficient oil in the gap ahead of the contact for the pressure build-up to occur. The motion of this 'oil-reservoir' has been examined in detail by Tipei.⁶ Because of the comparatively large volume of the oil ahead of the contact, and the small film thickness, the time taken for the volume of oil present to flow through the gap is considerably longer than the actual transit time of the gap. When the oil does

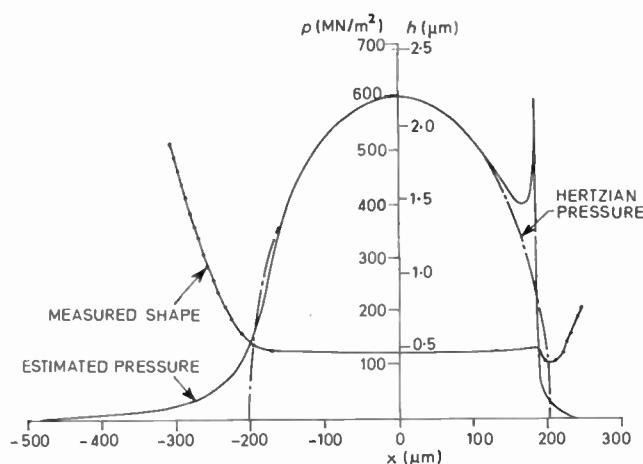


Fig. 2(a). Measured film shape and estimated pressure distribution along the centre line in the direction of rolling.

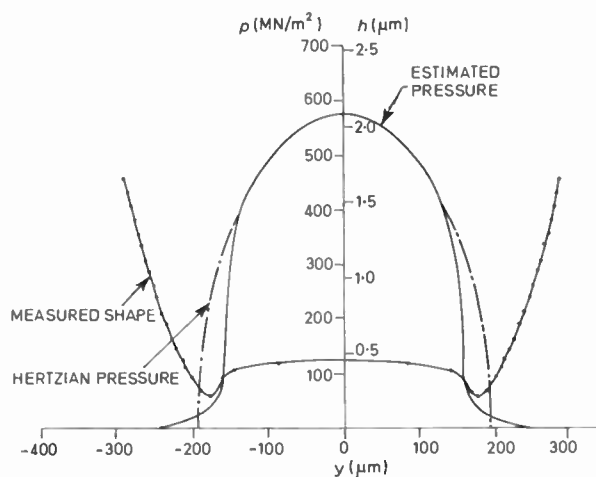


Fig. 2(b). Measured film shape and estimated pressure distribution in the transverse direction at the location of minimum film thickness.

pass through the gap it is subjected to such high pressures that, particularly with the more viscous oils, the liquid is 'super-preserved' or pressure-frozen.

Jacobson⁷ has measured the pressures at which lubricants freeze, and has shown these to be much less than a typical Hertz pressure. Poon⁸ has pointed out that due to the wide spread of molecular weights in common lubricants crystallization is unlikely to occur, particularly within the time available.

A possible structural relaxation in the glass transition has been discussed at length by Litovitz.⁹ Associated liquids in which the association is due to 'directed' forces between molecules, as is found in lubricants, tend to have a higher degree of order than non-associated liquids. Consequently structural relaxation becomes important as the orientating of molecules during crystallization involves the breaking of these bonds. Thus these liquids tend to supercool and vitrify, and the association increases the activation energy, and slows up the rate of crystallization. In the region of the glass transition temperature the relaxation times for structural rearrangements can be of the order of minutes or longer. From these observations, and from experimental measurements in a lubricated contact, it has been suggested that the lubricant in passing through a contact forms what Litovitz has termed a 'pseudo-glass'—that is, it remains a liquid but with the properties of a glass. In addition Gentle¹⁰ has suggested the possibility of small volumes of glass or solid nucleating in the body of the liquid, giving it some of the physical properties of a powder.

5 Film Thickness Formulae

Unfortunately theory lags behind experiment when providing equations for point contact film thickness, due to computational problems. Nevertheless the available expressions are in moderate agreement. It is found that the variables which have the greatest effect on the film thickness are the viscosity at ambient pressure η_0 , the pressure viscosity coefficient, α , the effective radius of curvature of the contact, R' , and the combined contact speed U .

Westlake⁴ deduced the following empirical formula for h_0 :

$$\frac{h_0}{R'} = K_1 \cdot (U^*)^{a_1} \cdot (W^*)^{b_1} \cdot (E^*)^{c_1} \tag{5}$$

where U^* , W^* , E^* are the non-dimensional speed, load and materials parameters respectively, and

$$K_1 = 62(U^*)^{-0.063}$$

$$a_1 = \frac{1}{90} \log_{10} W^* + 0.89$$

$$b_1 = \frac{1}{43} \log_{10} U^* + 0.303$$

$$c_1 = 0.55.$$

As the mechanics of the experimental apparatus used in this work are identical in principle to Westlake's, equation (5) has been used when values of h_0 have been required.

6 Experimental Results

A variety of lubricants was used in the test rig, and they are listed in Table 1. It was found that the results were

Table 1

Lubricant	Viscosity at 100°F (centistokes)	Description
Squalane	20	Hydrocarbon C ₃₀ H ₆₂ . Stood over silica gel before use
Squalane 4 0.1% stearic acid	20	
5P4E	363	Polyphenyl ether; 5-phenyl 4-ether. A mixed isomer
TN 631	137.5	A medium viscosity mineral oil by Shell
Teresso V78	152	Paraffinic mineral oil, doubly filtered

independent of the lubricant, implying that the chemical nature of the fluid is unimportant in this context. Similarly different surface finishes were used on the disk, ranging from 0.254 μm c.l.a. to better than 0.2 μm c.l.a. The finish on the ball was always better than 0.025 μm c.l.a. The finish on the disk did not affect the results except where stated, that is, at low film thicknesses, within the range of asperity contacts; in addition changing the polarity of the applied voltage produced no change in the results.

It is found convenient to classify the experimental data according to the current range. Thus there are three broad groups of results; there is no sharp transition between one current range and the next.

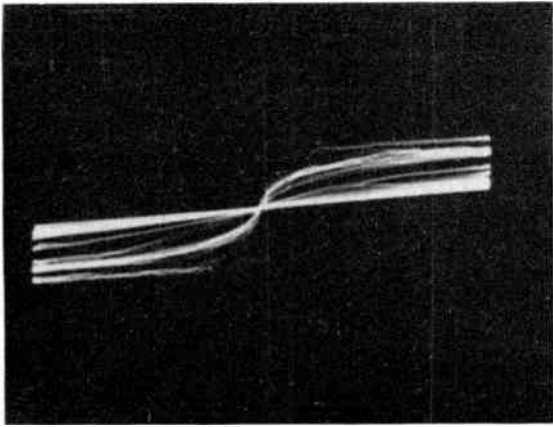
The first extends from zero to about 50–100 mA and may be described as the low-current regime. The high current regime begins at about 1.5 A, and has no apparent upper limit. Linking these two there is a rather indeterminate region in which characteristically unstable phenomena are observed. This is termed the intermediate current regime. The basic conduction processes in thin oil films are characterized by the low-current measurements, which will be described in detail.

6.1 //V Characteristics using a C.R.O.

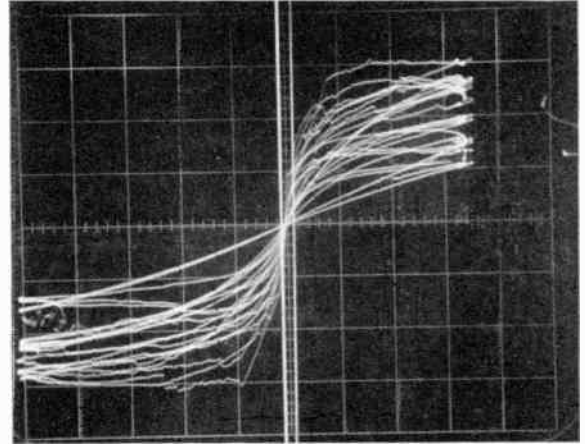
The current source was driven from a 1 kHz sinusoidal voltage generator and the voltages developed across the oil film and across a standard series resistor were displayed on the Y and X axes of the c.r.o., respectively.

A typical set of //V characteristics for different ball speeds is shown in Fig. 3.

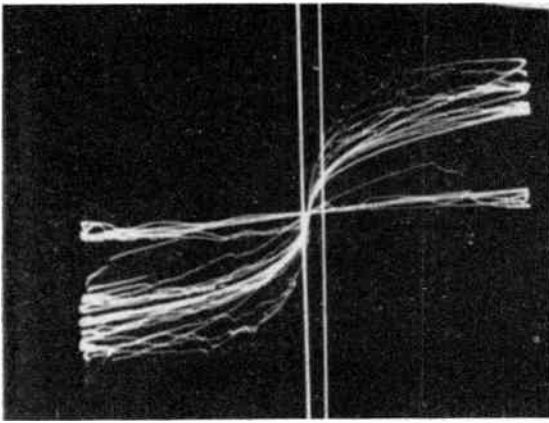
The absolute value of resistance at any point on the curves tends to increase with speed, and consequently with film thickness. In effect the maximum resistance at a given current level increases with thickness, although increasing the film thickness by no means precludes the occurrence of lower values. Indeed states of apparently zero resistance occasionally occur indicating a possible metallic contact, except in the higher speed ranges. At low speeds the characteristics were effectively continuous with time, whereas at high speeds they occurred intermittently—as a consequence the camera shutter was held open until suitable characteristics were recorded. At low speeds typical exposure times of 1/25 second were employed to record the //V characteristics.



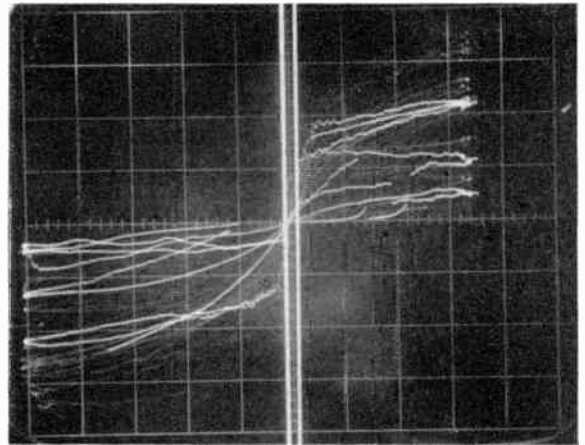
(a) 16.5 rev/min.



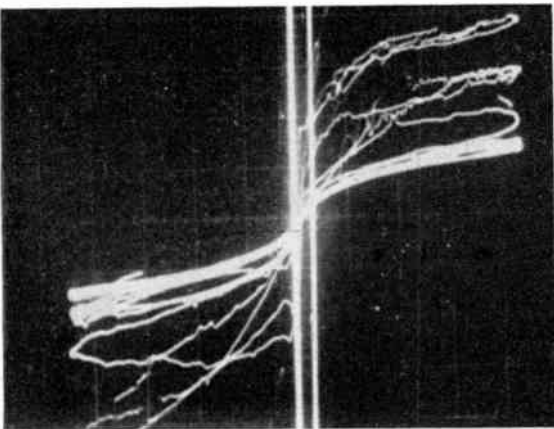
(a) 5 lb (2.27 kg).



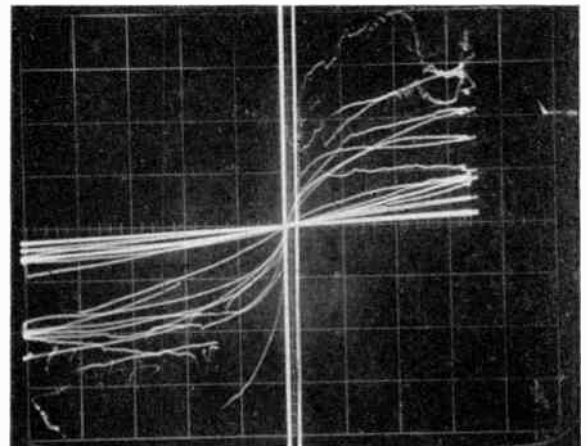
(b) 33.2 rev/min.



(b) 10 lb (4.54 kg).



(c) 77.8 rev/min.



(c) 15 lb (6.80 kg).

Fig. 3. I/V characteristics at different speeds. 5P4E, disk $0.019 \mu\text{m}$ c.l.a., load 2.3 kg, $x = 0.33 \text{ mA/div.}$, $y = 1 \text{ V/div.}$

Fig. 4. I/V characteristics at different loads. 5P4E, disk $0.076 \mu\text{m}$ c.l.a., ball speed 47.5 rev/min, $x = 0.66 \text{ mA/div.}$, $y = 1 \text{ V/div.}$

Figure 4 shows characteristics observed under similar conditions but with a varying load. The curves are all very similar, and due to the irregularity of the traces no firm conclusions can be drawn from them. However, at higher loads the incidence of a zero resistance is a little greater.

A selection of the curves obtained were sufficiently clear and apparently continuous to warrant further examination. These included I/V characteristics from all the lubricants tested, and the procedure was as follows. The corresponding values of current and voltage were measured from the trace using a travelling microscope, in order that the curve might be retraced in different forms. The following curves were then plotted using the values of current and voltage obtained from the photograph in order to find a meaningful analytical relationship describing the form of the curve.

- (i) $\log I$ vs. $\log V$ linearity implies $I \propto V^m$
 - (ii) I/V vs. V linearity implies $I \propto mV^2 + cV$
 - (iii) $\log I/V$ vs. V linearity implies $I \propto V \exp(mV)$
 - (iv) $\log I/V$ vs. $1/V$ linearity implies $I \propto V \exp(m/V)$
 - (v) $\log I/V^2$ vs. $1/V$ linearity implies $I \propto V^2 \exp(m/V)$
- where m is the appropriate gradient in each case.

Despite the apparent disparity between the curves studied two interesting results were found. In two cases a plot of type (i) gave a straight line of gradient 2, indicating that $I \propto V^2$. This was confirmed by plot (ii) also being linear and having the intercept $c = 0$. The other three graphs were non-linear. An example of these graphs is shown in Figs. 5 and 6.

6.2 I/V Characteristics using X-Y Recorder

The low-current characteristics of a 5P4E oil film were also studied using a Bryans X-Y plotting table, giving a time-average of the current-voltage values. An example of the trace obtained is shown in Fig. 7. Branch (a) was plotted as the current increased, whilst branch (b) was obtained by reducing the current. In this case the current was controlled by hand, using the panel control on the Roband Varex power supply, and it was found that above

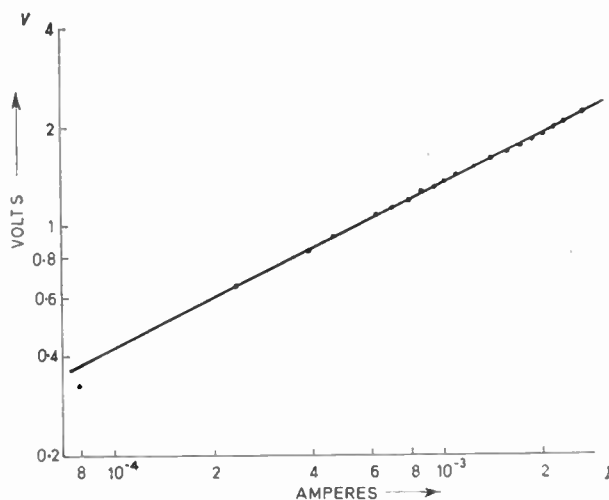


Fig. 5. Plot of $\ln V$ against $\ln I$ from curves of the type shown in Figs. 3 and 4; gradient = 0.5.

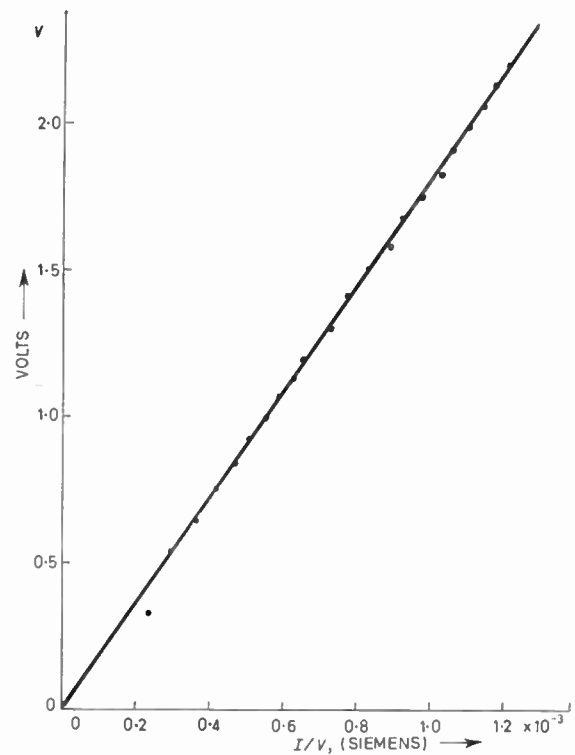


Fig. 6. Plot of V against I/V from curves of the type shown in Figs. 3 and 4; $I \propto V^2$.

a certain current the current increased even if the supply voltage was reduced, despite there being a 20 kΩ resistor in series with the oil film. The current 'runaway' began at about 1.5–2 μA, and it can be seen that although the supply voltage was decreased at 3 μA the current continued to rise. The return branch showed a marked linearity. Although the voltage values were non-reproducible between successive plots, the characteristic obtained was of the same form, with the return branches all linear and of approximately the same gradient. It was found that the voltage was very sensitive to the ball speed, and at high speeds the oil film acted as an effective open circuit, as far as these mean measurements were concerned.

By drawing a 'best fit' continuous curve through the experimental plot, it was possible to perform the same analysis as was carried out on the photographs obtained from the c.r.o. Again a plot of type (3) was linear, and is shown in Fig. 8. Similar results were obtained with the 5P4E and Teresso V79. With all these lubricants the maximum voltage developed across the film was non-reproducible, but nevertheless tended to increase with film thickness.

6.3 Time Dependence of V

The variation with time of the voltage dropped across the oil film was recorded photographically, using a c.r.o. and a single-sweep time-base. The effect of load, speed and maximum applied voltage was examined, using a 1 kΩ resistor in series with the oil film to limit the current drawn from the power supply. The results using 5P4E

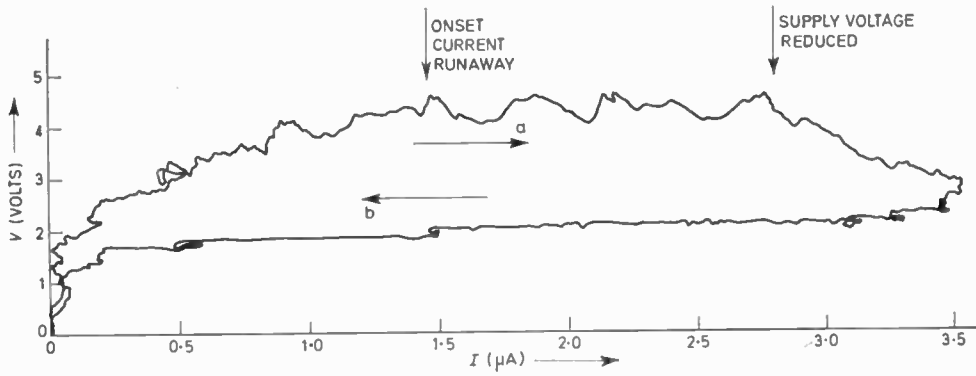


Fig. 7. Plot of V against I from X-Y recorder; TN (31, speed 92 rev/min, load 2.4 kg.

are shown in Figs. 9 and 10. It will be seen that there are in effect two resistive states of the oil film—one high, the other low. When in the low resistance state the mean voltage is effectively independent of both the film thickness and the current, which has maximum values of 10, 20 and 30 mA at the three voltage levels—see Figs. 9 (a), (b), (c) and 10 (a). The probability of finding the film in the low resistance state increases very markedly with the maximum applied voltage, and very slightly with decreasing speed. As the photographs displayed were taken with the same sweep speed it might be expected that the number of 'low' states in one frame increases with speed—this is indeed the case.

The most interesting effect is that of pressure. When the load is doubled, i.e. from Fig. 10 (a) to (b) the time spent in the 'low' state is increased dramatically. The 'low' state itself is independent of the load, and it would seem that the effect of the increase is to alter the ease of transition from the 'high' to the 'low' state. As both the number of transitions per unit time and the length of

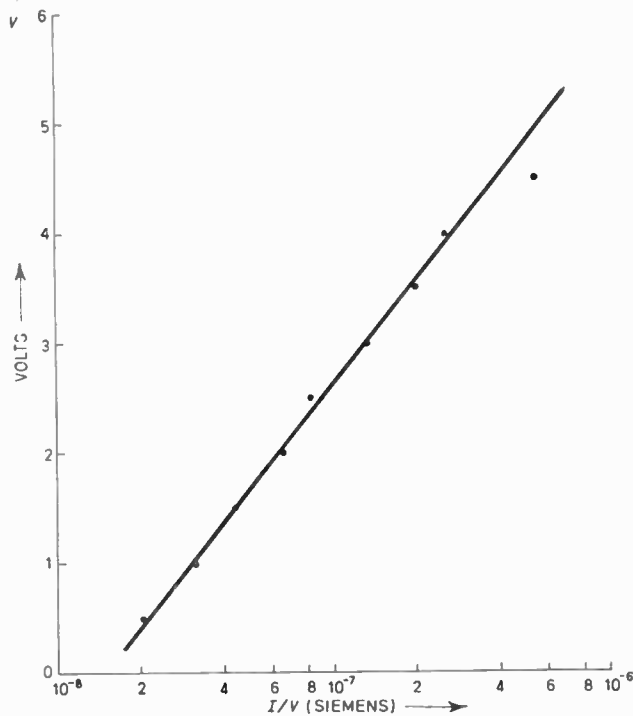
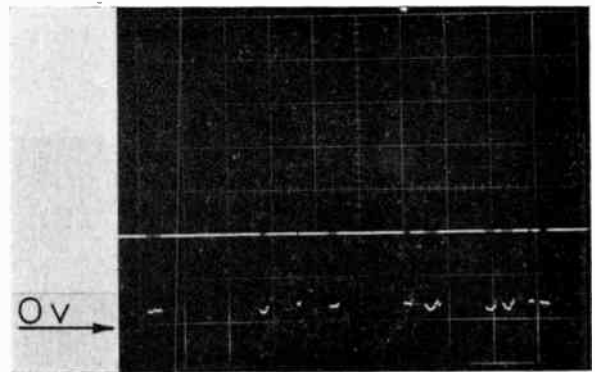
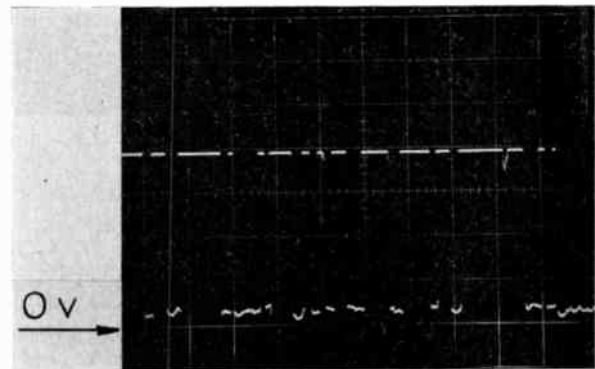


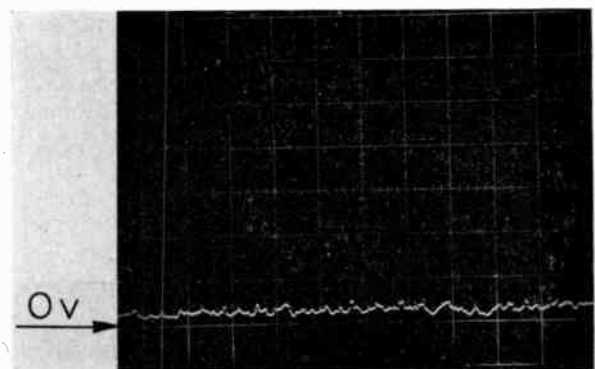
Fig. 8. Plot of V against $\ln I/V$ from Fig. 7; slope 0.716 V^{-1} .



(a) 10 V.



(b) 20 V.



(c) 30 V.

Fig. 9. V against time at different applied voltages. 5P4E, disk $2 \mu\text{m}$ c.l.a. load 2.4 kg, $x = 5 \text{ ms/div}$, $y = 5 \text{ V/div}$.

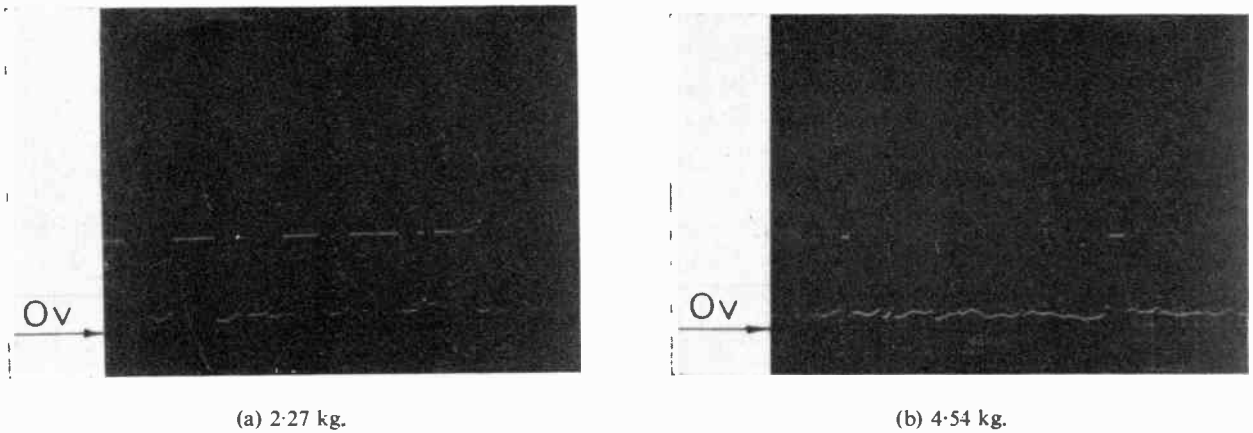


Fig. 10. V against time at different loads; 5P4E, disk $0.05 \mu\text{m}$ c.i.a., speed 61.5 rev/min , 10 V applied, $x = 5 \text{ ms/div}$, $y = 5 \text{ V/div}$.

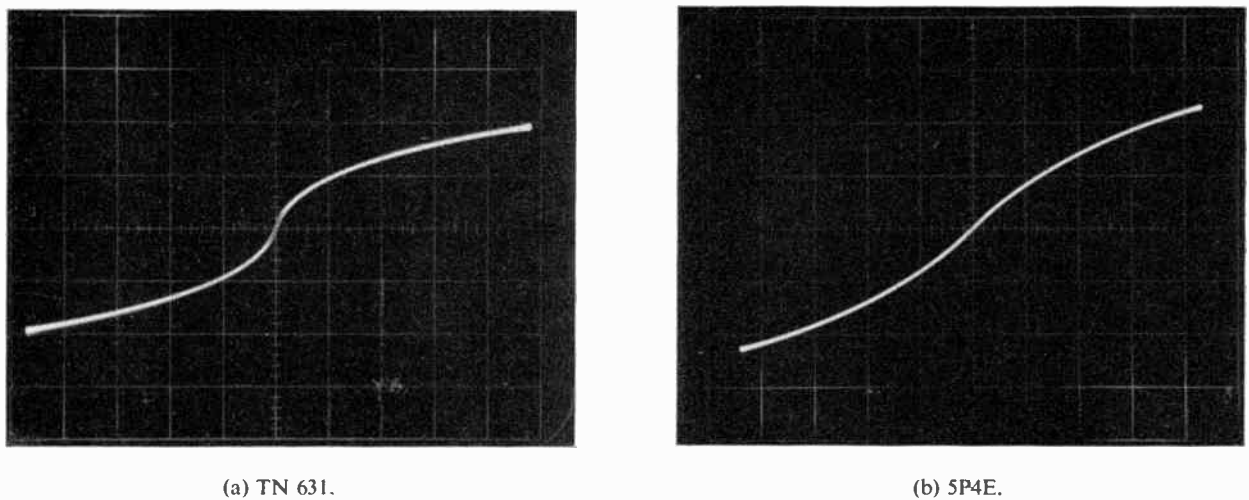


Fig. 11. I/V characteristics for static films; $x = 0.33 \text{ mA/cm}$, $y = 1 \text{ V/cm}$.

time spent in the high state is decreased by the pressure, it would seem that the reverse transition, that is from low to high, is made less probable by the pressure increase. Thus, rather than the mechanism itself which causes the transition being pressure dependent, it is the transition probability which is apparently pressure sensitive, unless the same mechanism is responsible for both types of transition. The mechanical effects of doubling the load can be determined from theory. The nominal contact area will increase by a factor of about 1.6, and the maximum pressure in the centre of the film will increase by a factor of 1.2. The film thickness will decrease by a factor of 0.925.

6.4 Static Oil Films

Measurements on static oil films were made using a 1 kHz current waveform and displaying the I/V characteristic on a c.r.o. Typical traces thus obtained are shown in Fig. 11 where it will be seen that the characteristics are non-ohmic.

It must be remembered that the mechanical conditions in the 'contact' in this case are very different from the dynamic situation. There is the obvious difference of

relative motion. In addition in order to establish a stationary oil film the loading between ball and steel plate is effectively zero. Hence there will be no Hertz pressure, and the ball will be undistorted. Similarly any asperities on the surfaces will stand up to their full height. Consequently the apparatus was exceedingly sensitive to the slightest vibration, there being no oil film under pressure to cushion any motion.

The curves were treated in exactly the same manner as those described earlier, but none of the plots (i)-(v) yielded a linear relationship.

6.5 Capacitance of Dynamic Oil Films

The capacitance of the ball and disk when separated by an e.h.l. film was measured using a Wayne Kerr B221 bridge with an external source. A c.r.o. was used as the detector.

The stray capacitance of the system with the ball not loaded against the plate, i.e. with a gap of about 6 mm between the two, was measured. This was then subtracted from the values measured under e.h.l. conditions to give the approximate capacitance of the oil film.

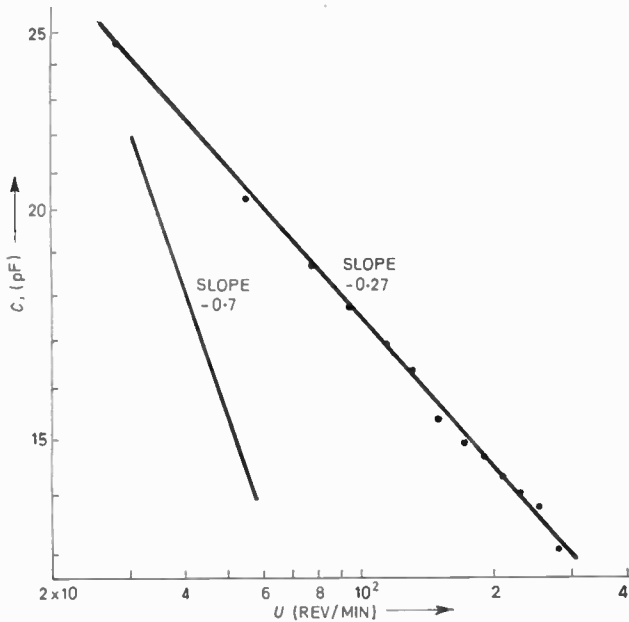


Fig. 12. Plot of ln (capacitance) against ln (ball speed) for fixed load (TN 631).

The variation of the capacitance with load and speed where TN 631 is the lubricant is shown in Figs. 12 and 13. Similar plots were obtained with other lubricants. In order to obtain the capacitance of the whole rig, the measured stray rig capacitance of 10.3 pF should be added to the values recorded.

It will be seen that the capacitance does not vary with speed quite as the film thickness does, otherwise the slope of Fig. 12 would be expected to be about 0.7. This is because a very large contribution to the measured values of capacitance comes from the surfaces just outside the contact. If the film thickness in the contact is increased by, say, 50%, the percentage increase of the separation of the surrounding surfaces will be much less due to their divergence. Thus the capacitance will not be as sensitive to ball speed as is the film thickness.

Similarly the variation with load is not as great as might be expected. This is despite the fact that the bulk dielectric constant of the oil is known to increase with pressure, and also increased pressure both increases the Hertzian radius and decreases the film thickness. All these factors assist in increasing the capacitance.

Assuming that the cross-section of the ball can be approximated by a parabola in the region of the contact, an approximate calculation shows that the capacitance C is given by

$$C = 4\pi\epsilon_0 \epsilon_1 r \log_e(r/4h) + \epsilon_0 \epsilon_2 \pi a^2/h$$

where the second term is the contribution from the contact area and the first is due to the peripheral surfaces. In addition,

- ϵ_0 is the permittivity of free space
- ϵ_1 is the relative permittivity of oil at ambient pressure (~ 2)
- ϵ_2 is the relative permittivity of oil at Hertz pressure (~ 5)
- r is the radius of ball (1.27 cm; 0.5 in)

- a is the Hertz radius ($\sim 127 \mu\text{m}$; 5×10^{-3} in)
- h is the film thickness ($\sim 0.5 \mu\text{m}$; 2×10^{-5} in).

Substituting typical values as shown in brackets, it is found that C has a value of about 23 pF, and the ratio of the first to second terms is about 50.

6.6 Summary of Results

The results described above were found to be insensitive to properties of both the oil and electrode surfaces. Synthetic and mineral oils were used, as well as a hydrocarbon, and surface finishes ranging from 0.2 to 0.25 μm . Both filtered and unfiltered oils were used, with no marked change in properties.

At low currents the conductivity was found to rise with voltage, as $\exp(\alpha V)$. The value of α was about 0.3 V^{-1} . The ability to conduct was shown to be very pressure-dependent, and also to be sensitive to either the maximum current that is able to flow through the film or the maximum voltage that may appear across it.

At high currents, that is, about 1.5 A the mean voltage drop across the film is approximately constant at about 0.3-0.35 V. This is independent of both film thickness and current.

6.7 Discussion of Results

Comparing the static with the dynamic measurements it is clear that, as the lubricant passes through the contact, the mechanical processes to which it is subjected alter the electronic properties considerably.

From the results the current is proportional to $V \exp(\alpha V)$ which is characteristic of space-charge limited current in the presence of a uniform distribution of traps. Space-charge limited current has been shown to occur in thin films of organic polar liquids associated with metal surfaces by, for example, Brockman.¹¹ We therefore

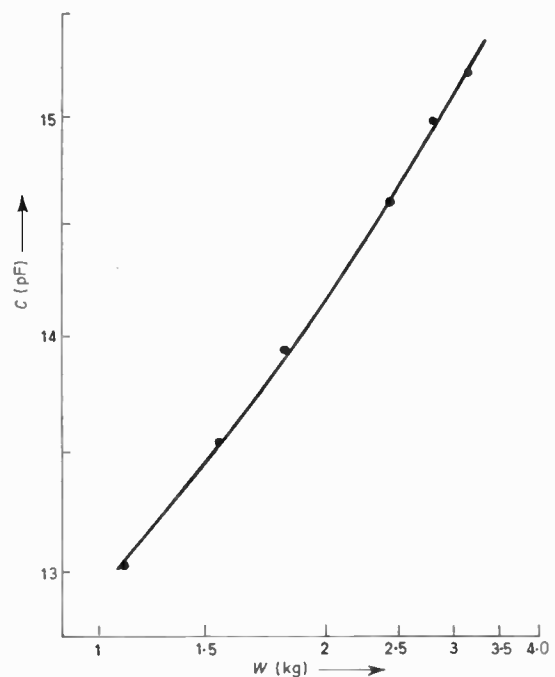


Fig. 13. Plot of log (capacitance) against log (load) for fixed speed (TN 631).

require to explain the presence of trapping centres in the oil film and to confirm that the conditions are favourable for the establishment of the space charge in this situation.

As discussed earlier, the oil film is highly compressed to a quasi-solid state in the contact so that it is possible for electron trapping centres to exist. Since the material is polar, polarization around the trapping centre will increase its energy depth in the band gap. Mott¹² has shown that localized states can exist in an amorphous material and Caserta *et al.*¹³ demonstrated the existence of a band structure, with a uniform distribution of traps, in amorphous organic films.

As the oil passes through the contact it is proposed that the following process occurs. Due to the very high pressures involved the oil will be compressed beyond the pressure at which it freezes at the particular operating temperature. So long as the time of transit of the oil through the contact is greater than the structural relaxation time, the oil will form a solid—possibly crystalline but more probably vitreous due to the time scale involved. Associated with this highly compressed glassy material there will be a fairly well defined band structure and trap distribution within the energy gap. As the rate of the passage of oil through the contact is increased a point will be reached at which the probability of glass formation by freezing becomes very low. Because the relaxation time is essentially a statistical function there is no guarantee that an element of the lubricant will not freeze, but the probability becomes vanishingly small. Thus as the speed is increased the nature of the trap distribution might be expected to alter. Nevertheless, due to the pressures applied to the liquid, with consequent rapid changes of density, traps will still be formed in the film. In addition it has been demonstrated that liquid molecules—hydrocarbons and others—are capable of trapping electrons in their structure

The conductivity of liquid 5P4E at low pressures has been studied by Reed¹⁴ who demonstrated that the conduction mode was that of single charge injection space charge limited current (s.c.l.c.). The carriers were assumed to be electrons that were attached to molecules to form negative ions. This is of interest when considering Fig. 5, which is a typical s.c.l.c. characteristic. Using the data from this figure and assuming that it is described by the Mott and Gurney law, an order of magnitude for the mobility μ can be determined. If the area of the conducting material is taken to be the Hertzian area, μ is found to be 10^{-12} cm²/Vs, which is extremely low. Even if the current path occupies only a small fraction of the contact area the value of μ would still be orders of magnitude below the lowest measured values as found in liquids and solids in the absence of traps.

In the presence of a single or dominant trap, Barbe and Westgate¹⁵ have shown that the current density is given by

$$J = \frac{2}{3} \epsilon \mu V^2 / d^3 \frac{N_c}{n_t} \exp \left(\frac{E_t - E_c}{kT} \right)$$

where N_c is the density of conduction states,
 n_t is the density of trapping states,
 E_c is the conduction band energy and
 E_t is the energy of trapping level.

For a given value of J this will give a larger value of μ than does the Mott and Gurney law. It is therefore proposed that the band structure of the oil film may have a single or dominant deep trap of large cross-section, which will effectively reduce the current. Simmons and Taylor¹⁶ have shown that under non-equilibrium steady-state conditions, a distribution of traps in the band gap leads to an energy-localized peak in the probability of occupancy within the band gap. This has the same effect as that of a single trap of large capture cross-section, and experimentally a distribution of traps may be indistinguishable from a single trapping level. This was particularly apparent in the case of an amorphous material exhibiting the 'tail' to the density of states due to intrinsic disorder, as predicted by Mott.¹² Thus it would seem that the apparent single trap observed in this case is in fact a characteristic of a trap distribution under particular steady-state conditions. The result obtained below for the trap distribution implies that the Simmons and Taylor¹⁶ conditions do not always apply in this situation.

Now the exit of the film is in many respects analogous to a deep trap, as the charge that is drawn out of the film is effectively lost to the conduction process. However the 'exit trap' does not contribute to the space charge, and merely acts as a current sink. The contribution to the current is small. Nevertheless a simple criterion can be evolved on the basis of the 'exit trap' to determine the combination of film speed and thickness at which charge is no longer able to cross the film in the time available. If a charge is injected into an element of oil as soon as it enters the contact, in order for the charge to be collected by the other electrode before the element of oil is expelled from the contact it must have travelled at least half the distance between the surfaces. As the oil film is assumed to divide down its centre line into two equal portions on cavitation, the charge will then be removed by the oil on the collecting electrode and still have a finite chance of contributing to the conduction current.

Assuming a uniform field throughout the contact, the time taken by the charge to cross half the oil film, of thickness h_0 , in a field E is

$$t_{\frac{1}{2}} = \frac{h_0}{2E\mu}$$

where μ is the mobility. The transit time of the contact is

$$t_c = \frac{2a}{U}$$

where a is the Hertz radius and U the surface speed of the ball. For conduction,

$$t_c > t_{\frac{1}{2}}$$

or

$$\frac{2a}{U} > \frac{h_0}{2E\mu}$$

Using 5P4E it is found that at speeds in excess of 20 cm/s, at film thicknesses of the order of 2 μ m and a Hertz radius of 125 μ m, the film is apparently an almost continuous open circuit at 10 V applied voltage. Using these figures a maximum value for μ of about 2×10^{-6} cm²/Vs is arrived at.

Using the value of the mobility thus obtained, an order of magnitude calculation may be made to show that the data obtained are consistent with the accumulation of space charge. The calculation compares the amount of carriers that are known by experiment to enter the film with the rate at which charge would cross the film assuming ohmic conditions.

If C is the capacitance of the contact itself, of cross-sectional area A and thickness h_0 , then the electron density at a voltage V can be written as

$$n_e = \frac{CV}{Ah_0 e} \text{ cm}^{-3}$$

where e is the electronic charge. Now the current density J at a field E , assuming ohmic conditions, is given by

$$J = n_e e \mu E.$$

In the terms of the number of electrons N_e flowing through the film

$$N_e = \frac{JA}{e} = n_e e \mu EA = \frac{CV^2 \mu}{h_0^2} \cdot \frac{\mu}{e}$$

In the capacitance measurements the value of C was found to be 4×10^{-13} F, and the other variables took the following values

$$\begin{aligned} V &= 2 \text{ V} \\ \mu &= 2 \times 10^{-6} \text{ cm}^2/\text{Vs} \\ h_0 &= 10^{-4} \text{ cm} \\ e &= 1.6 \times 10^{-19} \text{ C}. \end{aligned}$$

Thus $N_e = 5 \times 10^8$ electrons/s.

Now the measured injection current is 1 mA under these conditions, or 6×10^{15} electrons/s. It will be seen that this figure is far in excess of the result derived if the film was ohmic, and hence the conditions are favourable for the accumulation of charge necessary for s.c.l.c.

6.8 The Influence of the Surfaces

In the above discussion it has been assumed that the metal surfaces make ohmic contacts with the oil film, that is, they provide an effectively infinite supply of electrons to the oil film and the solid-liquid interface offers a negligible potential barrier to the current flow. If there was a potential or Schottky barrier at the surface there should be a detectable difference between the behaviour of the film when different surface finishes were used on the disk. A rougher surface should assist in the injection of electrons through a Schottky barrier due to the field concentration at asperity tips. In practice, surfaces ranging from 0.012 μm c.l.a. to 0.25 μm c.l.a. roughness were used, and there was no detectable difference which could be attributed to the comparative ease of charge injection by field emission. Any potential barrier will probably be independent of the metal work function, and will be a function of the charge distribution in the liquid. Morant¹⁷ showed that any potential barrier would be lowered by the space charge to give an effective barrier height, at 300 K, of

$$\phi_{\text{eff}} = 1.115 - \frac{1}{40} \log_e(n_i)$$

where n_i is the density of accumulated charge.

Using a result derived below, namely that the liquid may support a possible trap density of $10^{16} \text{ cm}^{-3} \text{ eV}^{-1}$, and assuming that the distribution of traps covers only 0.3 eV and only 10% of these traps are occupied, the effective barrier height would be of the order of 0.3 eV. With the space-charge screening predicted by Simmons¹⁸ causing a very thin barrier—of the order of angstroms—to be formed, the surfaces can be regarded as an effective ohmic contact.

6.9 The Trap Density and Trap-filled Limit

From the plots of $\log I/V$ vs. V , the value of α in the relationship

$$I \propto V \exp \alpha V$$

has been shown to be typically 0.3 V^{-1} . From Caserta *et al.*¹¹ α is given as

$$\alpha = \frac{C}{n_i h_0 e k T}$$

where C is the capacitance/unit area of film

e is the electronic charge

k is Boltzmann's constant and

T is the temperature in kelvins.

At a film thickness of 1 μm C has a value of approximately $4 \times 10^{-13} / 1.5 \times 10^{-4} \pi \text{ F/cm}^2$. Thus at 300 K,

$$n_i \approx 10^{16} \text{ cm}^{-3} \text{ eV}^{-1}.$$

It is of interest, perhaps, to compare this value for n_i with that obtained by Caserta *et al.*, who were investigating thin films of organic polymers. Their measurements led to a value for n_i which ranged from 10^{14} to $10^{18} \text{ cm}^{-3} \text{ eV}^{-1}$. The value of $10^{16} \text{ cm}^{-3} \text{ eV}^{-1}$ arrived at above does not, therefore, appear to improbable.

As the current level is increased a point will be reached at which all the traps in the material have been filled, and the 'exit trap' is flooded. This effectively reduces the capture cross-section of the traps to zero, and any charge injected into the film will make an unimpeded passage to the other electrode. Thus a sudden increase in the current level will be observed, and this has been noted in the discussion of Fig. 7. There are two further points to be made in this context. As fresh lubricant is being drawn into the contact which is not in the trap-filled limit (t.f.l.), the current increase will not be as rapid as might be expected with a static specimen, as the fresh lubricant has to be subjected to charge injection before reaching the trap-filled state. In addition, the transition will not be sharp. As the traps become filled the effective value of n_i will decrease, causing J to increase, and only when n_i is effectively zero will the t.f.l. be attained.

The conduction process in this instance acquires many of the qualities associated with switching phenomena, as the film has been transformed into an apparently high conductivity state. The explanations of switching phenomena have frequently invoked a transition temperature, above which conduction is by a low resistance 'hot' filament in the film, and involving a dramatic reduction in the voltage drop across the film. In the phenomenon examined here the effect is rather a very marked increase in the current flow, a characteristic of conduction in the trap-filled limit. The voltage level, of necessity, does not

fall, otherwise the t.f.l. would not be maintained and fresh oil would not be suitably conditioned.

The conduction in the t.f.l. must be through a limited part of the contact area, which can be regarded as a conducting filament. If at an instant of time the density of filled traps within the film reaches saturation point, almost the whole film will be in the t.f.l. state. But after a short period of time some of the 't.f.l. oil' will have been swept out of the contact, and fresh oil will enter upstream. The conducting part of the film will therefore be concentrated at the downstream end of the contact, and this will effectively shunt the incoming oil, thus forming a low resistance path or filament. In order to maintain the t.f.l., the voltage across the film must be kept at a sufficient value to ensure that the fresh oil eventually becomes trap-filled in order to prevent the filament collapsing. Because the stability of the t.f.l. state is dependent upon the voltage level being maintained, the transition can be stabilized by means of an external resistor—an effect which is not possible with the Ovshinsky type of switching phenomenon. The formation and destruction of the t.f.l. filament will vary with dynamic conditions. An increase in pressure will increase the probability of trap formation and hence of the formation of a t.f.l. filament. An increase in speed, which gives a thicker film, will decrease the probability of forming a t.f.l. state. This is in general agreement with the experimental results.

7 Conclusion

Under conditions of elasto-hydrodynamic lubrication oil films exhibit quasi-solid properties. In particular the low-current conductivity fits with the model of space-charge limited current in the presence of traps. An apparent switching-type behaviour is accounted for by the current reaching the trap-filled limit value. The onset and duration of trap-filled limit conduction depends upon the dynamic conditions in the film, due to speed and load.

8 Acknowledgments

The authors wish to thank Dr. A. Cameron for his constant interest in the work and for the laboratory facilities provided. One of us (W. G. F.) acknowledges with gratitude the financial support of the Science Research Council and the Mobil Oil Company.

9 References

1. Brix, V. H., 'An electrical study of boundary lubrication', *Aircraft Engineering*, **19**, p. 294, 1947.
2. Cameron, A., 'Surface failure in gears', *J. Inst. Pet.*, **40**, p. 191, 1954.
3. Fiennes, W. G. and Anderson, J. C., 'An analysis of voltage discharge measurements in lubrication research', *I. Mech. E. Tribology Convention Proc.*, 1972.
4. Westlake, F. J., 'Interferometric Study of Ultra-thin Fluid Films', Ph.D. Thesis, University of London, 1970.
5. Wedeven, L. D., 'Optical Measurements in Elastohydrodynamic Rolling-contact Bearings', Ph.D. Thesis, University of London, 1970.
6. Tipei, N., 'Boundary conditions of a viscous flow between surfaces with rolling and sliding motion', *Trans. Amer. Soc. Mech. Engrs*, **90**, p. 254, 1968.
7. Jacobson, B., 'On the lubrication of heavily loaded spherical surfaces, considering surface deformation and solidification of the lubricant', *Acta Poly. Scand.*, ME 54, 1970.
8. Poon, S. Y., Contribution to discussion of 'Traction in elasto-hydrodynamic contacts', *Proc. Instn. Mech. Engrs*, **182**, Pt. I, p. 326, 1967.
9. Litovitz, T. A., 'Liquid relaxation phenomena and the glass state', in 'Non-crystalline solids', ed. Frechette, V. D., pp. 252-66 (Wiley, New York, 1962).
10. Gentle, L. R. and Cameron, A., 'Granular aspects of elasto-hydrodynamic traction', *Wear*, **27**, p. 71, 1974.
11. Brockman, I. H. 'Electrical properties of thin films of organic liquids associated with metal surfaces', Conference on Electrical Insulation and Dielectric Phenomena, NAS/NRC Publication No. 1870, p. 46, 1970.
12. Mott, N. F., 'Conduction in non-crystalline systems: I. Localized electronic states in disordered systems', *Phil. Mag.*, **17**, p. 1259, 1968.
13. Caserta, G. *et al.*, 'Space-charge-limited current and band structure in amorphous organic films', *Phys. Stat. Sol.*, **35**, p. 237, 1969.
14. Reed, C. W., 'Electrical conduction in polyphenyl ether fluids using electron injection for carrier generation', Conference on Electrical Insulation and Dielectric Phenomena, NAS/NRC Publication No. 1356, p. 59, 1965.
15. Barbe, D. F. and Westgate, C. R., 'Bulk trapping states in β -phthalocyanine single crystals', *J. Chem. Phys.*, **52**, No. 8, p. 4046, 1970.
16. Simmons, J. G. and Taylor, G. W., 'Non-equilibrium steady-state statistics and associated effects for insulators and semiconductors containing an arbitrary distribution of traps', *Phys. Rev. (B)*, **4**, No. 2, p. 502, 1971.
17. Morant, M. J., 'Equilibrium space-charge at the contact of a metal and a pure highly insulating liquid and its influence on high field conductivity', *J. Electrochem. Soc.*, **107**, p. 671, 1960.
18. Simmons, J. G., 'Conduction in thin dielectric films', *J. Physics (D)*, **5**, No. 4, p. 613, 1971.

Manuscript received by the Institution on 16th July 1973. (Paper No. 1572/CC 190.)

© The Institution of Electronic and Radio Engineers, 1974

Factors affecting the design and construction of thin-film magnetic recording heads

ALAN J. COLLINS, Ph.D., B.Eng.(Tech.) *
and

IVOR PREECE, Ph.D., B.Sc., M.Inst.P.

SUMMARY

This paper describes two of the basic types of thin film magnetic recording heads which have been proposed. The advantages and disadvantages of the heads are discussed. The production techniques and magnetic materials which have been employed in the manufacture of these heads are critically examined. Finally, the available experimental results on thin-film magnetic recording heads are compared with the theoretical predictions.

* Wolfson Centre for the Technology of Soft Magnetic Materials, University of Wales Institute of Science and Technology, 30 The Parade, Roath, Cardiff CF2 3AD.

1 Introduction

During the last few years there has been considerable interest in thin-film magnetic recording heads which can be batch fabricated using techniques similar to those employed in integrated circuit technology. An excellent review of the subject has been given by Valstyn¹ and this paper extends that review to include the latest developments. The interest has arisen because: (1) The small size of these heads offers the possibility of higher track densities; furthermore the manufacturing techniques make it possible to position them very accurately with respect to one another, thus allowing fixed head per track recording systems to be manufactured at a reasonable cost. (2) The fast switching properties of the ideal thin film heads in which the magnetization changes take place by coherent rotation, which is a faster process than domain wall motion, would allow higher frequency applications. (3) Theoretical calculations have indicated that the heads would have higher resolution than conventional heads.

2 Types of Head

Basically two types of miniature recording heads have been proposed. The first of these was the 'vertical' head¹ in which the magnetic films forming the magnetic circuit are perpendicular to the plane of the recording medium (Fig. 1). The gap is formed by a conductor sandwiched between the films.^{2,3}

In the second type or 'horizontal' head (Fig. 2), the

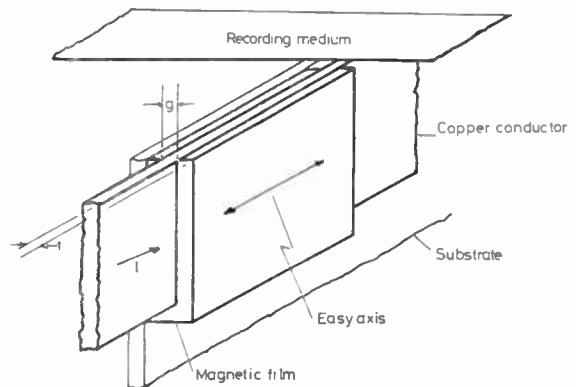


Fig. 1. Vertical head: gap width g , film thickness t , drive field current I .

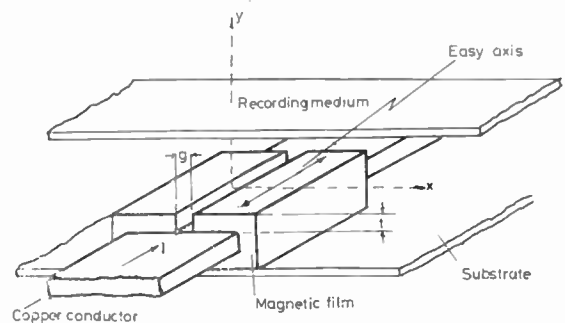


Fig. 2. Horizontal head: gap width g , film thickness t , drive current I .

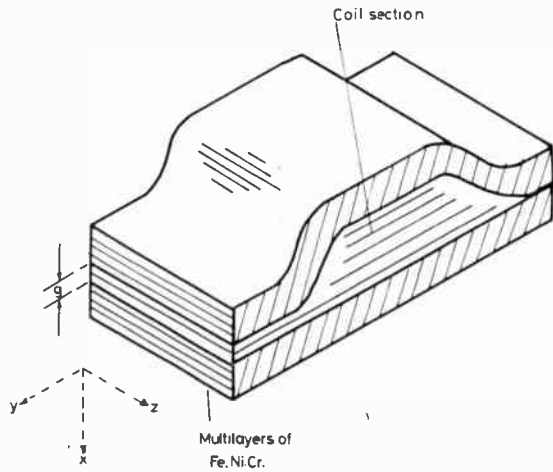


Fig. 3. Multi-turn vertical head manufactured by Lazzari and Melnick.⁹ The insulating layers are of SiO₂. Each leg consists of alternate layers of FeNiCr and SiO₂. *g* is the gap length.

magnetic films are parallel to the plane of the recording medium, and the gap is formed in the magnetic film nearest the recording medium.⁴

In both types of head writing is accomplished by passing a current through the conductor, thus magnetizing the core circumferentially and producing a fringing field at the gap. Reading is accomplished by detecting the voltage pulse induced in the conductor when a magnetization transition in the recording medium passes the gap. In both types of head the magnetic films are normally made anisotropic with the easy axis of magnetization parallel to the gap, so that when writing the film is driven in the hard direction. This is done because in an ideal uniaxial film magnetization changes in the hard direction take place by coherent rotation and secondly the magnetization changes are non-hysteretic and hence there is no remanence. In actual heads because of the magnetization dispersion and demagnetizing fields these ideal reversal conditions are not attained, but they can be approached by suitable choice of material and head geometry. The magnetization dispersion is a function of (1) the magnetocrystalline anisotropy and the magnetostrictive constants of the material, (2) the easy axis skew.⁵ The intrinsic magnetization dispersion is expected to be small in materials in which $K_1 \rightarrow 0$ and $(\lambda_{100} - \lambda_{111}) \rightarrow 0$.^{6,7}

Both types of head have advantages and disadvantages. In the case of the horizontal heads, the complete head can be manufactured using integrated circuit techniques, though the etching of narrow gaps (1–2 μm) in 2 μm of magnetic film, a thickness which is theoretically required if the heads are to be capable of writing into conventional recording materials,⁸ does pose problems. Secondly, because of the thickness of the magnetic material, the horizontal head suffers from the disadvantage that the slightest amount of wear will destroy it. In the case of the vertical head producing a narrow separation between the magnetic films presents little difficulty, but the gap has to be finished by cutting and polishing or lapping.⁸

A disadvantage of both types of single-turn heads is that relatively large currents are required for writing,

and they generate low read signals. For this reason several integrated multi-turn vertical heads have been proposed^{8,9,10} Figure 3 shows the multi-turn head fabricated by Lazzari and Melnick.⁹ The layered structure of the magnetic legs was adopted to reduce the demagnetizing effects.

To overcome the problem of the low sense signals in single-turn heads, Kaske *et al.*¹¹ developed a horizontal read head in which the head magnetization was detected and not the flux from the recording medium. In this head (Fig. 4) the easy axis is perpendicular to the gap, and there is an additional conductor, the read line, perpendicular to the gap. In reading, a recorded domain is positioned above the gap, and a current pulse is applied to the read line of sufficient magnitude to produce a field which saturates the head in the hard direction: On reduction of this hard axis field, the head magnetization is steered into one of the easy axis directions, the direction being determined by the polarity of the recorded domain. The head magnetization linking the sense line changes from effectively zero to the saturation magnetization of the head.

3 Production of Thin-film Heads

3.1 Manufacturing Methods

The magnetic materials used in integrated heads have been deposited by evaporation and electroplating. Though evaporation offers the advantage that all the materials, i.e. magnetic, conducting and insulating if required, can be deposited by the one technique, the method does suffer from certain disadvantages. Firstly, control of the composition of the magnetic film, which is usually a binary or ternary alloy is difficult because of the problems of fractionation. Secondly, because highest efficiency is achieved if the magnetic circuit is closed except for the gap, it is desirable that the top magnetic film is continuous at the edge of the conductor. Because in evaporation the evaporant travels in straight lines, one would expect that this continuity would be difficult to maintain in one evaporation, especially where the thickness of the conductor is greater than the magnetic film. Romankiw *et al.*¹² deposited permalloy films by electroplating from a chloride-nickel iron bath and claimed that control of the composition and the forming of a complete magnetic circuit did not present any great problems. However, the method does suffer from the disadvantage that if non-conducting substrates are used

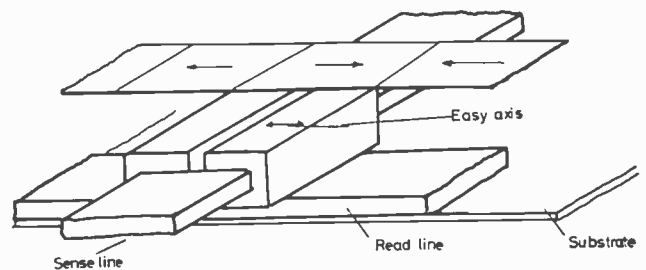


Fig. 4. Read head manufactured by Kaske *et al.*¹¹ Magnetic material NiFe 0.2 μm thick, gap 1.5 μm, sense and read lines copper 2 μm thick.

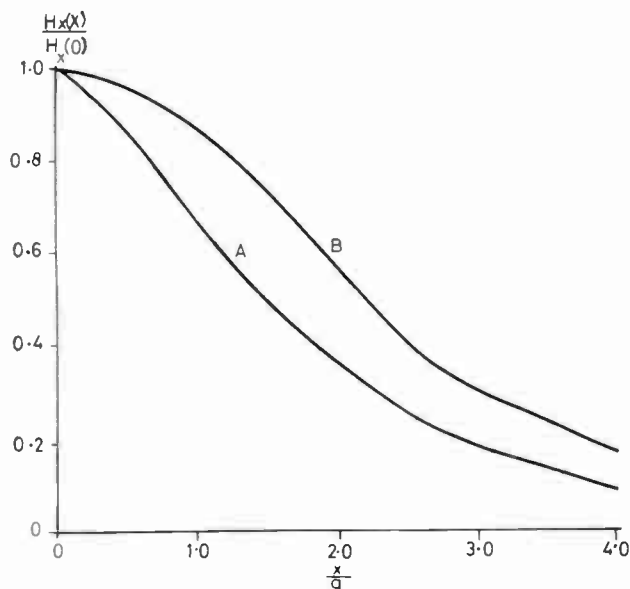


Fig. 5. X component of the write field of a single turn horizontal head (Fig. 2) as a function of x/g for $k/g = 2$ and $y/g = 1$ (curve A), compared to that of a conventional head for $y/g = 1$ (curve B), due to Valstyn and Kosy.⁸

an initial conducting layer must be deposited, also if insulating layers are required then they too must be deposited by other methods. One method which does not suffer from any of these disadvantages is r.f. sputtering, which is currently being employed at the Wolfson Centre for the deposition of high permeability alloys for integrated head applications.

The gaps in vertical heads may be formed either by depositing an insulating layer between the magnetic film or by extending one of the conductors to the pole face. In the case of the horizontal head, forming the narrow gap is somewhat more difficult. Romankiw *et al.*¹² formed a $2\ \mu\text{m}$ wide strip of electron sensitive resist at the gap location before electroplating the top layer. Kaske *et al.*¹¹ used a photo resist, laser exposure and conventional etching technique. Gaps as small as $1.5\ \mu\text{m}$ were formed in $0.2\ \mu\text{m}$ thick Ni-Fe films. No indication was given of the minimum gap widths which could be achieved in films 1 to $2\ \mu\text{m}$ thick. Other possible techniques for forming the gaps are by ion beam milling or sputter etching. The head and conductor patterns can be formed using normal photo-etching techniques.

3.2 Magnetic Material Requirements

The magnetic material used in the head should have a high saturation induction M_s , low uniaxial anisotropy and low magnetization dispersion; this would then result in a high intrinsic permeability. In an ideal thin film the hard axis permeability is given by M_s/H_k where H_k is the anisotropy field. The heads reported in the literature have been made of the binary permalloy composition^{11,12} or permalloy based alloys with small additions of Cr to reduce the anisotropy field⁹ or Co to reduce the dispersion.¹² Additions of Cr however increase the dispersion¹³ while Co causes an increase in anisotropy field.⁹ Other high permeability alloys have been produced in thin film form¹⁴ with lower anisotropy and

magnetization dispersion comparable with the binary permalloys, and though they suffer from the disadvantage that they have a lower saturation induction the limited published work indicates that they have a higher permeability. One high permeability alloy which does offer promise as a head material is Sendust (85% Fe, 5.4% Al, 9.6% Si). Films of this material have been produced at the Wolfson Centre by r.f. sputtering with anisotropy fields as low as 160 A/m (2 Oe) and angular dispersion α_{50} of 3° . This material also has the advantages of a high saturation induction (1.1 tesla, 11 000 gauss) and it is extremely hard wearing. A thick film ($50\ \mu\text{m}$) video head has recently been reported¹⁵ in which the magnetic material was Sendust, deposited by sputtering.

4 Comparison of Experimental Results with Theory

4.1 Horizontal Head

Valstyn and Kosy⁸ calculated by means of a micro-magnetic analysis that a single-turn horizontal head made of permalloy films $2\ \mu\text{m}$ thick would be able to write into conventional particulate coatings with currents of a few hundred milliamperes at a distance of $2\ \mu\text{m}$ from the gap. They also predicted that in writing the resolution of the horizontal head was superior to that of the conventional head (Fig. 5).

Watanabe *et al.*¹⁶ was the first to report the manufacture of a version of the horizontal head in 1969, but this head was not however used for magnetic recording. Romankiw *et al.*¹² using heads with $2.5\ \mu\text{m}$ thick permalloy films and gaps of $2\ \mu\text{m}$ succeeded in writing into conventional oxide recording materials. In these experiments the heads were placed in contact with the medium which was slowly moved across the gap while current pulses were applied to the head. The current required to approach saturation near the gap was in excess of 1 A.

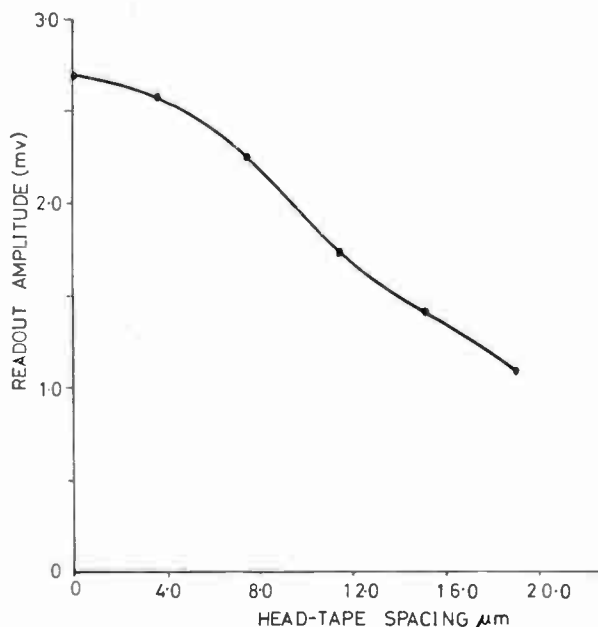


Fig. 6. Output signal as a function of head-to-medium spacing, for the thin film head of Fig. 4.

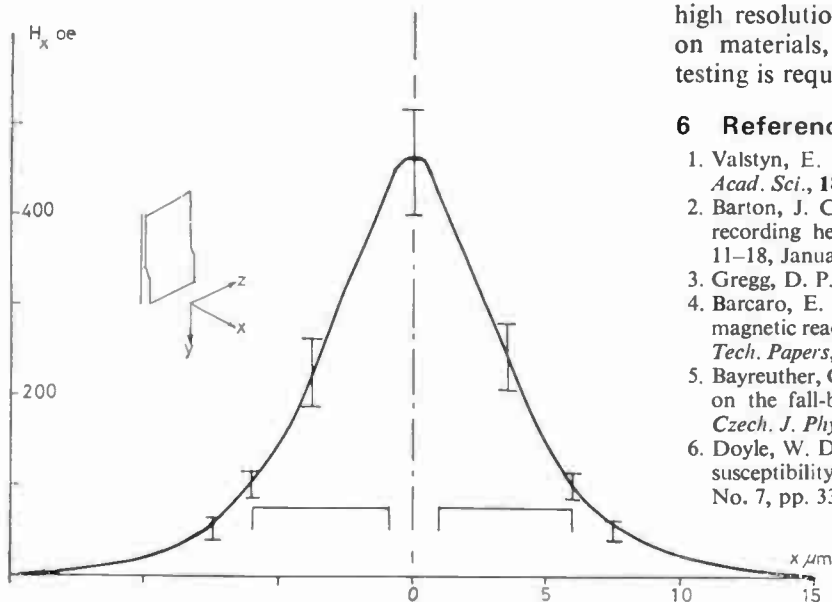


Fig. 7. Measured H_x plotted against x with $y = 0$ for multi-turn vertical head of Fig. 3.

Subsequently Kaske *et al.*^{11,17}, reported writing tests with heads employing permalloy films 1.15 μm thick and gap lengths of 17.5 μm . Densities as high as 150 flux reversals per millimetre were written in Fe films having a coercivity of 6400 A/m (80 Oe) with a head to medium spacing of 4 μm . The amplitude of the current pulses necessary to write was again in excess of 1 A. The only read tests reported using horizontal heads were reported by Kaske *et al.*^{11,17} using the read head of Fig. 4. Figure 6 shows the output signal as a function of separation for a density of 31.5 reversals/mm in conventional oxide materials. The theoretically predicted high resolution and frequency capabilities¹⁸ have not been investigated experimentally.

4.2 The Vertical Head

High resolution¹⁹ and efficiency²⁰ have been predicted for the single-turn vertical head, but there have been no experimental results published on these heads. Multi-turn vertical heads of the type shown in Fig. 3 have been investigated both theoretically and experimentally by Lazzari *et al.*^{9,21,22} Their theoretical analysis of the field contours was in good agreement with experimental results obtained by electron probe measurement of the field distribution. Figure 7 shows the measured write field component of the vertical head shown in Fig. 3. The total thickness of each magnetic arm was 5 μm and the gap width was 2 μm . This type of head was tested on a vibrating head recorder; using a CrCo film recording medium having a coercivity of 48 000 A/m (600 Oe) and a head to medium spacing of 6 μm . Both writing and reading were achieved.

5 Conclusion

Because of the limited amount of experimental work, it is not possible to predict whether thin-film integrated magnetic recording heads are capable of approaching their theoretically predicted operating characteristics of

high resolution and frequency response. Further work on materials, manufacturing techniques and dynamic testing is required.

6 References

1. Valstyn, E. P., 'Integrated head developments', *Annals N.Y. Acad. Sci.*, **18**, pp. 191–205, 1972.
2. Barton, J. C. and Stockel, C. T., 'A novel type of magnetic recording head', *The Radio and Electronic Engineer*, **26**, pp. 11–18, January 1964.
3. Gregg, D. P., US Patent 3,334,237, September 1967.
4. Barcaro, E. B., Best, D. T. and Zajackowski, J. S., 'A new magnetic read only memory', *Int. Solid-State Circuits Conf. Dig. Tech. Papers*, **10**, pp. 80–81, February 1967.
5. Bayreuther, G. and Hoffmann, H., 'Influence of ripple and skew on the fall-back angle α_{80} in thin uniaxial permalloy films', *Czech. J. Phys.*, **B21**, pp. 541–5, 1971.
6. Doyle, W. D. and Finnegan, T. F., 'The effect of strain on the susceptibility of polycrystalline NiFe films', *J. Appl. Phys.*, **39**, No. 7, pp. 3355–64, June 1968.
7. Fujii, T., Uchiyama, S., Tsunashima, S. and Sakaki, Y., 'An experimental verification of dispersion theory in soft magnetic films', *IEEE Trans. on Magnetics*, **MAG-5**, pp. 223–6, September 1969.
8. Valstyn, E. P. and Kosy, D. W., 'The write field of a magnetic film recording head', *IEEE Trans.*, **MAG-5**, pp. 442–5, September 1969.
9. Lazzari, J. P. and Melnick, I., 'Recording integrated magnetic heads', *IEEE Trans.*, **MAG-6**, pp. 601–2, September 1970.
10. UK Patent 1,169,869, 1969.
11. Kaske, A. D., Oberg, P. E., Paul, M. C. and Souter, G. F., 'Vapour deposited thin film recording heads', *IEEE Trans.*, **MAG-7**, pp. 675–9, September 1971.
12. Romankiw, L. T., Croll, I. M. and Hatzakis, M., 'Batch fabricated thin film magnetic recording heads', *IEEE Trans.*, **MAG-6**, pp. 597–601, September 1970.
13. Cohen, M. S., 'Magnetic properties of Ni-Fe-Cr films', *J. Appl. Phys.*, **35**, No. 3, pp. 834–5, March 1964.
14. Flur, B. L. and Griest, A. J., 'Properties of thin films of high permeability alloys', *J. Appl. Phys.*, **37**, No. 3, pp. 1478–80, March 1966.
15. Shibuya, H., 'Fabrication of narrow-track video head with sendust-sputtered films', N.H.K. Laboratories Note, Serial No. 154, July 1973.
16. Watanabe, Y. S., Matsumoto, S. N. and Yajima, N., 'Fabrication of grouped magnetic recording heads', *IEEE Trans.*, **MAG-7**, pp. 689–95, September 1971.
17. Sauter, G. F., Paul, M. C., Oberg, P. E. and Kaske, A. D., 'Transverse recording using thin film recording heads', *IEEE Trans.*, **MAG-8**, pp. 194–200, June 1972.
18. Thompson, D. A., 'Exchange eddy current effect in thick magnetic films', *Intermag. Conf. Paper 242*, 1970 (Digest in *IEEE Trans.*, **MAG-7**, p. 674, September 1970).
19. Potter, R. I., Schmalian, R. J. and Hortmann, K., 'Fringe field and readback voltage computations for finite pole tip length magnetic recording heads', *IEEE Trans.*, **MAG-7**, pp. 689–95, September 1971.
20. Paton, A., 'Analysis of the efficiency of thin-film magnetic recording heads', *J. Appl. Phys.*, **42**, No. 13, pp. 5868–70, December 1971.
21. Augier, D. and Lazzari, J. P., 'Write-process study on integrated magnetic heads', *IEEE Trans.*, **MAG-7**, pp. 679–83, September 1971.
22. Lazzari, J. P. and Wade, R. H., 'Electron probe measurements of field distributions near magnetic recording heads', *IEEE Trans.*, **MAG-7**, pp. 700–4, September 1971.

Manuscript received by the Institution on 12th March 1973. (Paper No. 1573/CC 191.)

© The Institution of Electronic and Radio Engineers, 1974

A frequency domain stability criterion for non-linear feedback systems

C. F. HO,

M.Sc., Ph.D., C.Eng., M.I.E.E., M.I.E.R.E.*

SUMMARY

A criterion for the investigation of the stability of a certain class of non-linear system with sinusoidal input is proposed. It is derived from the concepts of the describing function method and the circle criterion. If the non-linear system satisfies the restrictions of describing function analysis and if the characteristic of the non-linearity is bound in a sector $\frac{Y}{e} \in [a, b]$, there exists a critical region in the inverse polar plane which contains all possible describing functions of non-linearities bounded in this sector. Sufficient condition for the stability of the system is assured if the locus of the linear element does not intersect the critical region.

* Department of Electrical Engineering, University of Hong Kong.

1 Introduction

Among the methods used for stability analysis in non-linear systems, the describing function¹⁻⁴ enjoys a wide popularity. It belongs to those methods of solving non-linear differential equations based upon the existence of an assumed solution. As such, the non-linear element characteristic is described in a quasi-linear sense, hence enabling linear technique to be used in the analysis.

The recently developed circle criterion⁵⁻¹⁰ is also a notable contribution in control engineering. Sufficient condition for the stability of a large class of non-linear systems is assured if the locus of the linear element does not intersect in the same plane a critical region which is derived dependent upon the bounding sector of the non-linearity and not upon the actual non-linearity. The mechanics of determining the stability conditions are similar to the describing function method, and represent an extension of linear techniques into the analysis of non-linear systems.

This paper proposes a criterion developed from the concepts of describing function analysis and circle criterion. It shows that if the non-linear system satisfies the restrictions of describing function analysis and if the characteristic of the non-linearity is bounded in a sector $\frac{Y}{e} \in [a, b]$, there exists a critical region which contains all possible describing functions of non-linearities bounded in this sector. This may be compared with the boundary curve which Fukuma and Matsubara¹¹ obtained by using describing function and by normalizing the non-linear characteristic in the inverse polar plane.

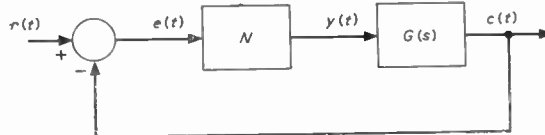


Fig. 1. A basic feedback system.

2 Statement of the Problem

Consider the basic feedback system of Fig. 1 where it is assumed that all the system non-linearities can be grouped into a block labelled N and the linear components into a block labelled $G(s)$. It is also assumed that:

- (i) the non-linear element is time invariant,
- (ii) all poles of $G(s)$ lie in the left half s -plane,
- (iii) when the input to the non-linear component is a pure sine wave, i.e. $e(t) = E \sin \omega t$, then no zero-frequency component and no subharmonic terms exist, and all higher harmonics of the Fourier series of $y(t)$ are sufficiently attenuated by $G(s)$.

Under these conditions the system of Fig. 1 meets all the requirements for application of describing function analysis. Thus, the stability of the system may be investigated by considering the characteristic equation of the system

$$1 + N(E) G(j\omega) = 0, \quad (1)$$

where $N(E)$ is the describing function of the non-linearity and is given by

$$N(E) = n_1(E) + jn_2(E) \tag{2}$$

$$n_1(E) = \frac{2}{ET} \int_0^T y(t) \sin \omega t \, dt \tag{3}$$

$$n_2(E) = \frac{2}{ET} \int_0^T y(t) \cos \omega t \, dt. \tag{4}$$

Let the non-linearity be bounded in a sector defined by

$$a \leq \frac{y(t)}{e(t)} \leq b \quad (b > a \geq 0) \tag{5}$$

as shown in Fig. 2. It is desired to find the boundary envelope of the describing function for the non-linearities $\frac{y(t)}{e(t)} \in [a, b]$ in the inverse polar plane.

3 The Derivation

In general, the describing function $N(E)$ is a complex quantity. We take the problem of determining the boundary envelope as the problem of finding the maximum (minimum) imaginary part of $N(E)$ for all allowable real parts of $N(E)$.

3.1 The Upper Boundary Curve

Determination of the maximum imaginary part of $N(E)$ for all allowable real parts gives an upper curve of the boundary envelope. To tackle this problem let us formulate the state equations representing the real and imaginary parts of the describing function such that we may make use of Pontryagin's maximum principle.¹²⁻¹⁴ Consider the state equations

$$\dot{x}_1(t) = \frac{2}{ET} y(t) \sin \omega t \tag{6}$$

$$\dot{x}_0(t) = \frac{2}{ET} y(t) \cos \omega t \tag{7}$$

where

$$T = \frac{2\pi}{\omega} \quad (0 \leq t \leq T)$$

and

$$X_1(0) = X_0(0) = 0.$$

Define that at $t = T$, $X_1(T)$ and $X_0(T)$ represent the real and imaginary parts of the describing function, i.e.

$$n_1(E) = x_1(T) \tag{9}$$

$$n_2(E) = X_0(T). \tag{10}$$

The describing function $n_1 + jn_2$ depends on the time function $y(t)$ which in turn depends upon the characteristic of the non-linear element. From eqn. (5)

$$ae(t) \leq y(t) \leq be(t) \quad (\text{for } e(t) > 0) \tag{11}$$

$$ae(t) \geq y(t) \geq be(t) \quad (\text{for } e(t) < 0). \tag{12}$$

Let $e(t) = E \sin \omega t$ and define

$$y(t) = \left[\frac{b+a}{2} + u(t) \frac{b-a}{2} \right] E \sin \omega t, \tag{13}$$

where $u(t)$ is the control variable and is constrained in magnitude by

$$|u(t)| \leq 1 \quad (\text{for all } t). \tag{14}$$

Thus, the state equations (6) and (7) become

$$\dot{x}_1(t) = \frac{2}{T} \left[\frac{(b+a)}{2} + u(t) \frac{(b-a)}{2} \right] \sin^2 \omega t \tag{15}$$

$$\dot{x}_0(t) = \frac{2}{T} \left[\frac{(b+a)}{2} + u(t) \frac{(b-a)}{2} \right] \sin \omega t \cos \omega t. \tag{16}$$

Equations (15) and (16) represent the state equations of a system to which Pontryagin's maximum principle may be applied. The problem is interpreted as follows: Consider a hypothetical system described by a single state, eqn. (15) which represents the real part of the describing function with $x_1(0) = 0$, the initial state, and $t = 0$, the initial time. It is desired to determine the control function, $u(t)$ which takes the system from the initial state, $x_1(0)$, to its final state, $x_1(t)$ as time t varies from $t = 0$ to the end-time $t = T$ such that the cost functional, the imaginary part of the describing function

$$J(u) = \int_0^T \dot{x}_0(t) \, dt \\ = \frac{2}{T} \int_0^T \left[\frac{(b+a)}{2} + u(t) \frac{(b-a)}{2} \right] \sin \omega t \cos \omega t \, dt \tag{17}$$

is maximized. Thus, the problem stated is a fixed end-point fixed time problem.

Pontryagin's maximum principle states that relative to the problem formulated above, if $u^*(t)$ is the optimal admissible control function which maximizes the cost functional $J(u)$, and $x_1^*(t)$ is the optimal trajectory corresponding to $u^*(t)$, there exists a non-negative constant P_0^\dagger and a function $P_1^*(t)$ such that at any time t (except possibly at points where u is discontinuous) the Hamiltonian function evaluated along $x_1^*(t)$ corresponding to the optimal control $u^*(t)$ is at least as large as that corresponding to any other admissible control function $u(t)$. That is, the Hamiltonian

$$H[u^*(t), t] = \frac{2P_0}{T} \left[\frac{(b+a)}{2} + u^*(t) \frac{(b-a)}{2} \right] \times \\ \times \sin \omega t \cos \omega t + \frac{2P_1^*(t)}{T} \times \\ \times \left[\frac{(b+a)}{2} + u^*(t) \frac{(b-a)}{2} \right] \sin^2 \omega t \tag{18}$$

satisfies the inequality

$$H[u^*(t), t] \geq \frac{2P_0}{T} \left[\frac{(b+a)}{2} + u(t) \frac{(b-a)}{2} \right] \times \\ \times \sin \omega t \cos \omega t + \frac{2P_1^*(t)}{2} \times \\ \times \left[\frac{(b+a)}{2} + u(t) \frac{(b-a)}{2} \right] \sin^2 \omega t, \tag{19}$$

† In the literature P_0 is commonly chosen to be equal to unity.

where $P_1^*(t)$ satisfies the canonical equations

$$\dot{x}_1^*(t) = \frac{\partial H}{\partial P_1} \tag{20}$$

$$\dot{P}_1^*(t) = -\frac{\partial H}{\partial x_1^*} = 0 \tag{21}$$

with the boundary conditions

$$x_1^*(0) = 0, \quad x_1^*(T) = N_1^* \tag{22}$$

From equations (18) and (21) it is seen that

$$\dot{P}_1^*(t) = -\frac{\partial H}{\partial x_1^*} = 0 \tag{23}$$

which implies that

$$P_1^*(t) = P_1 = \text{constant (for all } t) \tag{24}$$

Hence equation (18) becomes

$$H[u^*(t), t] = \frac{2 \sin \omega t}{T} \left[\frac{(b+a)}{2} + u^*(t) \frac{(b-a)}{2} \right] \times [P_0 \cos \omega t + P_1 \sin \omega t] \tag{25}$$

or

$$H[u^*(t), t] = \frac{2P}{T} \left[\frac{(b+a)}{2} + u^*(t) \frac{(b-a)}{2} \right] \times \sin \omega t \sin(\omega t + \phi)$$

where

$$P = \sqrt{P_0^2 + P_1^2}$$

and

$$\phi = \tan^{-1} \frac{P_0}{P_1} \quad (0 \leq \phi \leq \pi) \tag{26}$$

Since $u(t)$ is constrained in magnitude by $|u(t)| \leq 1$ and $(b-a)/2 > 0$, the Hamiltonian of equation (26) satisfies the inequality (19) if

$$u^*(t) = \text{sgn} [\sin \omega t] \text{sgn} [\sin(\omega t + \phi)] \tag{27}$$

Therefore, as shown in Fig. 3

$$u^*(t) = \begin{cases} 1 & (0 \leq \omega t \leq \pi - \phi) \\ -1 & (\pi - \phi \leq \omega t \leq \pi) \\ 1 & (\pi \leq \omega t \leq 2\pi - \phi) \\ -1 & (2\pi - \phi \leq \omega t \leq 2\pi) \end{cases} \tag{28}$$

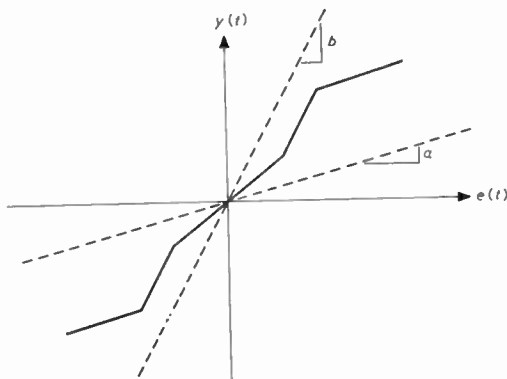
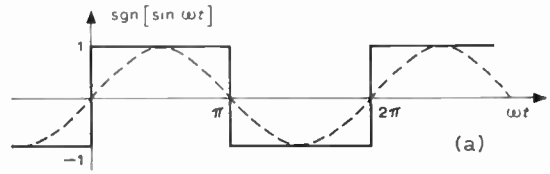
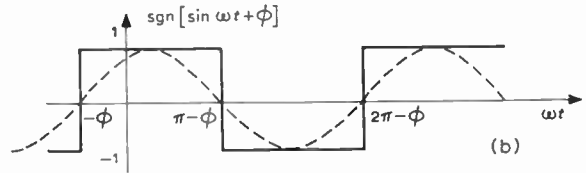


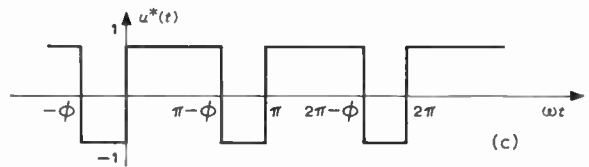
Fig. 2. Non-linearity bounded in the sector $[a, b]$.



(a) $\text{sgn} [\sin \omega t]$ versus ωt .



(b) $\text{sgn} [\sin \omega t + \phi]$ versus ωt .



(c) $u^*(t)$ versus ωt .

Fig. 3.

It has been defined that at $t = T$, $x_1(T)$ and $x_0(T)$ represent the real and imaginary parts of the describing function. Let N_1^* and N_2^* be the real and imaginary parts of the describing function respectively that correspond to $u^*(t)$ which is the control function that maximizes the imaginary part. From equations (15) and (16) we have

$$N_1 = \int_0^T x_1^*(t) dt = \frac{2}{T} \int_0^T \left[\frac{(b+a)}{2} + u^*(t) \frac{(b-a)}{2} \right] \sin^2 \omega t dt \tag{29}$$

$[\dot{x}_1(0) = 0]$

$$N_2^* = \int_0^T \dot{x}_0^*(t) dt = \frac{2}{T} \int_0^T \left[\frac{(b+a)}{2} + u^*(t) \frac{(b-a)}{2} \right] \sin \omega t \cos \omega t dt \tag{30}$$

$[\dot{x}_0^*(0) = 0]$.

Substituting equation (28) into equations (29) and (30) and integrate with respect to $\theta = \omega t$

$$N_1^* = \frac{1}{\pi} \left[\int_0^{\pi-\phi} b \sin^2 \theta d\theta + \int_{\pi-\phi}^{\pi} a \sin^2 \theta d\theta + \int_{\pi}^{2\pi-\phi} b \sin^2 \theta d\theta + \int_{2\pi-\phi}^{2\pi} a \sin^2 \theta d\theta \right] = \frac{1}{\pi} \left[\int_0^{\pi-\phi} b(1 - \cos 2\theta) d\theta + \int_{\pi-\phi}^{\pi} a(1 - \cos 2\theta) d\theta \right] = b + \frac{(a-b)}{\pi} \phi - \frac{(a-b)}{2\pi} \sin 2\phi \tag{31}$$

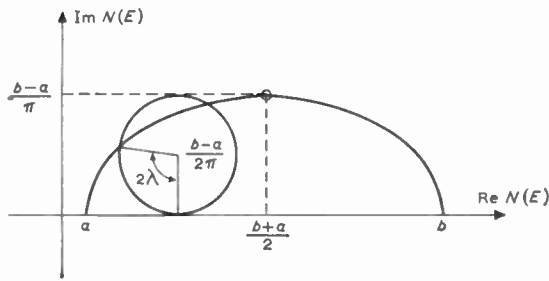


Fig. 4. Graphical interpretation of maximum describing function as a function of λ ($0 \leq \lambda \leq \pi$).

$$\begin{aligned}
 N_2^* &= \frac{1}{\pi} \left[\int_0^{\pi-\phi} b \sin \theta \cos \theta \, d\theta + \int_{\pi-\phi}^{\pi} a \sin \theta \cos \theta \, d\theta + \right. \\
 &\quad \left. + \int_{\pi}^{2\pi-\phi} b \sin \theta \cos \theta \, d\theta + \int_{2\pi-\phi}^{2\pi} a \sin \theta \cos \theta \, d\theta \right] \\
 &= \frac{1}{\pi} \left[\int_0^{\pi-\phi} b \sin 2\theta \, d\theta + \int_{\pi-\phi}^{\pi} a \sin 2\theta \, d\theta \right] \\
 &= \frac{(b-a)}{2\pi} [1 - \cos 2\phi].
 \end{aligned} \tag{32}$$

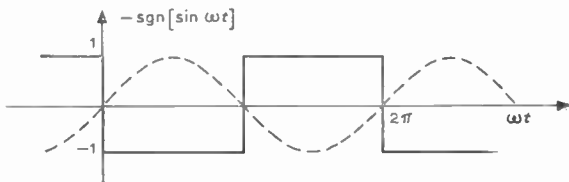
Let

$$\lambda = \pi - \phi \quad (0 \leq \lambda \leq \pi). \tag{33}$$

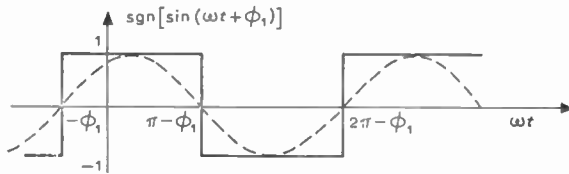
Equations (31) and (32) become

$$N_1^* = a + \frac{(b-a)}{2\pi} [2\lambda - \sin 2\lambda] \tag{34}$$

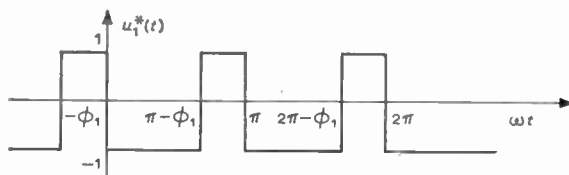
$$N_2^* = \frac{(b-a)}{2\pi} [1 - \cos 2\lambda] \tag{35}$$



(a) $-\text{sgn}[\sin \omega t]$ versus ωt .



(b) $\text{sgn}[\sin(\omega t + \phi_1)]$ versus ωt .



(c) $u^*(t)$ versus ωt .

Fig. 5.

Thus,

$$N(E)_{\max} = N_1^* + jN_2^* \tag{36}$$

which dictates the upper boundary curve or which may be defined as the maximum describing function in the sense that: given an allowable real part N_1^* where corresponds a $\lambda = \lambda'$ such that the imaginary part N_2^* is maximum for this λ' .

The geometrical interpretation of equation (36) is shown in Fig. 4.

3.2 The Lower Boundary Curve

We have obtained the maximum upper bound on the imaginary part of the describing functions for all non-linearities bounded in the sector $[a, b]$. In order to define a region which contains all of the describing functions under consideration, we must concern ourselves with the lower boundary curve as well. We consider the single-state system of equation (15) as before with the cost functional equation (17), and determine the control function $u(t)$ which minimizes the cost functional.

After a series of manipulations equivalent to these for the upper boundary curve, we find that

$$\begin{aligned}
 N(E)_{\min} &= N_1^* - jN_2^* \\
 &= \overline{N(E)_{\max}}
 \end{aligned} \tag{37}$$

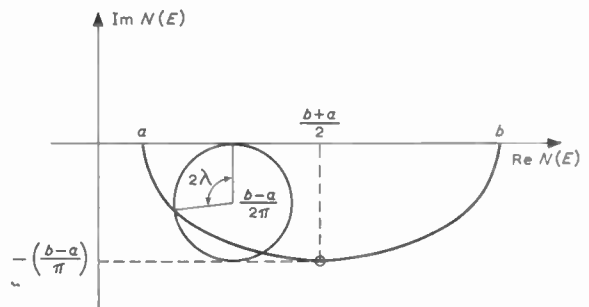


Fig. 6. Graphical interpretation of minimum describing function as a function of λ ($0 \leq \lambda \leq \pi$).

represents the lower boundary envelope of the describing functions of all non-linearities bounded in a sector $[a, b]$. This is shown in Fig. 6.

3.3 The Boundary Envelope

The two curves described by equations (36) and (37) define the maximum and minimum bounds respectively on the imaginary part of the describing function of non-linearities bounded in the sector $[a, b]$ for a given allowable real part. Combining these two curves yields a region R_N within which all describing functions of non-linearities bounded by the sector $[a, b]$ must lie. That is

$$R_N = a + \frac{(b-a)}{2\pi} (2\lambda - \sin 2\lambda) \pm j \frac{(b-a)}{2\pi} (1 - \cos 2\lambda) \tag{38}$$

To illustrate the relation between the describing function of a given non-linearity and the boundary region dictated by equation (38) let us consider the characteristic of a relay with hysteresis and dead zone

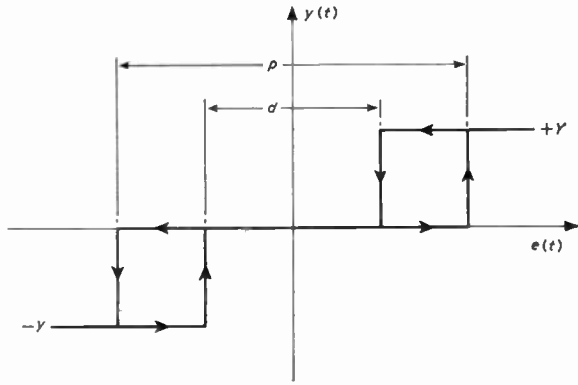


Fig. 7. Characteristic of a relay with hysteresis and dead zone.

$$e(t) = E \sin \omega t$$

$$y(t) \begin{cases} +0 & 0 \leq \omega t \leq \alpha \\ +Y & \alpha \leq \omega t \leq \pi - \beta \\ 0 & \pi - \beta \leq \omega t \leq \pi + \alpha \\ -Y & \pi + \alpha \leq \omega t \leq 2\pi - \beta \\ 0 & 2\pi - \beta \leq \omega t \leq 2\pi \end{cases}$$

$$\alpha = \sin^{-1} \frac{P}{2E}$$

$$\beta = \sin^{-1} \frac{d}{2E}$$

shown in Fig. 7. The describing function is given by

$$N(E) = \frac{2y}{\pi E} [(\cos \alpha - \cos \beta) + j(\sin \beta - \sin \alpha)]$$

where

$$\alpha = \sin^{-1} \frac{P}{2E}$$

$$\beta = \sin^{-1} \frac{d}{2E} \tag{39}$$

Let $y = 1$ and $d = 2$. Then the non-linearity is bounded in a sector with $a = 0$ and $b = 1$. A family of describing functions as functions of the variable E is obtained by assigning p with various values. This family of curves along with the boundary region R_N is shown in Fig. 8.

One must bear in mind that this boundary region was derived on the basis of the bounding sector of the non-linearity and not on the actual non-linearity. The non-linearity of Fig. 7 is one of many non-linearities bounded in the section $[0, 1]$. It is noted that the family of describing functions occupies only a portion of the boundary region R_N . Other non-linearities bounded in this sector will produce describing functions occupying other portions of the region.

4 Stability Analysis

The closed-loop transfer function of the model of Fig. 1 is given by

$$\frac{C}{R}(j\omega) = \frac{N(E, \omega)G(j\omega)}{1 + N(E, \omega)G(j\omega)} \tag{40}$$

The system will support sustained oscillation only if

$$e(t) = -c(t) \tag{41}$$

or in other words

$$N(E, \omega)G(j\omega) = -1. \tag{42}$$

It is more convenient to write equation (42) as

$$-N(E, \omega) = \frac{1}{G(\omega)} \tag{43}$$

and plot in the inverse polar plane. Equation (43) states that in order for sustained oscillations to exist there must be a pair of E and ω which causes $-N(E, \omega)$ to equal $1/G(\omega)$. The conditions for which the system is stable may be found graphically using a modified Nyquist plot.

In linear system theory, the absolute and relative stability may be found from the polar or inverse polar plot by considering the relative locations of the critical point -1 , and the open loop transfer function. In the describing function method, however, there exists not one critical point but a locus of critical points given by $-N(E, \omega)$, that is, the -1 point moves with changes in signal level. With this modification the stability analysis of the non-linear system using Nyquist criterion is similar to that of linear systems. The actual analysis is best explained through an example.

Example. Consider the non-linear system shown in Fig. 1 with the non-linearity being a relay with dead zone and hysteresis as given in Fig. 7.

The describing function is derived as

$$N(E, \omega) = \frac{2y}{\pi E} [(\cos \alpha - \cos \beta) + j(\sin \beta - \sin \alpha)]$$

or

$$\frac{2y}{\pi E} \sqrt{2(1-AB) + 2\sqrt{(1-A^2)(1-B^2)}} \times \tan^{-1} \frac{B-A}{\sqrt{(1-A^2)+\sqrt{(1-B^2)}}$$

where

$$A = \frac{p}{2E} \quad B = \frac{b}{2E}$$

With $y = 1$, $d = 2$ and $p = 3$, the describing function is plotted in Fig. 9. Also given in the same Figure is the plot of $1/G(j\omega)$ for different values of gain K for $G(j\omega)$.

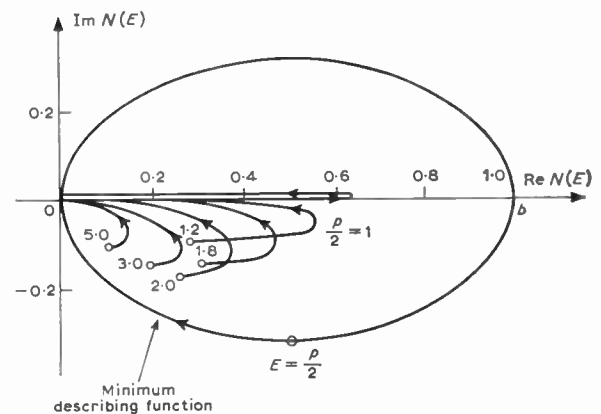


Fig. 8. Boundary region and a family of describing functions for the non-linearity of Fig. 7.

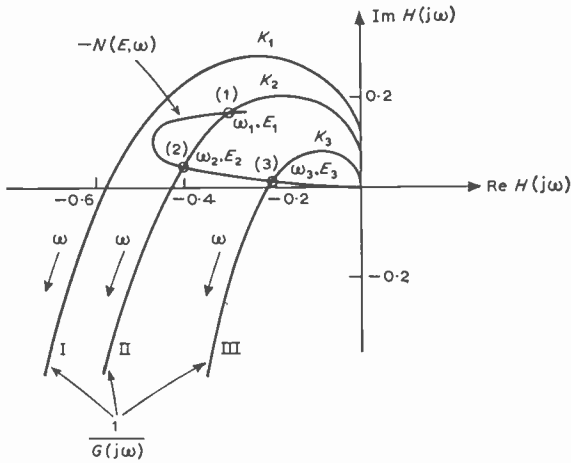


Fig. 9. Inverse polar plot for stability analysis.

The system is said to be stable if the plot of $1/G(j\omega)$ does not intersect or enclose $-N(E, \omega)$ locus. The region enclosed by a curve is taken here as the region to the right of the curve when the curve is traversed in the direction of increasing frequency. Thus, Fig. 9 shows the system to be stable if $K = K_1$ but is unstable if $K = K_2$ or K_3 . There are three intersections of $1/G(j\omega)$ and $-N(E, \omega)$ in the cases of K_2 and K_3 . These intersections represent limit cycles which may be stable or unstable. A limit cycle is stable if in the presence of perturbation the operation of the system tends to return to the equilibrium point. If the operation of the system settles to a different equilibrium point in the presence of disturbances the limit cycle is unstable. Hence, in the case of curve K_3 , assuming the system is operating at point (3). If E increases, the critical point on $-N(E, \omega)$ moves to the right of (3), then E tends to decrease and the system operating point returns to (3). Similarly, a decrease in E moves the critical point to the left of point (3) and the system becomes unstable; then E tends to increase and the system operating point again returns to (3). Therefore, point (3) represents a stable limit cycle. A similar inspection of points (1) and (2) reveals that point (1) is an unstable limit cycle while point (2) is a stable one.

In the preceding Sections we have derived the conditions that if the non-linearity is bounded in a sector $[a, b]$, there exists a curve (or an envelope) given by equation (38) which dictates all describing functions of non-linearities bounded by this sector. Hence by replacing $-N(E, \omega)$ with $-R_N$ in equation (43) the stability analysis method applies. We may formally state the criterion as follows:

Consider the basic feedback system of Fig. 1 whose non-linearity is bounded by a sector $[a, b]$ and the system meets all the constraints for the application of describing function analysis.

There exists a region described by

$$-R_N = a + \left(\frac{b-a}{2\pi}\right)(2\lambda - \sin 2\lambda) + j\left(\frac{b-a}{2\pi}\right)(1 - \cos 2\lambda) \quad (0 \leq \lambda \leq \pi)$$

in the inverse polar plane. The stability of the system

is guaranteed if the locus of $G(j\omega)^{-1}$ does not intersect with or enclose this region.

It should be remarked that intersection of $G(j\omega)^{-1}$ and R_N does not necessarily imply the system being unstable, because this region depends upon the actual location in the region R_N of the describing function of the particular non-linearity under consideration. For instance, a single-valued non-linearity such as the one shown in Fig. 10 which produces real describing function will lie on the real axis inside the boundary region (see Appendix). As long as the locus of $G(j\omega)^{-1}$ does not cut the real axis, intersection with the boundary region R_N will still yield a stable system. A more precise boundary region could be defined for a given non-linearity, of course, if desired.

Stability analysis of non-linear system using this criterion is the same as the describing function method. The only difference is that there exists a critical region instead of a critical curve in the inverse polar plane. Similarly to the circle criterion, the proposed criterion yields sufficient and not necessary conditions and tends to be conservative. Thus, the criterion is not intended to substitute for the describing function method for system analysis. It is useful when in system design, a quick estimate of the stability condition is required particularly when it is more desirable to alter the non-linearity than to compensate for the linear part of the system.

It is interesting to note that equation (38) is precisely the same as the equations (30) and (31) given in Reference 16 in which an extension of Fukuma and Matsubara jump resonance criterion by the use of describing function was discussed. This indicates that the proposed criterion may also be used to ensure sufficient conditions of non-existence of jump resonance of the system if the non-linearity is bounded in the section $[a, b]$.

5 Comparison of the Circle Criterion and the Proposed Criterion

Since both the circle criterion and the proposed criterion yield sufficient conditions for stability of a system by dictating a critical region which the locus of the linear element of the system must not enclose or cross, it is of interest to compare these critical regions

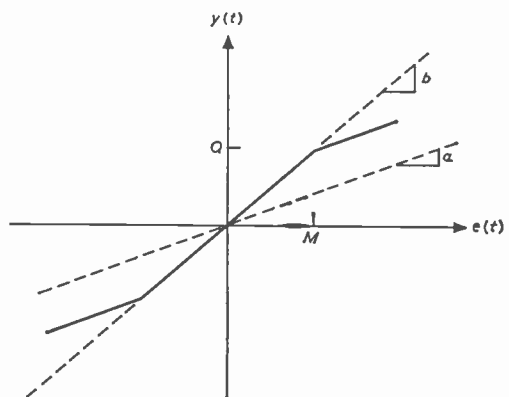


Fig. 10. Non-linearity characteristic.

although there are differences in the conditions imposed on the non-linear system by the two criteria.

The circle criterion describes critical regions bounded by circles in the polar plane which the locus of $G(j\omega)$ must not enclose or cross. The proposed criterion, on the other hand, describes critical regions bounded by cycloids in the inverse-polar plane which the locus of $G(j\omega)^{-1}$ must not enclose or cross. In both cases the boundary curves are dictated by the sector bounding the non-linearity. In order to compare the critical regions given by the two criteria, one must perform a transformation to map the two regions in the same plane. Figure 11 shows the transformation of the critical regions of the circle criterion in the polar plane into the inverse polar plane by setting

$$H(j\omega) = \frac{1}{G(j\omega)}$$

$$G(j\omega) \neq 0,$$

where

$$H(j\omega) = h_1(\omega) + jh_2(\omega)$$

$$G(j\omega) = g_1(\omega) + jg_2(\omega). \tag{44}$$

Now, consider a basic feedback system whose non-linearity is bounded in the sector $[a, b]$. Assume that the system meets all conditions imposed by circle criterion and the proposed criterion. The circle criterion thus describes a critical region in the inverse polar plane given by

$$[h_1 + \frac{1}{2}(b+a)]^2 + h_2^2 = [\frac{1}{2}(b-a)]^2 \quad b > a \geq 0. \tag{45}$$

While the proposed criterion gives a critical region described by equation (46)

$$-R_N = -a - \left(\frac{b-a}{2\pi}\right) (2\lambda - \sin 2\lambda) \mp j \left(\frac{b-a}{2\pi}\right) (1 - \cos 2\lambda). \tag{46}$$

The two regions are plotted in Fig. 12.

It is seen that the bounds on the real axis for both regions are precisely the same as they correspond to the slopes of the lines bounding the non-linearity in the sector. The imaginary parts of the bounding curves differ but only by a maximum difference of $(1/2 - 1/\pi)$.

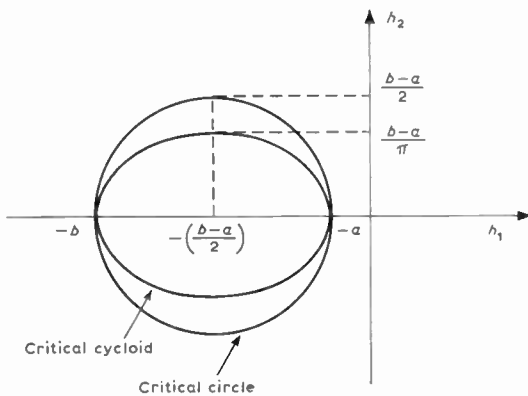


Fig. 12. Critical regions described by circle and cycloid criteria.

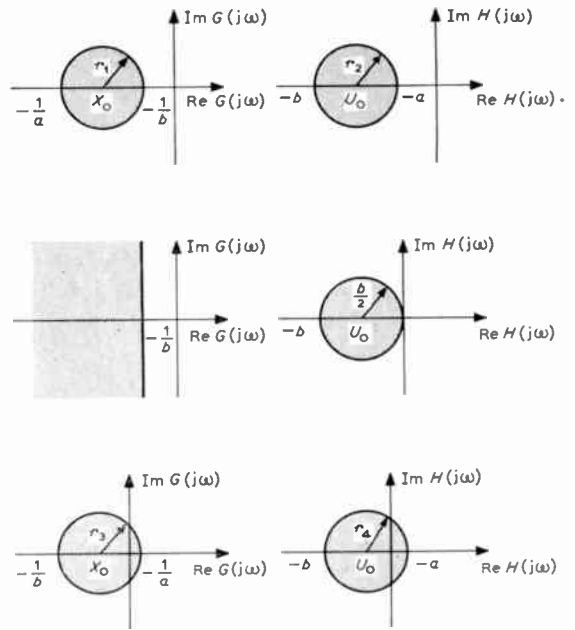


Fig. 11. Transformation of critical regions of circle criterion in the polar plane into the inverse polar plane.

The smaller region described by the proposed criterion implies that it is less conservative in the estimate of the stability condition for the system in this particular case.

6 Discussions and Conclusions

The stability condition dictated by the circle criterion is dependent upon the sector which bounds the non-linearity and not upon the actual non-linearity. This concept is very useful in system design particularly when it is more desirable to alter the non-linearity than to compensate for the linear plant of the system. This paper proposes a criterion based on this concept by the use of describing function and Pontryagin's maximum principle. Since the criterion stems from describing function analysis, the system being investigated using this criterion is constrained by similar restrictions as the describing function imposes on it. However, from the engineering point of view these restrictions are minor ones and are usually met by the control system being considered, because most control systems are higher order systems and naturally low-pass. Also, one of the first assumptions in modelling a system is that the system be time-invariant.

The proposed criterion places relatively few restrictions on the non-linearity. Due to its generality, the criterion yields sufficient conditions to assure the stability of the non-linear system, and can be conservative in its estimation. The critical region defined by this criterion is based on the bounding sector of the non-linearity. The nearer the actual non-linearity function lies to this boundary cycloid, the better the correlation will be between the proposed criterion and the actual describing function analysis. Therefore, the proposed criterion is not intended to supersede the describing function method in system analysis. However, it is useful as a design tool since it quickly yields stability

conditions in a manner which is similar to the linear technique, providing an intuitive feel for the physical system.

7 Acknowledgments

The author wishes to record his thanks to Prof. S. Y. King, Héd of Electrical Engineering Department, University of Hong Kong, for his constant encouragements throughout the course of this work, and to the Referees for their constructive criticism of the paper.

8 References

1. West, J. C., 'Analytical Techniques for Nonlinear Control Systems' (English University Press, London, 1960).
2. Kochenburger, R. J., 'A frequency response method for analysing contactor servo-mechanisms', *Trans. Amer. Inst. Elect. Engrs*, 69, Pt. 1, pp. 270-84, 1950.
3. Gilson, J. E., 'Nonlinear Automatic Control' (McGraw-Hill, New York, 1963).
4. Sridhar, R., 'A general method for deriving the describing functions for a certain class of nonlinearities', *IRE Trans. on Automatic Control*, AC-5, No. 2, pp. 135-41, June 1960.
5. Sandberg, I. W., 'A frequency domain condition for the stability of feedback systems containing a single time varying nonlinear element', *Bell Syst. Tech. J.*, 43, No. 4, Pt. 2, pp. 1601-8, July 1964.
6. Zames, G., 'On the input-output stability of nonlinear time-varying feedback systems', *Proc. National Electronics Conf.*, 20, pp. 725-30, October 1964.
7. Sandberg, I. W., 'Some stability results related to those of V. M. Popov', *Bell Syst. Tech. J.*, 44, No. 9, pp. 2133-48, November, 1965.
8. Zames, G., 'On the input-output stability of time-varying nonlinear feedback systems—Part I: Conditions derived using concepts of loop gain, concity and positivity', *IEEE Trans.*, AC-11, No. 2, pp. 228-39, April 1966.
9. Zames, G., 'On the input-output stability of time-varying nonlinear feedback systems—Part II: Conditions involving circles in the frequency, plane and sector nonlinearities', *IEEE Trans.*, AC-11, No. 3, pp. 465-76, July 1966.
10. Hsu, J. C. and Meyer, A. U., 'Modern Control Principles and Applications' (McGraw-Hill, New York, 1968).
11. Fukuma, A. and Matsubara, M., 'Jump resonance criteria of nonlinear control systems', *IEEE Trans.*, AC-11, No. 4, pp. 699-707, October 1966.
12. Pontryagin, L. S., Boltyanskii, V. G., Gamkrelidze, R. V. and Mishchenko, E. F., 'Mathematical Theory of Optimal Processes' (English translation) (Interscience, Wiley, New York, 1962).
13. Rozonoer, L. I., 'L. S. Pontryagin maximum principle in the theory of optimum systems', *Automation and Remote Control*, 20, Pt. I, pp. 1288-1302, Pt. II, pp. 1405-1421, Pt. III, pp. 1517-32, 1959.
14. Athans, M. and Falb, P. L., 'Optimal Control—an Introduction to the Theory and its Applications' (McGraw-Hill, New York, 1966).
15. Cook, P. A., 'Describing function for a sector nonlinearity', *Proc. Instn Elect. Engrs.*, 120, pp. 143-4, Jan. 1973.
16. Ho, C. F., 'An extension to Fukuma and Matsubara jump resonance criterion by the use of describing functions', *The Radio and Electronic Engineer*, 42, No. 12, pp. 562-68, December 1972.

9 Appendix:

Describing Function of Single-valued Non-Linearity

In general, the describing function of a non-linearity is a complex quantity given by

$$N[E\omega] = \frac{B_1 + jA_1}{E}, \tag{47}$$

where A and B are the coefficients of the Fourier series for the signal at the output of the non-linearity with the input wave given by $E \sin \omega t$. If the non-linearity is single-valued, the describing function is real, that is

$$N[E] = \frac{B_1}{E}. \tag{48}$$

This real property is always stated in literature but rarely proved. We will give the proof here and also show that if the single-valued non-linearity is bounded by a sector (a, b) then the describing function lies on the real axis and bounded by

$$a \leq N[E] \leq b. \tag{49}$$

Let the input to the non-linearity be given by

$$e = E \sin \omega t \quad \left(\omega = \frac{2\pi}{T} \right) \tag{50}$$

and the output of the non-linearity be

$$y = f(e). \tag{51}$$

Any function may be uniquely broken into even and odd parts. Thus

$$f(e) = f_e(e) + f_o(e), \tag{52}$$

where $f_e(e)$ and $f_o(e)$ are the even and odd parts respectively of the function $f(e)$, and possess the following properties:

$$\begin{aligned} f_e(e) &= f_e(-e) \\ &= \frac{1}{2}[f(e) + f(-e)] \\ f_o(e) &= -f_o(-e) \\ &= \frac{1}{2}[f(e) - f(-e)]. \end{aligned} \tag{53}$$

Then, equation (51) becomes

$$y(t) = f_e(E \sin \omega t) + f_o(E \sin \omega t), \tag{54}$$

which is periodic and may be represented by a Fourier series

$$y(t) = \frac{A_0}{2} + \sum_{n=1}^{\infty} [A_n \cos n\omega t + B_n \sin n\omega t],$$

where

$$\begin{aligned} A_n &= \frac{2}{T} \int_{-T/2}^{T/2} y(t) \cos n\omega t \, dt \\ B_n &= \frac{2}{T} \int_{-T/2}^{T/2} y(t) \sin n\omega t \, dt \\ &\quad (n = 1, 2, 3, \dots). \end{aligned} \tag{55}$$

The definition of the describing function requires $A_0/2 = 0$ and A_n, B_n for $n \geq 2$ are negligible. Thus, the coefficients of interest are A_1 and B_1 .

From equations (51), (52) and (55)

$$\begin{aligned} A_1 &= \frac{2}{T} \int_{-T/2}^{T/2} f_e(E \sin \omega t) \cos \omega t \, dt + \\ &\quad + \frac{2}{T} \int_{-T/2}^{T/2} f_o(E \sin \omega t) \cos \omega t \, dt. \end{aligned} \tag{56}$$

Since $f_e(E \sin \omega t)$ is an even function of time with period $T/2$, its Fourier series is given by

$$f_e(E \sin \omega t) = \frac{A'_0}{2} + \sum_{n=1}^{\infty} A'_n \cos 2n\omega t \tag{57}$$

$f_o(E \sin \omega t)$ is an odd function of time with period T , its Fourier series is given by

$$f_o(E \sin \omega t) = \sum_{n=1}^{\infty} B'_n \sin n\omega t. \quad (58)$$

Thus, the integrals of equation (55) become zero, i.e.

$$A_1 = 0.$$

Similarly,

$$B_1 = \frac{2}{T} \int_{-T/2}^{T/2} f_e(E \sin \omega t) \sin \omega t dt + \frac{2}{T} \int_{-T/2}^{T/2} f_o(E \sin \omega t) \sin \omega t dt \quad (59)$$

The first integral of equation (59) is reduced to zero since $f_e(E \sin \omega t)$ is an even function. Thus, the describing function of a single-valued non-linearity is given by

$$\begin{aligned} N[E] &= \frac{B_1}{E} \\ &= \frac{2}{ET} \int_{-T/2}^{T/2} f_o(E \sin \omega t) \sin \omega t dt \\ &= \frac{2}{ET} \int_{-T/2}^{T/2} y(t) \sin \omega t dt \end{aligned} \quad (60)$$

and is a real function of E .

Now, for the non-linearity bounded by a sector (a, b) , i.e.

$$a \leq \frac{y(t)}{e(t)} \leq b, \quad (61)$$

thus

$$\begin{aligned} ae(t) &\leq y(t) \leq be(t) \quad (e(t) > 0) \\ ae(t) &\geq y(t) \geq be(t) \quad (e(t) < 0) \end{aligned} \quad (62)$$

Since $f_o(E \sin \omega t) \sin \omega t$ is an even function over the interval $-T/2 \leq t \leq T/2$ and since $E \sin \omega t$ is positive over this interval, equation (60) may be written as

$$\begin{aligned} N[E] &= \frac{4}{ET} \int_0^{T/2} y(t) \sin \omega t dt \\ &\leq \frac{4}{T} \int_0^{T/2} b \sin^2 \omega t dt \\ &\geq \frac{4}{T} \int_0^{T/2} a \sin^2 \omega t dt. \end{aligned} \quad (63)$$

Equation (63) indicates that when the non-linearity is single-valued and is bounded by a sector, the describing function is real and is bound by

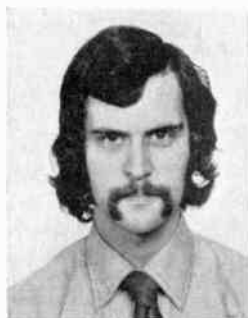
$$a \leq N[E] \leq b \quad (64)$$

Manuscript first received by the Institution on 9th May 1973, in revised form on 13th August 1973 and in final form on 16th October 1973. (Paper No. 1574/ACS 8.)

© The Institution of Electronic and Radio Engineers, 1974

Contributors to this issue

(Continued from page 118)



Mr. D. G. Jones obtained a first-class honours degree in electronic and electrical engineering at the University of Sheffield in 1971. He is at present reading for the degree of Ph.D. on the subject of microwave holography.



Dr. A. P. Anderson obtained his Ph.D. at University College London for research into millimetre waves, and then went to Ferranti Ltd. where he was employed on the development of microwave parametric devices. He subsequently joined RCA and worked on the design of microwave transistors until his present appointment at the University of Sheffield in 1967. His research interests are microwave holography, coherent optics and active antennas.



Dr. A. J. Collins received the B.Eng. (Tech.) degree in electrical engineering from the University of Wales Institute of Science and Technology, Cardiff in 1967, and a Ph.D. from the Wolfson Centre, UWIST, in 1971 for work on the effect of annealing on the magnetic properties of thin ferromagnetic films. From 1971-1973 he held a University of Wales Fellowship at the Wolfson Centre, to investigate the problems associated with r.f. sputtering of ferromagnetic materials. He is currently engaged in work on thin ferromagnetic recording heads at the Wolfson Centre.



Dr. I. Preece gained his B.Sc. in physics at Nottingham University in 1959. After spending two years in the Antarctic as a physicist, he entered the steel industry and was engaged on a variety of problems concerned with production and properties of electrical steels. In 1966 he joined the Electrical Engineering Department of UWIST and obtained a Ph.D. in 1970, for research on the domain structure of nickel-iron alloys. Since then he has studied a wide range of magnetic materials and applications and is at present Senior Physicist at the Wolfson Centre for the Technology of Soft Magnetic Materials in UWIST.

STANDARD FREQUENCY TRANSMISSIONS—January 1974

(Communication from the National Physical Laboratory)

Jan. 1974	Deviation from nominal frequency in parts in 10^{10} (24-hour mean centred on 0300 UT)			Relative phase readings in microseconds NPL—Station (Readings at 1500 UT)		Jan. 1974	Deviation from nominal frequency in parts in 10^{10} (24-hour mean centred on 0300 UT)			Relative phase readings in microseconds NPL—Station (Readings at 1500 UT)	
	GBR 16 kHz	MSF 60 kHz	Droitwich 200 kHz	*GBR 16 kHz	†MSF 60 kHz		GBR 16 kHz	MSF 60 kHz	Droitwich 200 kHz	*GBR 16 kHz	†MSF 60 kHz
1	0	0	0	688	584.6	17	-0.3	0	-0.1	697	586.5
2	0	+0.2	0	688	584.9	18	0	0	-0.1	697	586.7
3	0	0	0	688	586.1	19	+0.2	+0.1	-0.1	695	586.0
4	-0.2	-0.1	-0.1	690	587.3	20	+0.3	0	-0.1	692	585.6
5	-0.1	0	-0.1	691	587.7	21	-0.4	0	-0.1	696	585.6
6	-0.2	-0.1	-0.1	693	588.7	22	+0.2	0	-0.2	694	586.6
7	-0.2	-0.1	-0.1	695	589.3	23	0	-0.1	-0.2	694	587.4
8	0	-0.1	-0.1	695	590.7	24	0	0	-0.1	694	597.4
9	0	+0.1	-0.1	695	589.1	25	0	0	-0.2	694	587.6
10	+0.1	0	-0.1	694	589.3	26	-0.1	-0.1	-0.2	695	588.5
11	+0.1	+0	-0.1	693	588.0	27	-0.1	0	-0.2	696	591.1
12	-0.1	+0.1	-0.1	694	587.7	28	-0.1	-0.1	-0.1	697	592.3
13	0	+0.1	-0.1	694	587.2	29	0	0	0	697	591.4
14	0	0	-0.1	694	587.3	30	0	-0.1	0	697	592.5
15	-0.2	0	-0.1	692	586.3	31	-0.1	0	0	698	593.1
16	-0.2	-0.1	-0.2	694	586.9						

All measurements in terms of H-P Caesium Standard No. 334, which agrees with the NPL Caesium Standard to 1 part in 10^{11} .

* Relative to UTC Scale; $(UTC_{NPL} - \text{Station}) = + 500$ at 1500 UT 31st December 1968.

† Relative to AT Scale; $(AT_{NPL} - \text{Station}) = + 468.6$ at 1500 UT 31st December 1968.

A method for obtaining three-dimensional optical images with minimal primary distortion from microwave holograms

D. G. JONES, B.Eng.*

and

A. P. ANDERSON, Ph.D.*

SUMMARY

A new method is presented for the reconstruction of almost distortionless three-dimensional optical images from microwave (or other long wavelength) holograms. The strategy for overcoming the axial elongation of an optical image from a long wavelength hologram scaled down by a factor less than the ratio of the two wavelengths used, is demonstrated using a computer simulated microwave hologram.

* Department of Electronic and Electrical Engineering, The University of Sheffield, Sheffield, S1 3JD.

1 Introduction

Microwave holographic imaging has found application in synthetic aperture radar¹ and, on a much smaller scale, in the imaging of concealed objects.^{2,3} The means of remote sensing of objects by radio waves and reconstructing a visible, focused image is of great interest and has led to many different techniques of microwave holographic imaging.⁴⁻⁶ However, to the best knowledge of the authors, there has not been a realization of the three-dimensional image reconstruction which one associates with the term 'holography'.

It has long been recognized that when a hologram of a three-dimensional object is formed with one wavelength and the stored image reconstituted with another, a primary distortion results⁷ in which the longitudinal or axial magnification is proportional to the square of the lateral magnification, the lateral magnification also varying with the axial coordinate. Consequently, to realize ideal, distortionless, three-dimensional images, the lateral and axial magnifications must be made equal and the lateral magnification must also be independent of the axial coordinate. These conditions are completely satisfied only when the hologram is scaled both by the ratio of the two wavelengths used, and the ratio of the radii of curvature of reference and reconstructing waves.⁸ Since these conditions cannot always be satisfied, the image reconstructed by optical waves from a hologram recorded at a longer wavelength is usually distorted and too small for direct viewing. One method of relieving the problem of small image size when scaling by the wavelength ratio is a 'fractionating' technique which has been suggested⁹ in order to increase the image size without re-introducing distortion. Another proposed solution to the problem of three-dimensional optical image reconstruction from longer wavelength holograms is to compensate for the distorted image by viewing through a pair of prisms.¹⁰

These ideas appear to be practical when the wavelength change is relatively small, but in the case of microwave holography, where the ratio of microwave to optical wavelength is in the range 10^4 - 10^5 , the whole problem of obtaining a three-dimensional image is a severe one since reduction of the hologram dimension by the wavelength ratio is impractical. (Synthetic aperture radar is an exceptional case because of the effective hologram dimensions.) It is therefore the present intention to demonstrate the means by which three-dimensional optical images with minimal primary distortion can be obtained from a suitably formed microwave hologram reduced in dimension by a factor much less than the wavelength ratio. This approach reduces distortion and will also permit intermediate-size holograms of linear dimension $> 10^3$ wavelengths to be viewed directly by eye.

2 Principle of the Method

For reasons which will become apparent as the theory is developed, the Fourier transform hologram distribution is considered. Use of microwave lenses to perform the transformation in the hologram formation process is not generally possible, especially for the linear dimensions

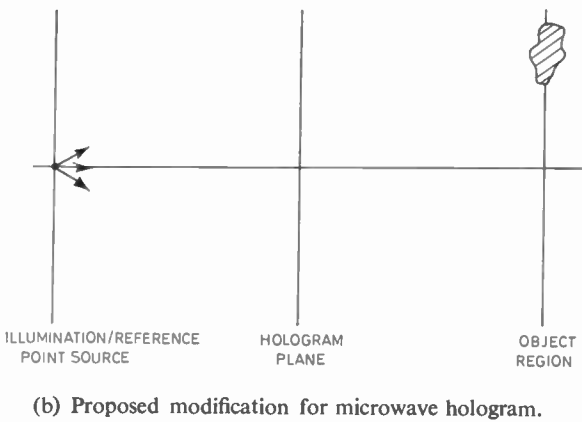
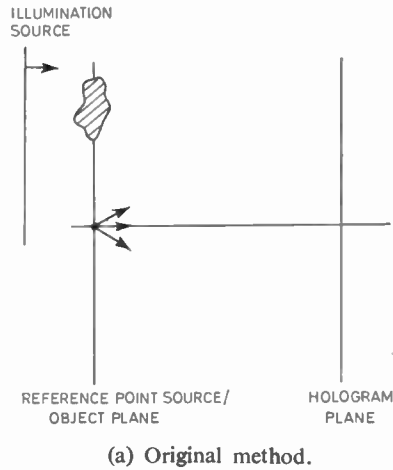


Fig. 1.

Formation geometry for a lensless Fourier transform hologram.

previously stated. However, the lensless Fourier transform technique,¹¹ originally devised for optical holography, emerges as an ideal basis for forming the microwave hologram. Just as this technique relaxes the film resolution requirement in optics, the microwave hologram can be adequately recorded by sampling the field distribution at predetermined intervals.¹² The original lensless Fourier transform technique shown schematically in Fig. 1(a) requires that the object be accessible. Since many applications of microwave holography are concerned with remote sensing, this hologram formation geometry is suitably modified by moving the object to the opposite side of the recording plane as shown in Fig. 1(b), such that source and object are equidistant from the hologram plane. The source now provides both the required reference field distribution and illumination of the object. Figure 2(a) shows the recording geometry of a microwave hologram of two object points with both lateral and axial spacing. Alternative methods for optical image reconstruction are shown in Figs. 2(b) and (c). The lateral magnification M_x of the optical image is given by¹³

$$M_x = \frac{\text{lateral image size at } \lambda_2}{\text{lateral object size at } \lambda_1} = \left\{ \frac{\lambda_2 Z_2}{\lambda_1 Z_1} \right\} K \quad (1)$$

where $K > 1$ is the hologram dimension reduction factor.

When the object point, O_{R1} , and the illumination source and reference, S , are equidistant from the hologram plane, a Fourier transform hologram distribution is formed within the paraxial limitations. In general, the object structure will be distributed in space around the (ξ, η) plane and $Z_1 \neq R_1$.

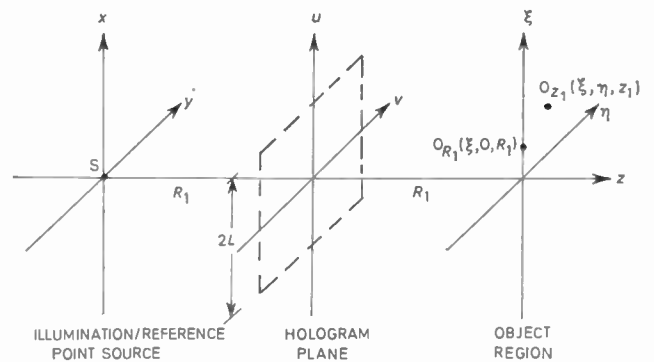
The axial magnification, M_z , is given by¹³

$$M_z = \frac{\text{axial image size at } \lambda_2}{\text{axial object size at } \lambda_1} = \frac{Z_2^2 \lambda_2 K^2}{Z_1^2 \lambda_1} = \frac{\lambda_1}{\lambda_2} M_x^2 \quad (2)$$

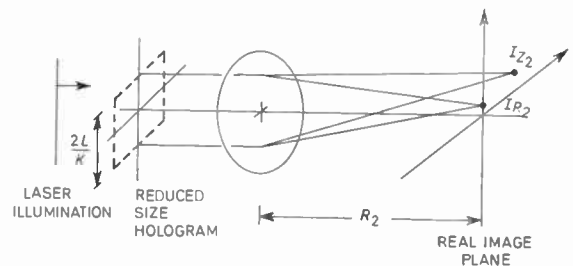
It is seen from equation (2) that the lateral and axial magnifications are not equal. Distortionless three-dimensional reconstructed images are obtained when $M_x = M_z$, and therefore

$$\frac{\lambda_1}{\lambda_2} M_x = 1 \quad (3)$$

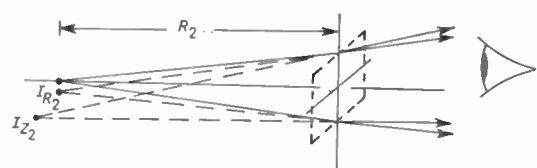
from equations (1) and (2). Hence, both lateral and axial magnifications are always equal to the wavelength ratio (λ_2/λ_1) when distortionless three-dimensional images are formed.



(a) Recording geometry for a microwave hologram of two object points.



(b) Optical real image reconstruction using a lens.



(c) Arrangement for viewing virtual image directly.

Fig. 2.

The focusing condition for the reconstructed image (analogous to the classical lens formula) is given by¹⁴

$$\frac{1}{Z_2} + \frac{1}{R_2} = -\frac{\lambda_2}{\lambda_1} K^2 \left(\pm \frac{1}{R_1} \mp \frac{1}{Z_1} \right) \quad (4)$$

where the upper signs refer to $Z_1 > R_1$ and the lower signs to $Z_1 < R_1$. Note that negative values of R_1 and Z_1 indicate that the two object points are located on the right-hand side of the recording aperture as shown in Fig. 2(a); a positive value of R_2 indicates that the reconstructing beam of light is convergent and that the images are real. These signs have been absorbed into equation (4).

Eliminating Z_2 from equations (1) and (4), and substituting the result in equation (3) yields the following quadratic equation in K :

$$K^2 Z_1 \frac{\lambda_2}{\lambda_1} \left(\pm \frac{1}{R_1} \mp \frac{1}{Z_1} \right) - K + \frac{Z_1}{R_2} = 0. \quad (5)$$

Solution of this equation gives two values of K at which the axial and lateral magnifications are equal. Using the binomial theorem, the following approximate solutions are then obtained:

$$K_1 = \left(\frac{R_1}{\pm Z_1 \mp R_1} \right) \frac{\lambda_1}{\lambda_2} - \frac{Z_1}{R_2} + \text{higher order terms} \quad (6a)$$

$$K_2 = \frac{Z_1}{R_2} + \text{higher order terms.} \quad (6b)$$

The higher-order terms contribute less than 1% for the typical range of values used in microwave holography and are therefore neglected. The solution, K_1 , is greater than the wavelength ratio and is therefore ignored but the second solution, K_2 , has flexibility and can be chosen by suitable design of the hologram formation and image reconstruction parameters.† Substituting $K_2 = Z_1/R_2$ into equation (5) leads to an exact solution of the quadratic if $Z_1 = R_1$, that is,

$$K = \frac{R_1}{R_2} \quad (7)$$

When $Z_1 = R_1$ over the whole object, a paraxially-limited Fourier transform hologram distribution is formed but the concept of a three-dimensional image is meaningless, the object there being planar. However when a Fourier transform hologram is formed with a three-dimensional object whose axial dimension is sufficiently small then the value of K given by equation (7) can be utilized. The quadratic phase deviation across a hologram resulting from such a three-dimensional object is given by

$$\phi = \left(\frac{2\pi}{\lambda_1} \right) \frac{L^2}{2} \left(\pm \frac{1}{R_1} \mp \frac{1}{Z_1} \right) \quad (8)$$

and is seen to be zero when the case of a Fourier transform hologram exists, that is when $Z_1 = R_1$. However, according to Diamond,¹⁵ the Fourier transform hologram distribution exists substantially over the range $-\pi/4 < \phi < \pi/4$, this being analogous to the Rayleigh

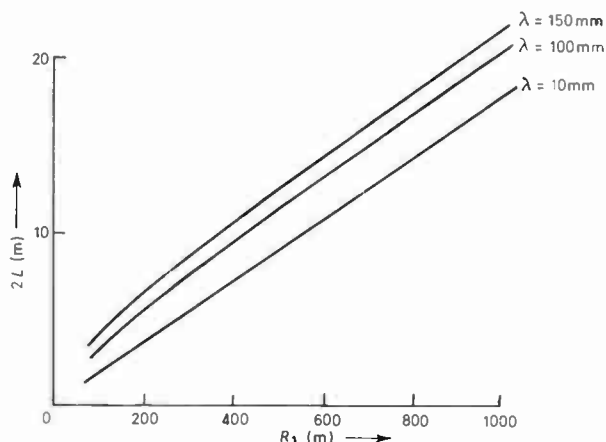
distance for an antenna at which the phase deviation across an illuminated aperture must be less than $\pi/4$ for generation of the far field pattern. Using this limit of ϕ , the maximum object depth which can be permitted is therefore given by

$$Z = \pm Z_1 \mp R_1 = \frac{R_1^2 \lambda_1}{(2L)^2 \mp R_1 \lambda_1}. \quad (9)$$

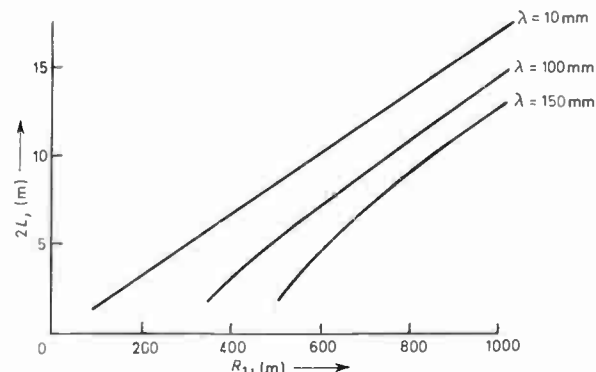
3 Computed Holograms and Optical Image Reconstructions

From the principal equations (7) and (9), curves of hologram aperture ($2L$), reduction factor (K) and reconstructing lens focal length (R_2), have been computed and plotted against reference distance (R_1) for a range of wavelengths (λ_1). Examples of these curves are shown in Figs. 3(a) and (b). The object depth (Z) was chosen initially to give an easily detectable image depth on reconstruction. It can be seen from these curves that although the object appears planar at the hologram recording plane, its axial component can be comparable to the reference distance.

A microwave hologram distribution of two object points has been computed on the basis of this theory



(a) $Z_1 > R_1, Z = 30$ m.



(b) $Z_1 < R_1, Z = 30$ m.

Fig. 3. Curves showing the relationship between hologram aperture and reference distance.

† The relationship between the proposed reduction factor and the ideal solution is given in the Appendix.

using the following parameter values:

object point spacing (laterally)	3 m
object point spacing (axially)	30 m
formation wavelength (λ_1)	10 mm
reference distance (R_1)	500 m
hologram aperture ($2L$)	10 m

The hologram distribution, generated on a 32-level intensity display system,¹⁶ is shown in Fig. 4. A reconstructed image obtained by illuminating the hologram with He-Ne laser light is shown in Fig. 5(a). The parameter values used in the reconstruction process are:

reduction factor K	10^3
reconstruction wavelength (λ_2)	0.6328 μm
reconstructing lens focal length (R_2)	500 mm

It should be noted that the value of K used is a factor of approximately 16 less than the wavelength ratio.

4 Interpretation of the Images

The reconstructed object points I_{Z_2} and I_{R_2} shown in Fig. 5(a) both appear in focus, indicating that they lie within the depth of focus of the lens, approximately 4 mm. The relative axial and lateral spacings in the microwave regime are found to be preserved in the optical regime. If the criterion for choosing K is not obeyed and the reduction factor increased by a factor of 2, then the distortion normally associated with wavelength change holography becomes obvious with the two points separated in depth by 9 mm, an axial elongation by a factor of 4.5. This distortion is shown in Fig. 5(b) as a defocusing of one of the reconstructed points.

In addition to the condition that the axial and lateral magnifications must be equal, the lateral magnification should also be independent of Z_1 for ideal distortionless three-dimensional imaging and this problem must be discussed with respect to the new solution. Substituting the focusing condition of equation (4) into equation (1)

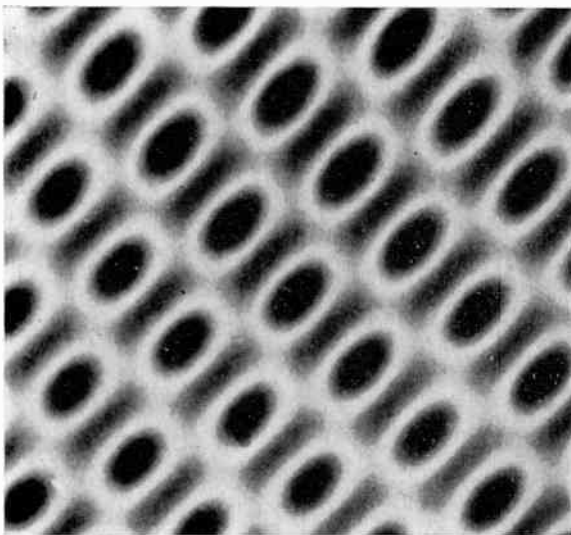
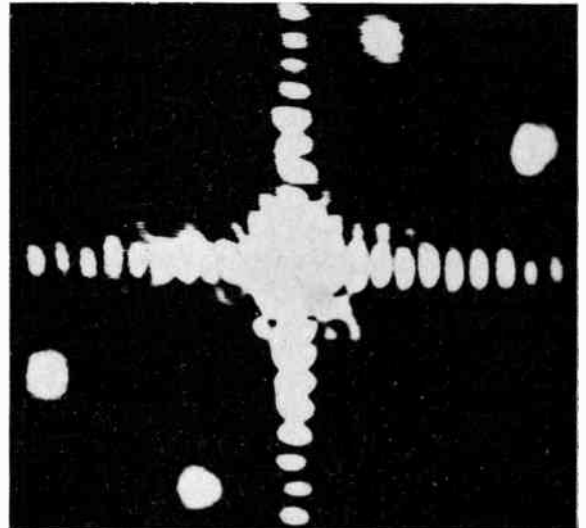
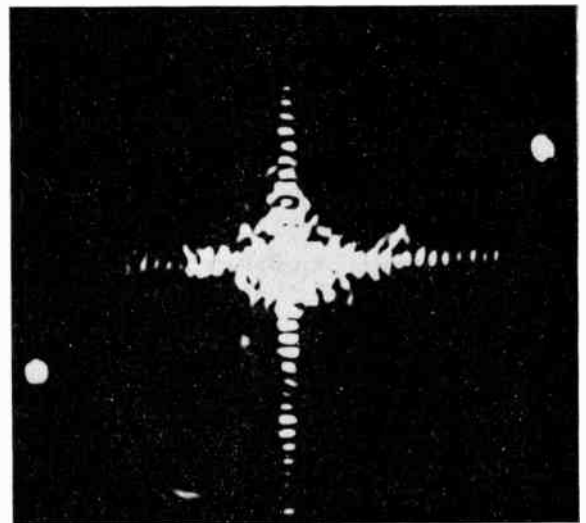


Fig. 4. Multilevel hologram of two object points.



(a) $K = 10^3$.



(b) $K = 2 \times 10^3$.

Fig. 5. Optical reconstructions of two points.

and eliminating Z_2 yields

$$M_x = \frac{(\lambda_2/\lambda_1) R_1 R_2 K}{(\lambda_2/\lambda_1) K^2 (\pm Z_1 \mp R_1) R_2 - Z_1 R_1} \quad (10)$$

Since $(\lambda_2/\lambda_1) K^2 R_2 (\pm Z_1 \mp R_1) \ll Z_1 R_1$ in the case of microwave holography, then

$$M_x \approx - \left(\frac{\lambda_2}{\lambda_1} \right) \frac{R_2}{Z_1} K.$$

Hence from equation (7)

$$|M_x| \approx \frac{\lambda_2}{\lambda_1} \left(\frac{R_1}{Z_1} \right) \approx \frac{\lambda_2}{\lambda_1} \left(\frac{R_1}{R_1 \pm Z} \right) \quad (11)$$

and shows the dependence of the lateral magnification on Z_1 for both $Z_1 > R_1$ and $Z_1 < R_1$. A graph of the lateral magnification against R_1 is shown in Fig. 6 for $Z_1 > R_1$ and for a constant object depth, Z . Since the lateral position of the imaged object point depends on the lateral magnification, the effect is manifested as a

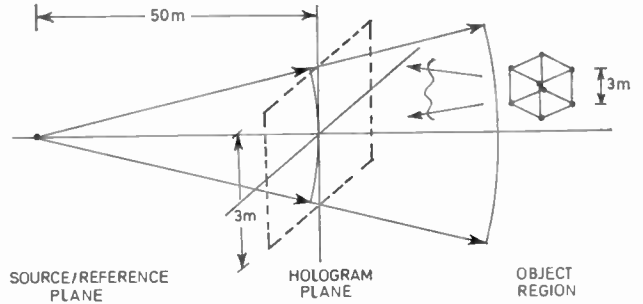
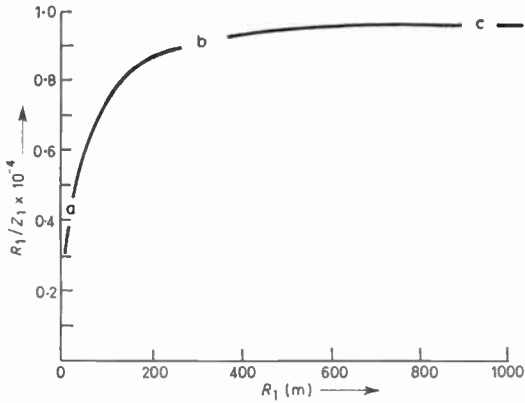


Fig. 7. Formation of the hologram of a cube showing dimensions used in the computer simulation ($\lambda_1 = 10$ mm).

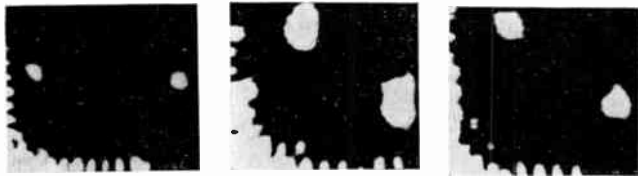


Fig. 6. Dependence of lateral displacement of a point for which $Z_1 \neq R_1$ on reference distance. Effect of parameters chosen at (a) $R_1 \approx Z_1$, (b) $R_1 = 9Z_1$ and (c) $Z_1 \rightarrow R_1$ is illustrated by reconstructed points.

lateral displacement of the point along a path joining the zero order axis of the system and the perfectly imaged object point. The graph shows that the correspondence between the image point I_{Z_2} and the perfectly imaged object point decreases as R_1 decreases, especially as R_1 approaches the object depth Z_1 . Only when $R_1 = Z_1$ and $M_x = \lambda_2/\lambda_1$ is there exact correspondence.

It is useful to consider how much distortion can be tolerated. The viewing of an image tends to be subjective depending on the type of image and how much distortion the viewer can accept before the image is no longer recognizable. Suppose (somewhat arbitrarily) that a disparity between the perfect and actual lateral magnifications of 10% is acceptable. Then for $Z_1 > R_1$ and using

equations (3) and (11) for the perfect and actual lateral magnifications,

$$\frac{\lambda_2}{\lambda_1} \frac{R_1}{Z_1} > 0.9 \frac{\lambda_2}{\lambda_1}$$

$$R_1 > 0.9 Z_1$$

or

$$R_1 > 9 Z_1 \tag{12a}$$

Similarly for $Z_1 < R_1$, the acceptable condition is

$$R_1 > 11 Z_1 \tag{12b}$$

Equations (12a and b) show that in order to limit the lateral distortion to a prescribed value, the reference distance must be greater than the object depth by the figures shown. The photographs in Fig. 6 show the three reconstructions under these conditions, namely, the undistorted image as $Z_1 \rightarrow R_1$, an image obtained from the condition $R_1 = 9 Z_1$, and an image with lateral distortion (shown by the orientation of the points) when $R_1 \approx Z_1$. It is observed that there is very little difference between the perfect case ($Z_1 = R_1$) and the case given by equation (12a). Similar results are to be expected from equation (12b). Since the holograms corresponding to the three images have different aperture and reference distances, the object point, O_{R_1} , will produce higher spatial frequencies in the hologram plane as R_1 is decreased. Hence the image of O_{R_1} moves further from the axis and its lateral position is in fact proportional to

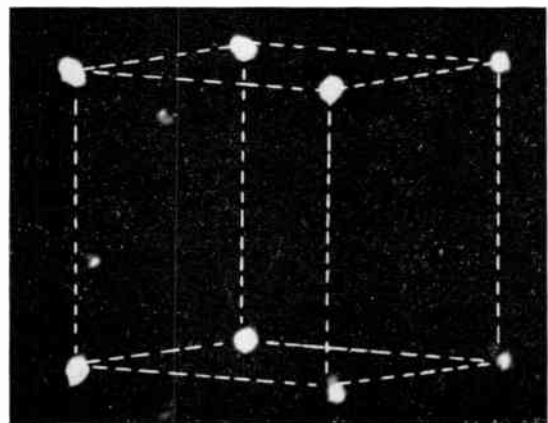
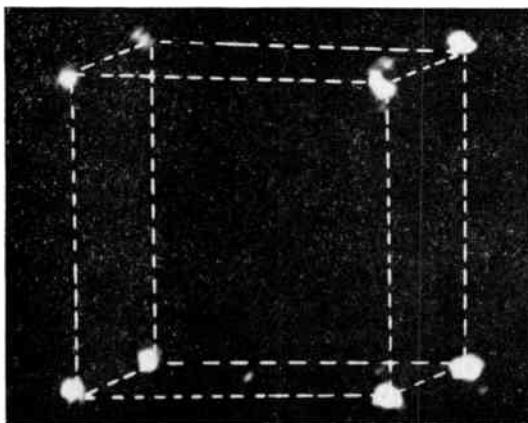


Fig. 8. Optical reconstructions of the cube. (a) Rotated 20° around ζ -axis, (b) rotated 40°.

$(2L/R_1)$. Thus, as R_1 decreases while maintaining $Z_1 > R_1$, the point I_{z_2} moves towards the axis as the image O_{R_2} moves away which explains the distortion seen in Fig. 6 as R_1 approaches Z .

The whole operation of hologram formation and image retrieval is shown convincingly for eight object points forming the shape of a cube. The dimensions used in the computer simulated microwave regime are shown in Fig. 7. Two views of the reconstructed object are shown in Figs. 8(a) and (b).

5 Conclusions

New criteria have been developed for the reconstruction of almost distortionless three-dimensional optical images from microwave (or other long wavelength) holograms. Hitherto, the requirement for distortionless three-dimensional images has been that the long wavelength hologram must be scaled by the wavelength ratio and hence such images have not been realized. The proposed criteria permit the hologram to be scaled by a factor much less than the wavelength ratio and this result has been verified in practice using a computed hologram.

An expression is given for the maximum permitted object depth when using the new scaling factor and also a relationship between reference distance and object depth which sets a limit on the lateral distortion

Although in principle the reduction factor can be chosen at will by suitable manipulation of the parameters for any object, in practice the final image size may be a critical factor in determining K ; if the object is too small, then it will be impossible to view the image directly. When the object size permits direct viewing of the reconstructed image, the scaled microwave hologram must be illuminated by a diverging optical wave of the correct radius of curvature. Only in this case is the full three-dimensional character of the image retained. However, in cases where the reconstructed optical image requires magnification, elimination of gross primary distortion is still desirable, and, in some cases, the whole almost undistorted image can be arranged to be within the depth of focus of the optical viewing system.

6 Acknowledgment

The authors gratefully acknowledge the financial support from Science Research Council, U.K.

7 References

1. Leith, E. N., 'Quasi-holographic techniques in the microwave region', *Proc. Inst. Elect. Electronics Engrs*, **59**, pp. 1305-19, 1971.
2. Farhat, N. H. and Guard, W. R., 'Millimeter wave holographic imaging of concealed weapons', *Proc. IEEE*, **57**, pp. 354-5, 1969.
3. Orme, R. D. and Anderson, A. P., 'High resolution microwave holographic technique', *Proc. Instn Elect. Engrs*, **120**, pp. 401-6, 1973.
4. Tricoles, G. and Rope, E. L., 'Reconstructions of visible images from reduced scale replicas of microwave holograms', *J. Opt. Soc. Amer.*, **57**, pp. 97-9, 1967.

5. Iizuka, K., 'In situ microwave holography', *Applied Optics*, **12**, pp. 147-9, 1973.
6. Augustine, C. F., 'Microwave holograms using liquid crystal displays', *Proc. IEEE*, **57**, pp. 354-5, 1969.
7. Gabor, D., 'Microscopy by reconstructed wavefronts', *Proc. Roy. Soc. (London)*, **A197**, pp. 454-87, 1949.
8. Leith, E. N., Upatnieks, J. and Haines, K. A., 'Microscopy by wavefront reconstruction', *J. Opt. Soc. Amer.*, **55**, pp. 981-6, 1965.
9. Thurstone, F. L., 'On holographic imaging with long wavelength fields', *Proc. IEEE*, **56**, pp. 768-9, 1968.
10. Winter, D. C., 'Correction of unequal longitudinal and lateral magnification in holography', *Applied Optics*, **10**, pp. 2551-3, 1971.
11. Stroke, G. W., 'An Introduction to Coherent Optics and Holography' (Academic Press, London, 1966).
12. Anderson, A. P., 'Some basic experiments on the optical resolution of sampled microwave holograms', *Opto-Electronics*, **3**, pp. 127-30, 1971.
13. Devellis, J. B. and Reynolds, G. O., 'Theory and Applications of Holography' (Addison-Wesley, New York, 1967).
14. Meier, R. W., 'Magnification and third-order aberrations in holography', *J. Opt. Soc. Amer.*, **55**, pp. 987-92, 1965.
15. Diamond, F. I., 'Magnification and resolution in wavefront reconstruction', *J. Opt. Soc. Amer.*, **57**, pp. 503-8, 1967.
16. Whitaker, A. J. T. and Anderson, A. P., 'Improved optical images using a multilevel display system for non-optical hologram distributions', *Laser & Optics Technol.*, **5**, pp. 28-9, 1973.

8 Appendix

The relationship between the reduction factors obtained in equations (6a and b) and the ideal solution⁸ is seen as follows. Consider the quadratic equation in K given by equation (5). The solution gives two values of K at which the condition of equal lateral and axial magnifications is satisfied. However, as previously stated, the other condition which must be satisfied for a perfect solution to the three-dimensional problem is that the lateral magnification must be independent of the axial co-ordinate. Since the lateral magnification is contained in equation (5), then it can be made independent of Z_1 by equating terms containing Z_1 to zero, that is,

$$\pm K^2 \frac{Z_1}{R_1} \left(\frac{\lambda_2}{\lambda_1} \right) + \frac{Z_1}{R_2} = 0$$

or

$$\mp K^2 R_2 \lambda_2 = R_1 \lambda_1. \tag{13}$$

Equation (5) now reduces to

$$K = \frac{\lambda_1}{\lambda_2}. \tag{14}$$

Substituting this expression for K in equation (13) yields the ideal reduction factor:

$$K = \frac{\lambda_1}{\lambda_2} = \pm \frac{R_1}{R_2}. \tag{15}$$

Manuscript first received by the Institution on 6th August 1973 and in final form on 17th October 1973. (Paper No. 1575/MST 2.)

© The Institution of Electronic and Radio Engineers, 1974

IERE News and Commentary

ICE Luncheon Club

Membership of the Luncheon Club at the Institution of Civil Engineers, Great George Street, Westminster, S.W.1, is open to members of other CEI Institutions without subscription and does not require special membership cards. Members of the IERE are entitled to make full use of the facilities of the Club and the only formality is that they may very occasionally be asked, as may Civil Engineers, to establish their identity and link with the IERE.

The Restaurant, Cafeteria, ICE Box Bar and Buttery at Great George Street are open daily from Monday to Friday between 12 and 2.30 (except at holiday periods). Members may bring guests (including ladies and children). It is advisable to book tables in the Restaurant—telephone 930 8373.

Changes of Address

Members are reminded that they should notify the Institution as soon as possible of any change in the address to which Journals and other membership correspondence are sent. The form printed at the back of most issues of the Journal can be used for this purpose but it is also helpful if an old address label is enclosed with the notification.

It should be appreciated that it is not possible to put such changes into effect immediately since labels for posting Journals are prepared some time in advance of the actual posting dates. Arrangements for forwarding of such communications are therefore recommended. The British Post Office makes a charge for redirection of 50p for a period not exceeding one month, for a period not exceeding three months 75p, and for 12 months £2.

Index to Volume 43

The index for the 1973 issues of the Journal, forming volume 43, will be ready in April. As stated in the December 1973 issue (page 761), copies will only be sent automatically to libraries and other organizations who subscribe to the Journal. Members of the Institution who wish to obtain a copy of the index may obtain one free of charge on application to Publications Department, IERE, 8-9 Bedford Square, London WC1B 3RG. As a limited number only will be printed it would be helpful if such requests are made without delay. Indexes will be incorporated in all bound volumes supplied by the Institution.

The Changing Role of Purchasing in the Telecommunications Industry

The Institute of Purchasing and Supply has formed a new Specialist Section covering Telecommunications and its first meeting will be held at the London Hilton on Thursday, 9th May.

The basic aims of the meeting are:

To assist top management and particularly those in Procurement, Marketing, Planning and Production to appreciate the additional demands of increased programmes and changing technology which will arise during the next decade or so of accelerating growth in Telecommunications.

To review present and future developments of components and materials and seek the views of experts in these fields.

The following contributions are to be made:

'Telecommunications and the Future—A Post Office View'
K. H. Cadbury, C.B.E., M.C. (*Senior Director, Planning and Purchasing, Post Office*)

The Eighth Clerk Maxwell Memorial Lecture

A record attendance was present at the London School of Hygiene and Tropical Medicine on March 21st to hear Dr. Wernher von Braun give his Clerk Maxwell lecture on 'Our space programme after *Apollo*'. The lecture will be published in full in an early issue of the Journal, together with a selection from the excellent slides which accompanied the presentation.

'The Collected Clerk Maxwell Memorial Lectures,' which comprises the first seven lectures given between 1951/71, may be obtained from the IERE Publications Department, price £2.50.

IERE Visit to ESTEC

The Institution has received an invitation for a small party to visit the European Space and Technology Centre (ESTEC) at Noordwijk in The Netherlands on Friday, 3rd May next. The party will be welcomed by Dr. O. Hammarström, Director of ESTEC, and the programme will include a tour of the Centre under the guidance of Dr. A. V. J. Martin, C.Eng. (Fellow). This will be followed by a presentation on European electronics projects in space. In addition to providing an opportunity to visit the Centre, this visit will be an excellent opportunity for members to meet and get to know some of their colleagues working in Europe.

It is proposed that the party should fly from London Airport to Amsterdam on the evening of Thursday, 2nd May, stay overnight at a hotel in or near Noordwijk, and return to London on the evening of Friday, 3rd May. A reception and dinner will be held following the visit at which wives (or other guests) will be welcomed. If there is a sufficient number of ladies in the party a tour of the bulb fields will be arranged during the day. The cost including air fare and overnight accommodation will be between £50 and £55 per person.

Further details may be obtained from Mr. R. C. Slater, Deputy Secretary, IERE, 8-9 Bedford Square, London WC1B 3RG.

A History of the Institution

'A Twentieth Century Professional Institution: The Story of the IERE' is still available in paper bound form, price £1.50. This 120 page book covers the history of the institution from its foundation in 1925 up to the granting of the Royal Charter and relates it to developments in radio science and the electronics industry. (A fuller description is given on the advertisement pages in this issue.) Orders for copies should be accompanied by a remittance and sent to the Publications Department, IERE, 8-9 Bedford Square, London WC1B 3RG.

'The Technological Revolution in Telecommunications and its Effect on Export Markets'

D. H. A. Scholey, M.B.E., C.Eng., F.I.E.E., F.I.E.R.E. (Technical Executive (Telephony), Private Communications Systems, Plessey Telecommunications Limited)

'Electronic Components for Telecommunications'

J. A. Everist (Advance Programmes Manager, ITT Semiconductors)

'The Essential Connection'

R. A. Leather, B.Sc., C.Eng., M.I.E.E., M.I.Mech.E. (Manager, Electrical Connections Group of Ferranti Limited)

'Transmission'

G. A. Dodd, M.B.E., C.Eng., F.I.E.E., A.I.R.S.E. (Divisional Director and General Manager, Telephone Cables Division, B.I.C.C. Limited)

The fee for this one-day meeting will be £19.80 for members of the Institute of Purchasing and Supply and £24.20 for non-members. These charges include luncheon, coffee, tea and V.A.T. A detailed programme is available from Mrs. G. Hine, Institute of Purchasing and Supply, York House, Westminster Bridge Road, London, SE1 (Telephone 01-928 1851).

CEI News

CEI and the Future of the Institutions

'The CEI and the Future of the Institutions' was the title of a forum organized by the Peterborough Joint Panel of the Institutions of Mechanical, Electrical and Marine Engineers on 11th February last. Chaired by Sir Leonard Atkinson, Chairman of CEI, the panel comprised Mr. M. W. Leonard (CEI), Dr. G. F. Gainsborough (IEE), Mr. J. G. Watson (ICE), Mr. J. S. Robinson (IMarE) and Mr. K. H. Platt (IMEchE).

A well-attended meeting heard various aspects covered by the speakers of the engineering institutions' current and future activities. Mr. Leonard spoke on the present activities of CEI in relation to H.M. Government, the Common Market and State Registration. Qualification standards, recruitment, training and re-training of engineers were covered by Mr. Watson. Dr. Gainsborough spoke on learned societies and professional conduct. From Mr. Stuart Robinson the audience heard about the funding of CEI activities in relation to the Institutions, and from Mr. Platt a summary of the personal services to members available from the institutions.

Streamlining CEI—the New Structure

By 1972 a stage had been reached in the evolution of the Council of Engineering Institutions when it was felt timely both to review the progress made by the Council since its inception in 1965 and to determine whether its existing structure was best adapted to meet future developments and requirements. A feeling prevailed that the Board itself, with its large representation from Constituent Members, was too cumbersome a vehicle to deal with the gathering momentum of day-to-day business being encountered by CEI. The first step towards implementing a more streamlined structure came in November 1972, when Presidents of Constituent Members concurred with a memorandum on CEI Phase II. This included a proposal that 'the Board would delegate powers to a small Executive body to deal with all Council business except that which the Board would specifically reserve to itself, e.g. changes in the Constitution, standards, new membership. The Executive Committee would advise the Council on policy and be responsible for seeing appropriate papers are initiated for the Council's consideration'.

In March of last year the Board decided that the principle of a small Executive be adopted and that an Interim Executive Committee should be set up to examine and progress its formation. This was formed in May with a brief to prepare formal proposals to place before the Board at its July meeting. In examining a framework and guidelines for its permanent successor, the Executive Committee itself, the Interim Executive produced some positive proposals that were accepted by the Board. One of these was that the Board should meet twice yearly in addition to the Annual Meeting and as

special occasion might demand. Another was that the Executive should meet regularly to see that much of the business previously undertaken by the Board was completed expeditiously.

It was also proposed that there should be some rationalization of the standing committee structure. Here it was envisaged that the work of the existing five standing committees—those for Education and Training, General Purposes and Finance, Membership, Overseas Relations, and Parliamentary Affairs—would in future be undertaken by the Executive Committee in conjunction with only three standing committees, 'A', 'B' and 'C'.

All these recommendations have now been implemented, and meetings have taken place both of the Executive and of the three new standing committees.

The work of Committee A, under the chairmanship of Professor J. F. Coales, concerns registration procedures for C.Eng. and all academic matters leading to qualification, registration, education and training of Chartered Engineers. The concern of Committee B, whose chairman is Mr. B. Hildrew, is that of CEI's internal affairs, and it will consider and advise on matters in which the Constituent Members must specifically participate in order to effect action. Committee C, under Sir Norman Rowntree, is for external affairs and it will consider and advise on any matters which involve organizations outside CEI and the Constituent Members.

As a result of this reorganization the IERE Council is making a number of new appointments to CEI. Professor W. Gosling (Vice-President) is to serve on Standing Committee Band a nomination will shortly be made to Standing Committee A on which it had been intended that the late Professor Emrys Williams should serve. Membership of Standing Committee C is on a group basis and the IERE is represented by an IEE member, Mr. R. T. Clayton. As far as representations on the Board itself is concerned, two vacancies have arisen, one due to the death of Professor Williams, the other because the President, Dr. I. Maddock is responsible, in his capacity of Chief Scientist of the Department of Industry, for certain important aspects of the Government's relationships with the Board. One of these vacancies is to be filled by Dr. P. A. Allaway (Vice President), and Council will make the second appointment shortly. The third IERE Board member will continue to be the Director, Mr. G. D. Clifford.

CEI Survey

Members are reminded that copies of CEI's 'Survey of Professional Engineers 1973', published in December (and fully commented upon in the December issue of *The Radio and Electronic Engineer*) are obtainable from the Council of Engineering Institutions, 2 Little Smith Street, London SW1, price of £4.50.

A tribute to

Professor Emrys Williams

B.Eng., Ph.D., C.Eng., F.I.E.E., F.I.E.R.E.

Members throughout the world will regret the death on 13th February 1974 of Emrys Williams, the 19th President of the Institution. It was in character with his deep involvement in Institution activities that he had just left the Annual General Meeting of the South Wales Section when he suddenly collapsed.



Born in Liverpool in 1910, Emrys Williams graduated from the University of Liverpool in 1932; his doctorate was conferred in 1934 for his work on electroacoustics. He then joined the Scientific Staff of the General Electric Company at Wembley and worked in the Electroacoustics, Telephony and Television Departments of the Research Laboratories. It was there, in 1936, that we met and talked about education, Institutions and the future of radio engineering.

His belief in the need to foster the teaching of radio engineering in the universities led him to secure, in 1937, a Lectureship at King's College, University of Durham. He retained this appointment for ten years, during which he married Dr Margaret Morrison, wrote the first of two standard textbooks—'Thermionic Valve Circuits'—and became a corporate member of the Institution in 1944. He was immediately appointed to the Committee of the North Eastern Section, of which he subsequently became Chairman.

Thus he began to demonstrate the sincerity of his convictions which also encompassed international freedom of opportunity. Much could be written of the liberal views of Emrys which he translated in later life by generously giving time and effort to deserving causes.

Having voluntarily worked for the need for universities to encompass radio and electronics as major departments he sought and obtained the Chair of Electrical Engineering at the University of North Wales, Bangor, in 1947. Seven years later he was appointed by the University College of South Wales and Monmouthshire to the Chair in Electrical Engineering and subsequently headed the separate Department of Electrical and Electronic Engineering—the post he was to hold for the remainder of his life. During that time he was a forceful advocate of full University status for each of the four colleges of the University of Wales.

Professor Emrys Williams spoke and wrote widely on technical and educational matters. His second, and now standard, textbook on 'Electric Wave Filters' was published in 1963 and he gave talks and papers to many Institutions on fundamental aspects of electronic engineering. His writings in *The Radio and Electronic Engineer* were on education and training; his Inaugural Address as President* in 1967 emphasized the need for specialization in engineering and is memorable for his description of electronics as 'the greatest intellectual "nosey parker" of all time'.

His ever growing reputation on training in the electronics field resulted in his being invited to be an external examiner to several British Universities; he was also a visiting professor to the Kumasi University of Science and Technology. In March 1967 Professor Williams made an overseas tour, with the Director, visiting the Indian Division and the newly formed Israeli Section.

Before the advent of the CEI, Emrys Williams was the IERE representative on the Joint Committee for National Certificates in Electrical and Electronic Engineering for many years, and also the Institution's representative on the Engineering Institutions Joint Council (EIJC)—the forerunner of CEI.

This testimony is to record the influence that Emrys Williams had on the welfare of the Institution of Electronic and Radio Engineers. For thirty years he was continuously involved in its affairs, both in the Sections and on the Council and its Committees. He was first elected to the Council in 1952 and apart from a statutory interval of a year's absence, as required by the Bye-Laws, he continuously served on it until last October; in 1954 he was Chairman of the Council and in 1957 was appointed a Vice-President; he was named a Charter Vice-President and in 1967 succeeded to the Institution's highest office.

In all the work which preceded the grant of the Royal Charter, Emrys Williams was a permanent representative of the Institution in the many negotiations which took place right up to the preparation of the Petition, the reply to the counter-Petition, and in the drafting of Bye-Laws. Indeed, he will be remembered by many for his diplomacy and skill as a negotiator, and in the Institution as a hardworking committee member and a tactful Chairman.

Ever since CEI was formed he was a member of its Board, and humbly undertook the duties of a committee member on Education and Training.

A writer and linguist of distinction, Emrys Williams delighted in exploration, mountaineering and music as hobbies. A delightful companion and a sincere friend, there will be many in and out of the Institution who will feel the mark of his work. All will have great sympathy with his wife and two sons; sadly, he missed by a few days the birth of his first grandson.

G.D.C.

* *The Radio and Electronic Engineer*, 33, pp. 1–8, January 1967.

Forthcoming Conferences

The History of Electrical Engineering

Following the success of the conference 'The History of Electrical Engineering' held in July 1973, the Science, Education and Management Division of the Institution of Electrical Engineers is organizing a second conference at Goldsmith College, University of London, from 12th-14th July 1974.

The conference programme will include lectures, lecture tours, visits to places of electrical history interest, including the Royal Institution to see the Faraday Museum and Archives, and talks on recent research in electrical history (for which offers are invited).

Further information and registration forms are available from the Secretary, IEE, Savoy Place, London WC2R 0BL, quoting the reference LS(SEM).

L.F. and D.C. Electrical Measurement Practice

The third in the series of vacation schools on electrical measurement practice is being organized this summer by the Institution of Electrical Engineers. Entitled 'L.F. and D.C. Electrical Measurement Practice' it is being held at the University of Lancaster from 7th-19th July 1974. The IERE, the British Calibration Service and the Institute of Electrical and Electronics Engineers (UKRI Section) will co-sponsor the school; Mr. A. G. Wray (Fellow) is representing the IERE on the organizing committee for the school.

Both the theory and techniques of electrical measurements at d.c. and low frequencies (up to 100 kHz) will be covered, including the maintenance and use of standards and equipment as well as aspects of laboratory management. There will be ample time for discussion.

The school is aimed at practitioners in electrical measurements in particular those engaged in the operation of standards and calibration laboratories and other measurement facilities and also at those involved in measurement education and training. Although a degree is not essential, it is likely that graduates and professional engineers will get the greatest benefit from the school.

Companies who send employees to this vacation school may record the time spent as days of training for General Grant claim from the Engineering Industries Training Board.

Further details are available from the Secretary, IEE, Savoy Place, London WC2R 0BL, quoting the reference LS(S).

Materials for use in Medicine and Biology

A two-day Conference is being organized by the Biological Engineering Society in association with the Institute of Physics (Materials and Testing Group), and the Hospital Physicists' Association. The subject of the Conference is 'Materials for use in Medicine and Biology' and it is to be held at Churchill College, Cambridge, from 18th to 19th July 1974.

The two major themes of the Conference will be Implant Stability and Incorporation, and Implant-tissue Compatibility. Included amongst the topics under discussion will be surgical adhesives, porous prostheses, tissue-implant inter-

facial reactions including blood compatibility, systemic effects following implantation, artificial joints, infection and implants, and dental implant materials.

Further information may be obtained from Mr. K. Copeland, Biophysics Department, University College London, Gower Street, London WC1E 6BT (Tel. 01-387 7050, Ext. 288).

Low Light and Thermal Imaging Systems

Papers are now invited for an international conference on 'Low Light and Thermal Imaging Systems' to be held at the Institution of Electrical Engineers, London, from 4th-7th March 1975.

The conference is being organized by the Electronics Division of the Institution of Electrical Engineers in association with the IERE, the Institute of Physics and the Institute of Measurement and Control. The IERE representatives on the Organizing Committee are Lt. Col. W. Barker and Mr. W. G. Gore (Members).

Sessions will include the following topics:

Phenomenological aspects: reflectivity, contrast, emissivity, radiance and transmission.

Optical system design: scanning, high-speed, stroboscopic, wide-angle, augmented, range-gated and assessment of optical imaging systems.

Detectors: imaging tubes, intensifiers, detectors, detector arrays and cryogenic systems.

Signal processing: image motion compensation, scan conversion picture recording and transformation, and target detection.

Displays: solid state, plasma, false colour, isothermal and man/machine interface.

Systems and applications: surveillance, location, recognition, underwater, airborne, space, security, medical, forensic, scientific, environment management and extreme environments.

Papers on phenomenological aspects and components should be directly relevant to complete low light or thermal imaging systems.

The Organizing Committee invites offers of contributions not exceeding 3000 words (i.e. maximum of six A4 pages including typescript and illustrations) for consideration for inclusion in the conference programme. Those wishing to offer a contribution should submit a synopsis of approximately 250 words to the IEE Conference Department by 1st May 1974. The full typescripts will be required for assessment by 14th October 1974.

Registration forms and further programme details will be available a few months before the date of the conference from the IEE Conference Department, Savoy Place, London WC2R 0BL.

Aerospace Instrumentation

The 8th International Aerospace Instrumentation Symposium will be held at Cranfield Institute of Technology, Cranfield, Bedford, England, from 24th to 27th March 1975. The Symposium is sponsored by the Cranfield Institute of Technology, the Royal Aeronautical Society, the Institute of Measurement and Control, and the Instrument Society of America. An exhibition of Aerospace Instrumentation equipment will be held in conjunction with the Symposium.

Papers are invited on subjects in the following list:

Transducer developments.

Instrumentation systems for: aircraft and helicopter flight test including environmental measurements; space flights; surface transport; hovercraft.

Avionic equipment for: aircraft and helicopters; communication satellites; external environmental monitoring from aircraft and spacecraft; aerial survey; navigational aids.

Telemetry systems including vehicle equipment, r.f. links and ground stations.

Tape recorder developments and applications.

Applications of new theoretical concepts and computer techniques to the problems of data gathering, transmission and analysis.

Authors who wish to present a paper are invited to send, by 1st June 1974, a brief (up to 100 words) synopsis on these or other related subjects to: Mr. N. O. Matthews, Symposium Organizer, Department of Flight, Cranfield Institute of Technology, Cranfield, Bedford, England.

Electrical Measurements in Europe

A residential specialist seminar on 'Electrical Measurements in Europe' will be held at the Université Libre de Bruxelles, Belgium from 2nd-5th September 1974. It is being organized jointly by the Institution of Electrical Engineers and the Société Royale Belge des Electriciens in association with the British Calibration Service.

The aim of the seminar is to provide a forum where senior men in the measurements field throughout Europe will be able to survey the present situation, identify industrial needs, highlight problems and consider possible solutions to these problems. It is hoped that the exchange of views will be frank and that it will be possible to achieve a measure of harmony in this field of technology.

There will be five half-day sessions devoted to: specification and certification, national standards and problems of traceability, national calibration facilities, the market for electrical instruments, and prospects of European co-operation.

Further details are available from the Divisional Secretary LS(S), IEE, Savoy Place, London, England WC2R 0BL.

Management in Engineering

A residential vacation school 'Management in Engineering' will be held from 7th to 13th September 1974 at the London Graduate School of Business Studies. It will be an intensive week's course to provide an understanding of the more important management skills for engineers who are in managerial positions or who are about to assume them.

Subjects to be included in the school are: company objectives and strategy; business planning; marketing; financial planning; organization; manpower planning; management development (including motivation); management of engineering activities; project management; and problems of engineering management in a mass production situation. The emphasis throughout will be on the integrated management approach, with lectures drawing on case studies from engineering situations. They will be supplemented by syndicate sessions, discussion groups and films.

The school will be organized by the Science, Education and Management Division of the Institution of Electrical Engineers, and further details will be available shortly from the Secretary, IEE, Savoy Place, London WC2R 0BL, quoting the reference LS(S).

Dielectric Materials, Measurements and Applications

Papers are invited for the conference 'Dielectric Materials, Measurements and Applications' to be held at Churchill College, Cambridge from 21st-25th July 1975. It is being

organized by the Science, Education and Management Division of the Institution of Electrical Engineers in association with the IERE, the Institute of Physics and the Institute of Electrical and Electronics Engineers (United Kingdom and Republic of Ireland Section). The representative of the IERE on the Organizing Committee is Dr. R. A. Waldron (Fellow).

The conference will be of interest to those involved with dielectrics and will cover the field widely, including frequency, temperature, pressure and other physical parameters. The areas to be covered will include: the behaviour and the underlying physical principles of solid, liquid and gaseous dielectrics (including biological materials); and the application of dielectric materials and techniques for measuring their properties.

The Organizing Committee invites offers of contributions of not more than 2000 words for consideration for inclusion in the conference programme. Those wishing to offer a contribution should submit a 200-300 word synopsis to the IEE, Conference Department by 29th July 1974. Full typescript will be required for assessment by 10th February 1975.

Registration forms and further programme details will be available a few months before the conference from the Conference Department, IEE, Savoy Place, London WC2R 0BL.

Fifth B.E.S. Conference

On the occasion of the 15th Anniversary of its foundation, the Biological Engineering Society is organizing a major International Conference, the fifth in its series on 'Recent Advances in Bio-Medical Engineering'. It will be held in Edinburgh during the week of 10th to 17th August 1975, immediately before the commencement of the Edinburgh Festival of Music and the Arts.

Under its Chairman Mr. W. J. Perkins, C.Eng., F.I.E.R.E., the Programme Committee is working out a new approach to avoid the formal presentation of ten-minute papers which invariably allow little time for discussion, and to encourage participation by all delegates. Subjects will be selected that are considered to be important, and these will be dealt with at seminars in which a chairman will control the discussion. Some chairmen may decide to have an opening speaker, and persons wishing to make a definite contribution to the discussion may be invited to become participants, rather than to present a formal paper. It is possible that one session will be devoted to the presentation of papers of merit that do not fit into the selected topics. Some twenty seminars are envisaged at present and the choice of subjects needs careful consideration. It is hoped that intending delegates will put forward their own ideas for seminar subjects at the planning stage. As an example—ultrasonics is a major topic, but too general and could be discussed under a title of 'Patient-acceptable methods of measurement' which could also introduce the necessary compromise with the quality of the measurement.

Appropriate emphasis will be given in the seminars to the significant advances which demonstrate the practical applications of bio-medical engineering in clinical practice and developments which enable those with various deficiencies to live fuller and more independent lives.

Scientific and commercial exhibits will be welcomed and will be located in close proximity to the Lecture Theatre. Accommodation has been arranged at University Halls of Residence or for those who prefer at hotels in Edinburgh. Further details can be obtained from Mr. K. Copeland, Biophysics Department, University College London, Gower Street, London, WC1E 6BT.

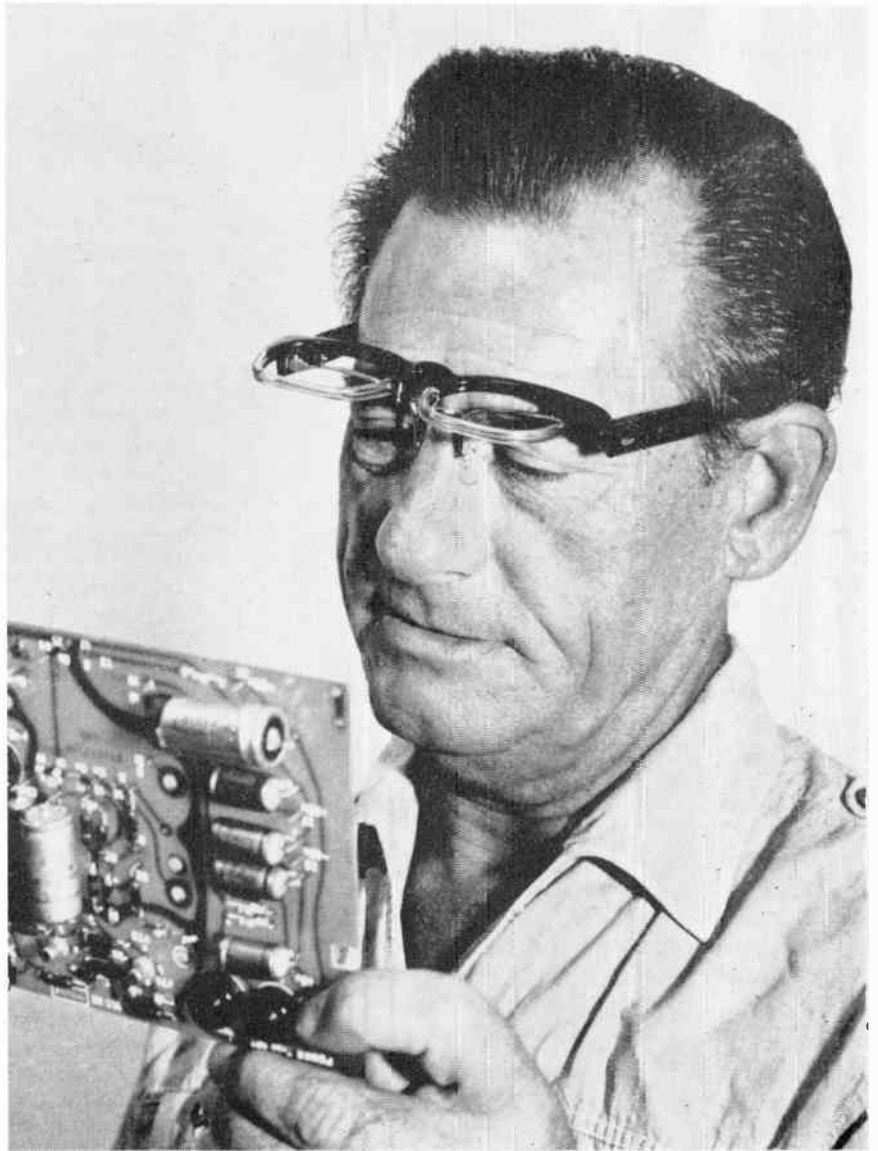
Eyes at Work

People do amazing things to overcome or avoid a vision handicap for which, if only they knew, the solution was simple. For example, an electrician used to turn his bifocal glasses upside down to do overhead work and risked costly repairs every time they fell off his face, while a fork-lift truck driver was on the point of giving up a job he liked because he was so distracted by overhead lights reflecting in his lenses as he drove around a warehouse.

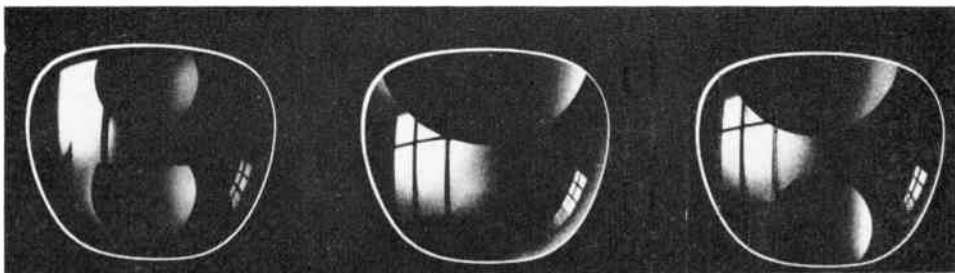
Most people regard their glasses as all-purpose aids, and end up fuming when the lenses will not serve some specialized need. Yet modern lenses can be made for almost any combination of seeing tasks, to improve personal comfort and performance.

The answer to the electrician's problem was a pair of special bifocal lenses with an extra portion at the top for viewing near-range work above eye-level. The fork-lift truck driver found his solution by having lenses treated to minimize the troublesome reflexions. In these and many other instances, the lenses were like tools of the trade—made with the individual's particular needs in mind. The special needs of those in other occupations can be catered for in the same way.

In the case of an engineer, any of the forms illustrated might perform more usefully than a conventional 'reading' bifocal. Points to consider are the direction of vision used (up, down, sideways) and the distances focused in relation to the particular sight problem involved. Thus the optician should be told precisely how eyes are used both at work and leisure.



A special spectacle frame shown in its alternative position—for reading and close work. The hinge in the frame (discreetly hidden behind the normal spectacle front) allows the lenses to be tilted well out of the way. With this frame, the spectacles do not have to be constantly removed for one visual task, and then replaced again.



Some of the various lens forms that might apply in the case of an engineer. *Left to right:*

A special bifocal allowing sections for close range work both at the top and bottom of the lens. Distance vision would be through the central portion.

A reversed bifocal, which gives a very large area at the bottom of the lens for close work, and a large section at the top for arm's length work.

A trifocal which allows a wide field of view at arm's length, with a large portion for near range vision. Distance vision is through the top of the lens.

British Electronics Exports

Some recent contracts gained in Europe, Africa, Asia, the Americas and Australasia

AFGHANISTAN

The Republic of Afghanistan is to install a new national telephone trunk transmission system using GEC open wire line carrier equipment over a 1448-km (900-mile) route which will link the main population centres of the country. The contract received by GEC Telecommunications covers 3- and 12-circuit telephony equipment and will include diesel generators and battery chargers to supply power for the system.

AUSTRALIA

Pye TVT has received a £250,000 order for the supply of a colour television outside broadcast unit to TCN9, one of Sydney's leading commercial stations. The vehicle to be supplied is part of this station's re-equipment programme in preparation for the introduction of colour television to Australia in March 1975 and is based upon the standard 4×LDK5 design. Initially the vehicle will be equipped with three colour cameras, with provision being made for the later installation of a fourth LDK5 and a further, hand-held camera. Among the particular requirements of the customer was the possibility of using the vehicle as a central control room for multi-vehicle productions.

Two leading British companies in the computer automation field Plessey and Ferranti, have combined to win an export contract worth £400,000. It covers supply, installation, commissioning and support of a system to provide electronic aids to vehicle drivers and a toll registration system for a new expressway being constructed south-west of Sydney by the Department of Main Roads in New South Wales. The new system will provide an emergency telephone service for road users and monitor traffic volume and speed. The control centre, which will direct all warning signs and the telephone system on the expressway, will be equipped with two Ferranti *Argus* 700 computers located at the Waterfall Toll Plaza.

CANADA

A £1.25M contract to equip the new 1805 ft high CN Tower in Toronto, Canada, with a complete antenna complex for f.m. radio and television broadcasting services has been won by the Telecommunications Division of EMI Sound & Vision Equipment, Hayes, Middlesex. When completed, Canadian National Railways observation and communication tower will be the tallest self-supporting structure in the world. The antenna system comprising initially four arrays surmounting the main concrete tower will be carried on a 220-ton needle-shaped steel structure over 300 feet tall.

CHINA

AEI Scientific Apparatus has topped the million pound mark for sales of its latest ultra-high resolution mass spectrometer, with an order from Peking. An earlier model had already been sold to Machimpex, the Chinese buying agency. In the current order, worth over £120,000, the company will supply an MS5074 mass spectrometer and an associated computerized data processing system for installation in a Chinese research institute.

Pye TVT has received an order from China for a £250,000 colour outside broadcast vehicle. The contract follows Chinese Trade Mission visits to Cambridge and participation by Pye companies in the British Industrial Technology Exhibition in Peking. The o.b. van, similar to those used by both the BBC and British commercial television companies, will be equipped with four LDK5 units and can function completely independently as a roving television studio control room.

ETHIOPIA

Racal transmitters have been chosen by the Ethiopian Imperial Civil Aviation Administration for use in air traffic control and the handling of meteorological information. This order, for three transmitters and associated equipment, represents a breakthrough into the Ethiopian civil aviation market for the Bracknell company.

The transmitters will be installed at Addis Ababa, transmitting to Jeddah, Khartoum and Nairobi as part of a British Overseas Development Administration loan 'package' which also includes instrument landing systems from another British company. Racal Communications has already installed transmitters for the Imperial Ethiopian Board of Telecommunications.

EASTERN EUROPE

Eastern European orders worth more than £120,000 for three computer-assisted automated draughting systems for printed circuit board manufacture have been secured by Quest Automation, Ferndown, Dorset. One package has been supplied to Videoton, Budapest, manufacturer of data processing equipment, and two systems have been ordered by the Polish Ministry for Machine Building.

IRAN

The Imperial Iranian Government has ordered further equipment for its *Rapier* low-level air defence systems, including a substantial number of radar trackers. The radar tracker was developed and is manufactured by Marconi Space and Defence

Systems for the *Rapier* system. Used in conjunction with existing *Rapier* equipment the radar tracker will give the systems a full 'blindfire' capability; it is mounted on an identical trailer to that used for the *Rapier* launcher and also includes other common components, thus simplifying logistic and maintenance support. The same automatic test equipment is used for maintenance of both the basic system and the radar tracker.

LIBYA

Plessey Telecommunications has won a major contract worth more than £1.3M for the supply of two Plessey 5005 Crossbar telephone exchanges to the Posts and Telecommunications Corporation of the Libyan Arab Republic. This is a market previously dominated by West German and Swedish suppliers. Plessey will install a 5,000 line exchange with an ultimate capacity of 20,000 lines at Misurata, a coastal town 125 miles from Tripoli, and a 3000 line exchange with an ultimate capacity of 15,000 lines at the provincial capital of Sebha.

NIGERIA

Pye TVT has a £1M order from Kano State Government, in Nigeria, for a television broadcasting service covering the State. The new broadcasting complex which comprises two main studios and a presentation suite, together with associated technical areas, will be housed in a new building due for completion during 1974. Television coverage of the State, which is about the size of Wales, will be by microwave link from the studio centre to the main transmitter and two ancillary transmitter stations. Because of the flat terrain of Kano State five aerial masts will be required ranging from 300 ft to 500 ft in height.

SAUDI ARABIA

Saudi Arabia has placed an order, valued at £1.4M with Plessey Radar for meteorological instrumentation. It is for three 'turn-key' upper atmosphere observation stations for installation at Dharan, Tabouk and Khamis Mushait airports, and the contract covers the supply, installation and commissioning of three Plessey 43S weather radar and radiosonde stations, electrical and hydrogen generators and buildings.

SIERRA LEONE

Pye TVT of Cambridge has signed a £750,000 contract with the Government of Sierra Leone. The contract includes provision of a new television transmitter and studio centre and a sound broadcasting complex. The new transmitting station will include a 10 kW Pye Band III transmitter with a 250 ft self-supporting tower. This transmitter will be fed by a microwave link from the studio centre which will include a main studio having three plumbicon cameras, a presentation studio having two cameras, together with a telecine suite and video tape recording equipment. The sound broadcasting complex will include a music studio, talks studio, commercial studio and a continuity suite together with a master control system and recording suite.

SINGAPORE

Marconi Communication Systems has won a £125,000 order from the Singapore Ministry of Culture's Department of Broadcasting for the supply, installation and commissioning of new 15 kW v.h.f. television transmitters. Singapore television is going on to colour in 1974 and the new programmes will be carried on the Marconi transmitters. Two existing transmitters, installed by Marconi in 1966, are to be modified to act as stand-by equipment.

SWEDEN

The Swedish Telecommunications Administration has ordered two u.h.f. transmitters from Marconi Communication Systems through Svenska Radio Ltd. Two 10 kW transmitters are to be installed at Karlstad on Lake Vänern in the south of Sweden. These will replace one existing Marconi transmitter, which is to be moved to the transmitting station at Varberg on the Kattegatt coast. Sweden has two television channels and the order is part of a

general consolidation programme for the second channel. The Marconi B7320 u.h.f. television transmitter is one of the range of i.f. modulated transmitters first introduced two years ago.

UNITED STATES

Marconi Marine has received an order from Mobil Shipping and Transport for the supply of communications installations to two 274,000 ton tankers currently under construction in Japan. Each installation will be based on Marconi Marine's high power *Conqueror* synthesized drive s.s.b. transmitter. It will be fitted with two *Apollo* s.s.b./d.s.b. digital display receivers which, together with a full emergency communications installation, will be housed in a low-line console/desk unit. A *Survivor* portable lifeboat transmitter/receiver is to be supplied for use in the lifeboats, while v.h.f. radio-telephone requirements will be met by an *Argonaut S* transceiver equipped with weatherproof bridge wing extension units. Other equipment to be supplied includes a *Lodestar IID* automatic radio direction

finder and two multi-standard television receivers complete with a v.h.f./u.h.f. aerial system.

WEST GERMANY

Pye Telecommunications has received a £200,000 export order from West Germany for some 1,300 mobile two-way radio equipment. The order has been placed by the company's German agents for a variety of customers including public utilities and private industry.

YUGOSLAVIA

Marconi Marine has received orders from Yugoslavian shipyards for the supply of communications equipment and navigational aids to six new vessels. All will have main communications installations based on Marconi Marine's *Conqueror* synthesized drive single-sideband transmitter and associated *Apollo* digital-display single-side-band receiver. The *Apollo* receiver, together with a full range of emergency equipment, will be housed in a low-line console/desk unit which Marconi Marine is supplying to each vessel.

Television and Radio Expansion

Matters concerning the expansion of television and sound broadcasting services in the United Kingdom were discussed in some detail at the recent quarterly meeting of the General Advisory Council of the BBC. The Council, which is one of the bodies through which the BBC seeks constructive criticism and advice on its activities, was considering a paper on the Use of Radio Frequencies for Sound and Television Broadcasting in the United Kingdom and the detailed comments made on it by a sub-committee.

It noted the fact that under the current expansion programme for bringing television reception to the whole population, 98% would be served by all three channels by 1979 at a cost of £4 M a year. The remaining 2% would comprise small communities numbering about 1000 people or less. The reasons, mainly outside the BBC's control, why this programme could not be further expedited, were generally accepted.

It supported the BBC's intention to continue with the expansion programme at a similar rate of expenditure annually thereafter until a situation was reached around the mid-1980s when, given the necessary frequencies, the size of isolated communities still to be served would have been substantially reduced. It was acknowledged that thereafter a point would be reached in which any supposed obligation to reach 100% coverage had to be weighed against steeply escalating costs. Consideration might have to be given to alternative forms of finance, possibly with the assistance of national or local government, bearing in mind that people living in areas

furthest from main centres of population might have a strong claim on public resources for access to popular entertainment and cultural influences.

On radio reception, the sub-committee of the Council recognized that the continued expansion of radio broadcasting throws an increasing load on channels at present allocated for broadcasting purposes. They accepted that the additional coverage required must be provided in the v.h.f. band, and they advised the BBC to pursue representations to the Ministry of Posts and Telecommunications as to the urgency of transferring service users to other bands in order to clear, at the very least, the 97.6-100 MHz band for broadcasting, as is the case in other countries.

They also suggested that the BBC should carry out a determined programme to inform listeners about the desirability of buying multi-wave receivers, having long, medium wave and v.h.f. capability, many of which are available at reasonable prices, in view of the likelihood that increasing reliance will have to be placed on v.h.f. in the future because of international frequency allocations.

The Council accepted that changes in the present frequency patterns for radio might be forced on the BBC by international developments. It urged, therefore, that specific and continuing research on current listening habits in terms of set and waveband usage should be undertaken so that any future changes which might become necessary could be designed to secure as much public acceptability as possible.

Members Appointments

CORPORATE MEMBERS

Mr. J. C. King (Fellow 1948, Associate 1946) has been appointed Managing Director of Thorn Radio Valves and Tubes Limited. Mr. King joined the Board in 1971 when he was General Manager of the company with whom he has been for the whole of his professional life. He was the first Chairman of the Kent Section.

Mr. C. J. Bulcock (Member 1966, Graduate 1962) who was a Technical Sales Engineer with English Electric, Stafford, concerned mainly with high voltage d.c. transmission, has been appointed Chief Engineer of Harrods Limited, London.

Air Commodore A. J. B. Clements (Member 1951) has been appointed Air Officer Signals, Support Command Signals Headquarters, Royal Air Force Medmenham. He was previously Assistant Controller (Operations), Headquarters Defence Communication Network.

Mr. K. J. Dickens (Member 1971) who went to the United States in 1970 as a Technical Field Support Specialist for mass spectrometers with AEI Scientific Apparatus Inc., is now Section Head in the Electronics Department of the James Franck Institute of Chicago University.

Mr. G. A. Duguid (Member 1971) has joined the Rank Video Organization as Senior Engineer concerned with computer controlled video editing. He has previously held appointments with Independent Television News, EVR Partnership and the Marconi Company.

Mr. J. L. L. Osborne (Member 1954) will retire later this year after completing 35 years with Mullard Company. For the past ten years he has been Manager of Central Technical Services at Mullard House. He was for many years particularly concerned with quality testing of receiving valves at the Company's radio valve works, Mitcham, and he has served on several industry and BSI committees.

Mr. G. White, C.G.I.A., (Member 1968, Associate 1966) has joined IVS (UK) Ltd. as Technical Director. He has held senior appointments during recent years with Memorex Corporation and with television broadcasting organizations. Mr. White served on the Committee for the recent IERE Conference on Video and Data Recording and he is the author of a book on 'Video Recording' published in 1972, in addition to articles in technical journals.

Mr. J. A. Wyatt (Member 1965, Graduate 1963) has been appointed Quality Assurance Manager with the Data Equipment and Systems Division of Standard Telephones and Cables Limited. He was previously Deputy Quality Assurance Manager in the Company's Step by Step Telephone Switching Division.

NON-CORPORATE MEMBERS

Mr. G. R. Billington, B.Sc., (Graduate 1973) who was an Electronics Development Engineer with the Lucas Electrical Company, Burnley, has joined RS Components Limited, London, as Technical Representative.

Mr. A. Butterworth (Graduate 1969) has moved from Dorman Smith Britmac (Preston) where he was a Technical Controller, to Corning-EEL Scientific Instruments Limited, Halstead, Essex, as Sales Engineer.

Mr. H. M. Morton, B.Sc. (Graduate 1973) has been promoted to Engineer with Plessey Telecommunications Limited, Beeston, whom he joined in July last year as an Assistant Engineer after graduating from the University of Strathclyde.

Mr. A. Smith (Graduate 1969) has joined Data Recognition Limited as Customer Services Engineer; he was previously Field Engineer with the West German subsidiary of Data 100 Limited.

Mr. H. P. White, B.Sc. (Graduate 1953, Associate 1945) has been appointed manager of Central Technical Services, Mullard Limited, in succession to Mr. J. L. Osborne (Fellow) who is retiring. He has been with the company since 1945, initially in the Valve Measurements and Applications Laboratory and subsequently in the Technical Services Department where he has been head of the Data and Publications Sections since 1955.

WO II J. Moore, REME (Associate 1973) is now with REME Technical Services BAOR as Defect Investigator and Electronic Adviser.

Mr. K. J. Pearson (Associate 1951) who has been with the Home Office for 34 years, latterly as Engineer in Charge of the Home Office Telecommunications Establishment near Cheltenham, retired at the end of the year because of ill health.

Obituary

The Council has learned with regret of the deaths of the following members.

Flight Lieutenant Patrick Michael Nagaur, RAF (Graduate 1969) died suddenly on 20th October 1973, aged 40 years. He leaves a widow and five children.

Flt. Lt. Nagaur entered the RAF in 1956 as a Junior Technician and by 1968 had reached the rank of Chief Technician. During this period he had obtained Higher National Certificate in Electrical and Electronic Engineering following part time studies at Harrow College of Technology. He was commissioned in 1971 with seven years seniority in the rank of flying officer and after completing his training at the RAF College, Cranwell, was posted to RAF Bawtry. At the time of his death he was at RAF Scampton, Lincoln.

Herbert Frederick Bell (Graduate 1964) died on 22nd December 1973, aged 53. He leaves a widow and two sons.

Mr. Bell was educated at Creighton School, Carlisle and served his apprenticeship in the Post Office Engineering Department. He later studied at Carlisle Technical

College and was awarded the Ordinary National Certificate in 1957 and in 1963 he obtained his Higher National Certificate. On both these occasions he received an IEE prize for his high standard. Mr. Bell joined the UKAEA in 1959 as an Instrument Mechanic and subsequently he was employed by British Nuclear Fuels Ltd. as the senior instructor in electronics in the Instrument Training School at Windscale and Calder Works. He played a major part in developing the City and Guilds 275 Course Part 3 syllabus taught in the School.

G.R.B.W.

Peter McGregor, Dip. El. (Member 1955, Graduate 1950) died on 31st December 1973 after being ill since August. He was 54 years of age and unmarried.

Mr. McGregor originally trained as an architect and surveyor but after War service with the Royal Engineers he obtained the Diploma in Electronics of the then University College of Southampton and entered the Royal Naval Scientific Service as an Assistant Experimental Officer. For

the majority of his professional life he was concerned with the development of sonar equipment serving at the Admiralty Underwater Weapons Research Establishment, Portland. In 1955 Mr. McGregor contributed a paper to the Journal on 'Trace to trace correlation in visual displays' which presented early work on elementary pattern recognition. In 1964 he was promoted to Senior Experimental Officer and was subsequently regraded as Senior Scientific Officer.

Mohammad Abdul Aleem Khan (Graduate 1963) died on 12th January 1974, aged 33. He leaves a widow.

Born and educated in Pakistan, Mr. Khan graduated with a general degree at the University of Karachi in 1958. In 1961 he came to England and studied engineering subjects at the Borough Polytechnic and Wandsworth Technical College, obtaining his HNC in Electronics with Electronics Measurements endorsement in 1963. From 1961 until 1966 he was a Scientific Technical Officer (Grade 2) at the Mining Research Establishment of the National Coal Board,

working on problems on intrinsically safe electrical equipment. For the next three years he was Deputy Manager of Philips Electrical Industries of Pakistan Limited, and at the end of 1969 he returned to Europe to work as an Engineer with Landis and Gyr of Zug, Switzerland, where he was concerned mainly with reliability evaluation on semiconductor devices. From July 1972 until the time of his death he had been working as a Development Engineer with Siemens-Albis of Zurich.

William Robert Roper (Member 1966, Graduate 1963) died on 14th January last at the London Hospital as a result of injuries received in a car accident a few days previously. He was 35 years of age and leaves a widow and two children.

Born in Warlingham, Surrey, Mr. Roper studied at the Mid-Essex and North-East Essex Technical Colleges, gaining the Higher National Certificate with endorsements in Electronic Measurements in 1962. He joined the Marconi Company in 1955 as a student apprentice and subsequently worked as an Engineer in the Display and Data Handling Laboratory. In 1964 he

moved to Elliot Bros (London) Limited as a Systems Engineer and he remained with the company until 1967, dealing mainly with data presentation. For the next four years he was with Cossor Electronics as manager of data systems engineering. He left the company in November 1970 to join Capital Cities Computers Limited at Watford where he was an area Manager concerned with data processing facilities for a number of customers.

Eric Rees (Member 1971) died in January at the age of 44 years after nearly a year's ill health. He leaves a widow and two children.

Mr. Rees received his secondary education in Sheffield and was then apprenticed to the electrical company, W.E. Burnand & Son Ltd. where he was involved in the repair and installation of electronic and electrical equipment. For four years from 1954 he was a field engineer with International Computers Ltd. working on installation and maintenance and for six years from 1958 he was with Davy & United Ltd. as a project engineer in charge of a team working on electrical and electronic services for steelworks rolling mills. During this time he followed a course of evening

study at the Sheffield College of Technology and obtained his Higher National Certificate in Electrical and Electronic Engineering at Rotherham College of Technology.

From September 1964 until his death Mr. Rees was senior electrical and electronic engineer to Husband & Company Ltd., consulting engineers, of Sheffield, who designed the Jodrell Bank Radio telescope. He worked on various similar projects throughout the world including one large steerable telescope which had a control system comprising of two digital computers with closed-loop drives and digital encoders.

From the date of his joining the Institution he maintained a very active part in local section affairs and had been Honorary Treasurer to the Yorkshire Section for the past two years and IERE representative on the Councils of both the Huddersfield and Wakefield Colleges of Technology and the Council of Stannington College of Further Education, Sheffield. He represented the Institution on the Yorkshire Section Committee of CEI.

He was a first class engineer, a hard worker and will be sorely missed, not only by his widow and his family, but also by the many friends which he had made throughout industry. P.A.B.

Forthcoming Institution Meetings (continued from opposite page)

Wednesday, 29th May

COMMUNICATIONS GROUP

Colloquium on MODELLING OF COMMUNICATIONS SYSTEMS

IERE Lecture Room.

Advance Registration necessary. Apply to Meetings Secretary, IERE.

Wednesday, 5th June

COMPONENTS AND CIRCUITS GROUP

Colloquium on J-FETS and MOSFETS

IERE Lecture Room.

Advance Registration necessary. Apply to Meetings Secretary, IERE.

South Midland Section

Wednesday, 24th April

Design for Automatic Testing

By J. W. Anstead (*Smiths Industries*)

To be followed by

ANNUAL GENERAL MEETING

The Foley Arms, Malvern, 7 p.m.

Friday, 10th May

Annual Buffet Dance

BBC Club, Evesham, 8 p.m.

Tickets necessary

South Western Section

Monday, 6th May

ANNUAL GENERAL MEETING

The Royal Hotel, College Green, Bristol, 7 p.m.

North Eastern Section

Wednesday, 10th April

Communication with Light

By Professor W. A. Gambling (*University of Southampton*)

Followed by **ANNUAL GENERAL MEETING**

The Main Lecture Theatre, Ellison Building, Newcastle Upon Tyne Polytechnic, Ellison Place, Newcastle Upon Tyne, 6 p.m. (Refreshments in Staff Refectory 5.30 p.m.)

North Western Section

Thursday, 9th May

ANNUAL GENERAL MEETING

Followed by **European Communication Satellites**

By A. Dickinson (*BAC*)

Lecture Theatre R/H10, Renold Building, UMIST, 6.15 p.m. (Tea 5.45 p.m.)

Yorkshire Section

Friday, 26th April

ANNUAL GENERAL MEETING

Leeds University, 7 p.m.

Merseyside Section

Wednesday, 24th April

ANNUAL GENERAL MEETING at 7 p.m. Followed by

Wide Ranging Applications of Metal Oxide Semiconductors

By J. A. Everist (*ITT Semiconductors*)

Department of Electrical Engineering and Electronics, University of Liverpool, 7 p.m. (Tea 6.30 p.m.)

South Wales Section

Thursday, 11th April

JOINT MEETING WITH IEE

Quadrophonics

By K. Barker (*University of Sheffield*)

University College, Swansea, 6.15 p.m.

Scottish Section

Thursday, 25th April

ANNUAL GENERAL MEETING

Glasgow College of Science and Technology, 7 p.m.

Forthcoming Institution Meetings

London Meetings

Wednesday, 10th April

COMPONENTS AND CIRCUITS GROUP

All-day Colloquium on SMALL POWER TRANSFORMERS AND CHOKES

IERE Lecture Room, 11 a.m. (Coffee 10.30 a.m.)

Transformers—The State of the Art 1974

By J. W. McPherson (*Gardiers Transformers*)

Magnetic Circuit Optimization for Miniature Power Transformers

By D. M. Fidler (*Tridem Transformers and Electronics*)

Life Testing of Chokes for Discharge Lamps

By Dr. T. R. Passmore (*Thorn Lighting*)

The Use of Matched Transformers for Synchro-Resolver Applications

By M. Pratt (*Ferranti*)

Constant Voltage Transformers

By A. Langley Morris

Designing for Production

By V. E. Cole (*Plessey*)

Ferrite Cored Transformers

By E. C. Snelling (*Mullard*)

For further details and registration forms, apply to Meetings Secretary, IERE

Wednesday, 17th April

AEROSPACE, MARITIME AND MILITARY SYSTEMS GROUP

Colloquium on ELECTROMAGNETIC COMPATIBILITY OR CONFUSION—EMC ON LAND, AT SEA AND IN THE AIR

IERE Lecture Room, 11 a.m. (Coffee 10.30 a.m.)

Technical Aspects of Electromagnetic Interference—Film

EMC—A Maintainer's Viewpoint

By Lt.-Col. W. Barker (*REME*)

Radio Interference from Road Vehicle Ignition Systems

By D. W. Morris (*Lucas Electrical*)

National and International Standards for the Control of Radio Interference

By A. S. McLachlan (*Ministry of Posts and Telecommunications*)

Problems of Measurement

By G. A. Jackson (*ERA*)

EMC Testing of Aircraft

By G. M. Smith (*A. & A. E. E., Boscombe Down*)

Mercantile Marine EMC

By M. Gibson (*Marconi International Marine Co.*)

EMC in Ships

By T. Morgan (*Formerly M.o.D., Bath*)

Advance Registration necessary. Apply to Meetings Secretary, IERE.

Tuesday, 23rd April

Please note change of date

COMMUNICATIONS GROUP

Uncertainties and Inertia in Long Range Telecommunications Planning

By A. A. L. Reid (*Post Office Long Range Studies Divisions*)

IERE Lecture Room, 6 p.m. (Tea 5.30 p.m.)

There are many sources of uncertainty in long range telecommunications planning. These include uncertainty about demand for new services, about technology, and about costs. Yet the enormous inertia of the telecommunications system, with over £3000M in assets having a long life, makes it difficult to change direction swiftly. In such a situation it is important to plan for uncertainty. This can be done through small added investment in 'hooks' upon which future services can be hung, and generally be selecting not the best technological strategy for a single future, but rather a strategy which will cope adequately with a wide range of possible futures.

Wednesday, 24th April

JOINT IERE/IEE MEDICAL AND BIOLOGICAL ELECTRONICS GROUP

Colloquium on HEARING AIDS

POSTPONED.

Wednesday, 1st May

COMPONENTS AND CIRCUITS GROUP

Colloquium on INTERACTIVE GRAPHICS FOR ELECTRONICS DESIGN

IERE Lecture Room.

P.C.B. Layout from Designer's Sketch to Artwork

By W. E. Hillier (*Redac Software*)

An Approach to Display Terminal Optimization for Computer Aided Circuit Design Applications

By J. J. O'Reilly (*University of Essex*)

The Use of a Storage Tube Graphic Terminal for Integrated Circuit Design

By J. D. Eades (*Department of Computer Science, University of Edinburgh*)

The Economics of using Interactive Graphics for Integrated and Printed Circuit Design in a Production Environment

By M. A. Northwood (*Calma Co.*)

Use of Small and Large Interactive Devices for Design and Drafting

By R. R. Gallant (*Computervision Corp.*)

An Interactive Graphical System for Circuit Analysis

By Dr. M. Apperley (*Imperial College of Science and Technology*)

Further details and registration forms from Meetings Secretary, IERE.

Wednesday, 8th May

EDUCATION AND TRAINING GROUP

The Teaching of Electronic Logic Systems

By Dr. K. J. Dean (*S.E. London Technical College*)

IERE Lecture Room, 6 p.m. (Tea 5.30 p.m.)

The rapid development of digital electronic systems has brought with it changes in teaching methods. Whereas in the past we have been primarily concerned with circuit design for linear systems, more emphasis is being placed on binary system design which is comprised of two-state circuits, the design of which is probably of less immediate concern than that of the system of which they are components. The lecture will discuss the impact this state of affairs makes upon teaching techniques and on syllabus content, and will be suitably illustrated.

Wednesday, 15th May

AEROSPACE, MARITIME AND MILITARY SYSTEMS GROUP

The US Navy Navigation Satellite System

By W. F. Blanchard (*Redifon Telecommunications*)

MEETING POSTPONED

Tuesday, 21st May

JOINT IEE/IERE COMPUTER GROUP

Colloquium on LARGE SCALE INTEGRATION—ITS USE AND ITS EFFECT ON SYSTEM ARCHITECTURE

IEE, Savoy Place, 2.30 p.m.

Further details and registration forms from the IEE, Savoy Place, WC2R OBL.

Wednesday, 22nd May

AUTOMATION AND CONTROL SYSTEMS GROUP

Automatic Frequency Response Testing of Non-Linear Control Systems

By M. C. De'Ath (*Marconi Space and Defence Systems*)

IERE Lecture Room, 6 p.m. (Tea 5.30 p.m.)

Friday, 24th May

JOINT IEE/IERE MEDICAL AND BIOLOGICAL ELECTRONICS GROUP

Colloquium on NON-INVASIVE MEASUREMENT OF CARDIAC OUTPUT

IEE, Savoy Place, 10.30 a.m.

Further details and registration forms from the IEE, Savoy Place, WC2R OBL.

(Continued on opposite page)

INSTITUTION OF ELECTRONIC AND RADIO ENGINEERS

Applicants for Election and Transfer

THE MEMBERSHIP COMMITTEE at its meetings on 28th December 1973 and 29th January 1974 recommended to the Council the election and transfer of 74 candidates to Corporate Membership of the Institution and the election and transfer of 6 candidates to Graduateship and Associateship. In accordance with Bye-law 21, the Council has directed that the names of the following candidates shall be published under the grade of membership to which election or transfer is proposed by the Council. Any communications from Corporate Members concerning these proposed elections must be addressed by letter to the Secretary within twenty-eight days after the publication of these details.

Meeting: 28th December 1973 (Membership Approval List No. 175)

GREAT BRITAIN AND IRELAND

CORPORATE MEMBERS

Transfer from Graduate to Member

ABEL, Dennis. *Slough, Buckinghamshire.*
ALEXANDER, Roger Martyn. *Stubbington, Hampshire.*
ANSELL, Michael John. *Welwyn, Hertfordshire.*
ARMSTRONG, Richard Henry. *Tonbridge, Kent.*
BARBER, David Ronald. *Great Wakering, Southend-on-Sea, Essex.*
BASSON, Keith. *Warrington, Lancashire.*
BRANDON, John Gregory. *Brentwood, Essex.*
BRADY, John Joseph. *Bangor, County Down, Northern Ireland.*
BROOK, Rodney Russell Victor. *Beckenham, Kent.*
BROWN, Colin. *Portchester, Hampshire.*
BURTON, Alfred William. *Cambuslang, Glasgow.*
CLISBY, Reginald George Kent. *Cranleigh, Surrey.*
CROSS, Ronald Anthony. *Harrow, Middlesex.*
D'SILVA, John Robert. *Bracknell, Berkshire.*
FITTER, Michael Adrian. *Hassocks, Sussex.*
FLETCHER, John Cedric. *Ringmer, Sussex.*
FRANKS, Frederick Arthur. *Bexley, Kent.*
GODDEN, Brian Frederick. *Sidcup, Kent.*
HALPIN, Robert Joseph. *Santry, Dublin.*
HORNE, John Michael. *London, N.15.*
JACKSON, Dennis Benjamin. *Portsmouth, Hampshire.*
JONES, Malcolm Edward. *London, N.W.2.*
KNIGHTSON, Keith Gerald, B.Sc. *Colchester, Essex.*
LEWIS Carey. *Stevenon, Berkshire.*
LIMPKIN, George Alan. *Meopham, Kent.*

LONGHORN, John Frederick. *Bronley, Kent.*
LOWE, David John. *Harthill, Sheffield.*
LOYNES, Albert Geoffrey. *Warrington, Lancashire.*
McCLURE, Robert Martin. *Wantage, Berkshire.*
McKINNEY, William John Maurice. *Belfast.*
MALTBY, Raymond George William, Captain. *Malvern Link, Worcester.*
MARTIN, Paul. *Lydiate, Lancashire.*
MAYNARD, Geoffrey Reginald. *Cranfield, Bedfordshire.*
MILLER, Alistair. *Edinburgh.*
NORTH, Ian Francis. *Loughborough, Leicester.*
O'CONNOR, John Colin. *Stoney Stanton, Leicestershire.*
PALMER, Geoffrey Ian. *Sherborne, Dorset.*
PELOW, James George. *Blackrock, County Dublin.*
PERRY, Terence James. *Bedford.*
PETTIT, Anthony George Rice. *Colchester, Essex.*
PETTIT, Christopher Richard. *Ruthin, Denbighshire.*
POMFRET, David John, B.Sc. *Woodford Green, Essex.*
POWELL, Douglas Reginald. *Colchester, Essex.*
ROSE, Michael John. *Didcot, Berkshire.*
ROSS, Donald, Mackenzie. *Chatham, Kent.*
SPENCER, Godfrey Stanley Gibson. *Rowlands Castle, Hampshire.*
SULLIVAN, Terence Eoghann. *London, S.E.2.*
TRINKWON, David Brian. *St. Albans, Hertfordshire.*
UNDERDOWN, Martyn Sinclair, Lieutenant. *Warsash, Southampton, Hampshire.*

WHITE, John Saunders. *Ascot, Berkshire.*
WILES, James Robert. *Romford, Essex.*
WILLINGTON, David John. *Harrow, Middlesex.*
WOOD, Royston. *Morrison, Swansea, Glamorgan.*
WRIGHT, Frederick Edward. *Chelmsford, Essex.*
YOUNG, David John. *Stockport, Cheshire.*

Direct Election to Member

BARKER, Paul Joseph. *Wasperton, Barford, Warwickshire.*
HEWITT, Michael Timothy. *Ipswich, Suffolk.*
LEAR, Eric Ernest. *Wallasey, Cheshire.*
MAHADEVAN, Ponnambalam, B.Sc., Ph.D. *Guiseborough, Yorkshire.*
OLIVE, Bryan Roy, Commander R.N. *Barrow-in-Furness, Lancashire.*
RAYNER, Stuart, Lieutenant Commander R.N. *Nutbourne, Chichester, Sussex.*
SMITH, Alfred Edward. *Haywards Heath, Sussex.*
STILL, Raymond George. *Fareham, Hampshire.*

OVERSEAS

CORPORATE MEMBERS

Transfer from Graduate to Member

BARNES, Brian William. *Kenya, East Africa.*
BECK, Arnon. *Afula, Israel.*
IP MIN WAN, Yukam. *Vacoas, Mauritius.*
JEFFRIES, Frederick John, Lieutenant R.N. *BFPO Ships.*
JOHNSON, Victor Adebayo. *Oniyarin, Ibadan, Nigeria.*
MANNAKKARA, Vimalasiri Senarath. *Kurunegala, Sri Lanka.*

Transfer from Associate to Member

GLASSCOTT, Eric Marcel. *Kingston, Jamaica, West Indies.*

Direct Election to Member.

COWL, Paul Edward, Major. B.Sc.(Eng.). *Alabama 35808, BFPO, 2.*
JEYABALASUBRAMANIAN, Kanthiah Dehiwela. *Sri Lanka.*
NWACHUKWU, Dominic Osundu Uzodinma. *Lagos, Nigeria.*
O'SULLIVAN, Patrick Joseph. *Jakarta, Indonesia.*

Meeting: 29th January 1974 (Membership Approval List No. 176)

GREAT BRITAIN AND IRELAND

NON CORPORATE MEMBERS

Transfer from Student to Graduate

JAWAID, Ahmed Ahsanuz Zaman, B.Sc. *London, N.W.2.*

Direct Election to Associate

COURT, Stephen John. *London, N.W.6.*

STUDENTS REGISTERED

ALLARD, Eric Stephen Powell. *Stowmarket, Suffolk.*
BLANEY, Gerald Henry. *Seaham, County Durham.*
BOTTING, Keith Charles. *Sanderstead, Surrey.*
BOYLE, Patrick Laurence. *Dublin 6, Eire.*

CLARK, Lorne. *Watford, Hertfordshire.*
COOK, Michael Kenneth. *Gateshead, County Durham.*
CRAWLEY, Peter Thomas. *Morden, Surrey.*
GILL, Martin George. *Ipswich, Suffolk.*
HIGGINS, Terence Michael. *Clifton, Bristol.*
KEARNEY, Robert John. *Ipswich, Suffolk.*
LAWER, Steven. *Woodbridge, Suffolk.*
LEUNG, Tsan Chung. *Newcastle upon Tyne.*
MAGHERA, Prem Singh. *Luton, Bedfordshire.*
MOHAMMED, Saidu. *Newcastle upon Tyne.*
MORSE, John Brian. *Hemel Hempstead, Hertfordshire.*
NAYLER, John Barry. *Ipswich, Suffolk.*
PINKNEY, William. *Seaham, County Durham.*
SEAGERS, Paul Lewis. *Woodbridge, Suffolk.*
TANYI-TANG, Enoch. *Southall, Middlesex.*
WHITING, Derek John. *Woodbridge, Suffolk.*

OVERSEAS

NON CORPORATE MEMBERS

Transfer from Student to Graduate

ABUBAKAR, Ibrahim Sarki. *Kaduna, Nigeria.*

Direct Election to Graduate

LEWIS, Martin, B.Sc. *Switzerland.*

Direct Election to Associate

HAFEEZ ALI. *Islamabad, Pakistan.*
LAKE, Arthur Henry. *Freetown, Sierra Leone.*

STUDENTS REGISTERED

LEOW, Huat Siong. *Singapore 11.*
PERRY, David Ernest. *Blair Athol, South Australia.*
TAN, Gim Seng. *Singapore 2.*

Notice is hereby given that the elections and transfers shown on List 173 have now been confirmed by the Council.